2014

The Synthesis and study of heterocyclic, dimeric and chiral ligands for the multidrug-resistance transporter

Scott Steiger
The University of Montana

Synthesis and study of heterocyclic, dimeric and chiral ligands for the

multidrug-resistance transporter

By

SCOTT ALLEN STEIGER

Ph.D Medicinal Chemistry, University of Montana, Missoula, MT, 2014

A Thesis

Presented in partial fulfillment of the requirements
For the degree of

Doctorate in Medicinal Chemistry

The University of Montana
Missoula, MT

Official Graduation Date: May 2014

Approved by:

Sandy Ross, Dean of The Graduate School
Graduate School

Nicholas R. Natale, Chair
The Department Of Biomedical & Pharmaceutical Science

Howard Beall
The Department Of Biomedical & Pharmaceutical Science

Charles Thompson
The Department Of Biomedical & Pharmaceutical Science

Keith Parker
The Department Of Biomedical & Pharmaceutical Science

Stephen Lodmell
Division of Biological Science

ABSTRACT

Steiger, Scott, Ph.D, December 2014,   Major
Medicinal Chemistry

Synthesis and study of heterocyclic, dimeric and chiral ligands for the multidrug-

resistance transporter

Chairperson: Nicholas R. Natale

        The development of multidrug resistance in tumor cells has been recognized as a major obstacle to successful cancer treatment. Tumor cells *in vitro* and *in vivo* can develop multidrug resistance (MDR) to the lethal effects of the cytotoxic drugs used to treat them, with about 40% of cancers going on to develop MDR. There are multiple factors that lead to MDR but the factor that we will be exploring in this dissertation is the expression of multiple drug resistance gene 1 and the over expression of multi drug resistance protein 1(MDR1, also known as P-glycoprotein or P-gp). MDR1 has also been shown to be a major contributor to the development of MDR in cancer, *via* preventing entry of therapeutically relevant drugs into the cancerous cell. As such, MDR1 is highly investigated as a drug target both for controlling absorption, distribution, metabolism and excretion (ADME) of clinically relevant compounds and for the production of MDR inhibitors.
        Our efforts in producing novel compounds to reverse MDR by inhibiting MDR1 have shown marked improvement from generation to generation of drug development. Our first generation of compounds had activitys that ranged from 10.9% to our lead compound showed a 61.2% inhibiton when compared to cyclosporine A. Our second generation had a slight increase in activity when we explored tethered compound with our lead compound showing a 63.0% inhibition when compared to cyclosporine A. Further exploration of tethered and dimer compounds in generation 3 showed a dramatic increase in inhibitory activity with our lead compound showing over a 200% inhibition when compared to cyclosporine A. With such a positive trend in activity generation 4 and 5 compounds where then designed to be more selective for MDR1. Currently, both generation 4 and 5 are in hand and are waiting for biological testing. Generation 4 compounds explore the effect that more steric groups in the 3-isoxazolyl position would have on MDR1 inhibition. While generation 5 componds explored chiralities effect on MDR1 inhibition and how it can be utilized in refining selectivity.
        Reversal of MDR is of interest for the clinical application; if a compound could effectly and safely reverse MDR, it would allow for major advancements in cancer chemotherapy. If successful, halting the function of MDR1 will stop the outward efflux of chemotherapeutic agents out of the cell. In combination with chemotherapeutic treatments, inhibitors could allow for greater penetration of drugs into an MDR cell and potential allow for the repurposing of out of date drugs where MDR has redered the drug ineffective. The exploration of this concept and the advancements that our group has added to this field will be explained in due course.

Table of Contents

List of Figures

Chapter 1

List of Tables

This paper was published in Future Medicinal Chemistry

Nicholas, Natale R.; Steiger, Scott., 4-Isoxazolyl-1,4-dihydropyridines: a tale of two

scaffolds. *Future Medicinal Chemistry*. **2014**, 6(8), 923-943

Chapter 1:

4-Isoxazolyl-1,4-dihydropyridiens: A tale of two Scaffolds

1.1 Introduction

The concepts of bioisoteric replacement,[1,2] privileged structures,[3-9] and scaffold hopping,[10,11] all have contributed to the process of drug development as medicinal chemists endeavors to develop approaches that arrive at bioactive candidates, and avoid excessive exploration of unproductive terrain. The term privileged structure was first introduced by Evans et al in 1988 and was defined as "a single molecular framework able to provide ligands for diverse receptors."[3] The development of novel compounds from known privileged structures has found general support due to the appearance of the 32 scaffolds in roughly half of known drugs.[4] Furthermore the inclusion of common moieties accounts for a large majority of side chains found in most drugs.[5] The exploration of privileged structures is an emerging theme in medicinal chemistry to aid in focusing synthetic efforts towards more active compounds. A privileged structure represents a substructure that is a common chemical motif capable of binding to given target with high affinity.[6-9] Considerable amounts of effort had been placed into increasing the success rates of novel drug discovery thus, the inclusion of so called privileged structures has been employed as a viable tactic for drug development. Conclusions drawn from using privileged structures and scaffolds lead in turn to the construction of common pharmacophore models, and as information emerge regarding the biomolecular target, to more detailed homology models to aid in drug development. The utility of privileged structures has increased our ability to synthesize libraries based upon core scaffolds and screen against a variety of targets to yield active compounds.

This review will focus on two of these structures and their application to complex drug development issues. Since the introduction of the term several groups have been shown to fit the criteria such as the 1,4-dihydropyridine (DHP) [12, 13] and the isoxazole [14] have been described as privileged structures. Both the isoxazole and dihydropyridine appear on Kubinyi and Muller's list of a dozen more common heterocycles in drug discovery, given their propensity for polypharmacology, these rings may well be referred to as the "dirty" dozen.[15]

The 1,2-oxazole or isoxazole 1 (Figure 1) was first isolated by Claisen in 1888 [16] and the name monoazole was suggested for the substructure. It was later named isoxazole by Hantzsch.[17] The inclusion of isoxazole in potential drug candidates have produced a range of pharmacological active compounds,[18] making the isoxazole of considerable interest to medicinal chemists. The isoxazole ring shows some aromatic character with the oxygen atom acting as an electron donating group and the nitrogen atom acting as an electron-withdrawing group.[19-23] The 4 position is the preferred position for electrophilic substitution and its reactivity is affected to the substituents at the 3 and 5 position. Electron donating groups activate the electrophilic substitution, while electron-withdrawing groups deactivate it. The 5 position is the thermodynamically more acidic proton in the ring in most instances.[24] The N-O bond is the weakest among the five bounds and can be reductively cleaved by many methods. The isoxazole has been considered by Bauman, et al, as one of the standard five-membered heterocycles to be considered in drug discovery.[18]
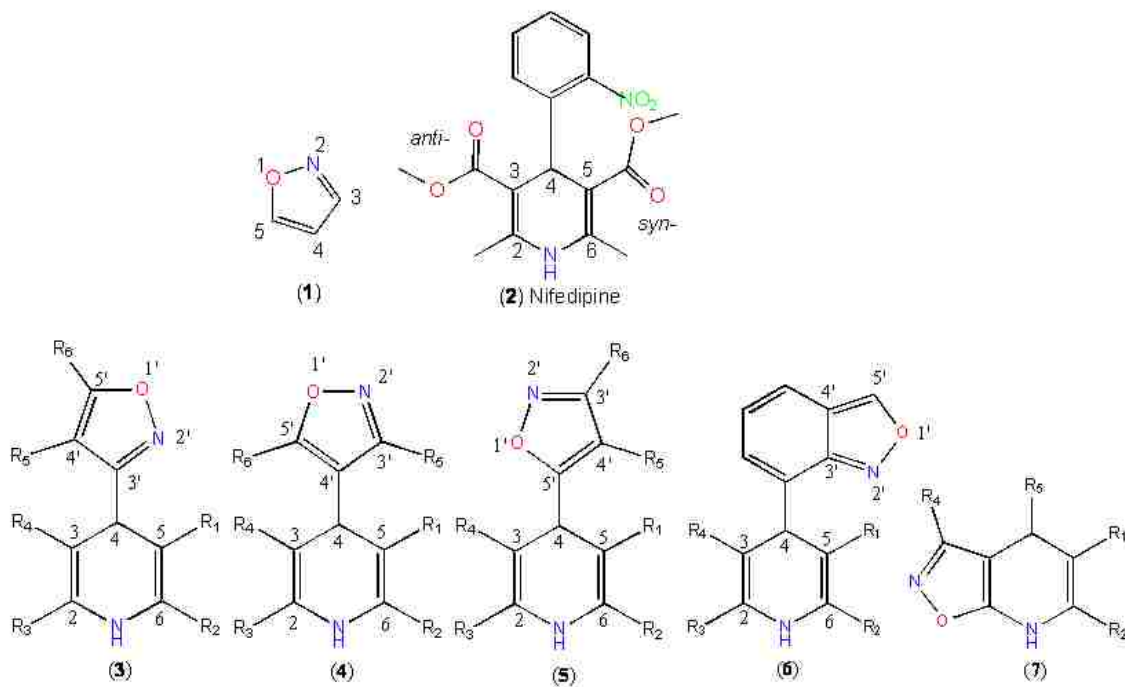
Figure 1.1: The isoxazole scaffold (1), and the dihydropyridine (DHP) (2), exemplified by the antihypertensive agent nifedipine. The esters at C-3 and C-5 of the DHP can attain either a synperiplanar or antiperiplanar conformation. . Representative known modes of isoxazole to DHP attachment isoxazol-3'-yl-4-DHP (3), isoxazol-4'-yl-4-DHP (4), and isoxazol-5'-yl-4-DHP (5), benzisoxazole (6,) and fused bicyclic system isoxazolo[5,4-b]pyridine (7).

The present review will focus on the type (4) IDHPs. The first synthesis of 1,4 DHPs was from acetoacetic acid esters, aldehyde and ammonia was first published in 1882 by Hantzsch.[25] Since then the synthetic procedure has proved to be highly versatile showing a considerable structural variation in the aldehydic component as well as in the 1,3 dicarbonyl compounds.[26, 27] As 1,4 DHPs have become more medicinally important variation of the synthesis have been explored to accommodate analog development.

4

Subsequently, the 1,4-DHP substructure has served as a scaffold for both second and third generation compounds that have shown improve activity.[28]

The 1,4 DHP has been important and highly effective drug substructure due to their wide range of biological activities. DHPs have a broad range of pharmacological actions such as vasodilation, brochodilation, antiatherosclerosis, antioxidant and anticonvulsant effects. The 1,4-DHP substructure is best known for their pharmacological action as calcium channel blockers, with the prototypical case being nifedipine 2 (Figure 1) which has been in general medical practice since 1975.[29,30,31]

It was noted early in the first generation of calcium channel antagonists exhibited cardiovascular action, this action was ultimately ascribed to the 1,4 –DHP substructure. Thus, the substructure is often included in compounds used to treat a variety of cardiovascular disorders such as hypertension. With further research on the substructure leading to the discovery that 1,4-DHP structure also having antitumor, antidiabetic, and anti-platelet aggregation properties. Additionally these compounds have also been utilized to promote drug transport across the blood-brain barrier,[31] which in turn lead to the use of DHPs to inhibit the Multidrug resistance transporter efflux pump (MDR, also known as P-gp).[32-34]

Potential connection of groups to the isoxazole can be accomplished through the 3'-,4'- and 5'- positions (Figure 1). This review will focus primarily on the potential connections to the 1,4-DHP in the 4'- position of the isoxazole ring system. The first example of the association of the two scaffolds was claimed in the patent literature, however, it is not clear whether the IDHP was actually prepared until the first fully characterized preparation of an IDHP was published in 1982 by Natale and Quincy.[35]

1.2 Isoxazol-3'-yl-4–IDHP

The connection of the isoxazole to the 3 position (3) is produced via the

producing an alcohol in the 3 positions of the isoxazole. From the alcohol the product is

oxidized to the aldehyde and subjected to the Hantzsch pyridine synthesis to produce the

DHP. The 3,4–IDHP was shown by Shafu and co-workers to have anti-tubercular

activity.[36] Due to multi-drug resistant strains of mycobacterium and to a high prevalence

of MDR tuberculosis the potential use of 3,4–IDHP as a MDR reversing agent was

proposed. The use of DHPs to combat MDR is an emerging trend in DHPs research that

is currently being explored by many groups including our own (*vide infra*). Further

analog development in this area where developed to explore calcium channel antagonist

activity.[37] Darybari *et al* observed that activity of these analogs was moderate at best

with maximum calcium channel antagonist activity approximately 10^{-7} M range

compared to the prototypical DHP nifedipine activity (1.10×10^{-8}M). This is expected in

light of Triggle's SAR principles [29] since para-phenyl substitution is well known to

lower voltage gated calcium channel (VGCC) affinity. Further exploration of analogs as

VGCC were not explored, it should be noted that these could potentially represent leads

for designing *against* the VGCC.

1.3 Isoxazol-4'-yl-4-IDHP

In the course of our early studies in this area,[35] the preparation of the isoxazole

connected to the DHP at the 4' position of the isoxazole (Figure 1, type (4)) was

rationalized by the structure activity relationship (SAR) developing at that time for

antihypertensive activity by virtue of blocking the VGCC: (1) that *para* substitution on

the 4-aryl ring lowered activity (the isoxazole has no *para* group) and (2) electron

withdrawing groups at the 4-aryl enhanced activity (the isoxazole is π-deficient). [28, 30, 38-46] We recognized that chemistry being developed in our laboratories at that time, lateral

metalation and electrophilic quenching of isoxazoles,[24, 47-51] could be applied to study

conformational and configurational issues in antihypertensive SAR. The structure activity

relationship (SAR) that emerges is distinct in critical points from known 4-

aryldihydropyridines (*vide infra*).[52] More recently we have recognized that IDHPs of

Type 4 bind the multi-drug resistance (MDR) transporter.[53,54]

1.4 Isoxazol- 5'-yl-4-IDHP

The connection of the isoxazole at position 5'- to the DHP was reported by

Mirzaei, and was performed by producing the 5'- alcohol followed by oxidation to the

aldehyde. The Hantzsch pyridine synthesis was then used to produce the 1,4-DHP.[55]

1.5 Fused Ring Systems

The preparation of benzo 2,1-isoxazole analogs of the 5',4-IDHP (5, where R_5

and R_6 are fused in a benzene ring) have also been achieved by Phillips.[56-57]

Alternatively, the benzoisoxazole was attached to the DHP via the benzene moiety (6),

analgous to isradipine. The exploration of these analogs was needed to systematically

probe differences in calcium channel activity. The fusion of the isoxazole at the 3 and 2

positions of the DHP to the Isoxazolo[5,4-**b**]pyridine (7), and their subsequent antitumor

activity, was studied by Hamama.[58] The fused isoxazole analogues were used to study

the receptor ligand interactions because these rigid, geometrically defined derivatives that

allow definition of spatial requirements for receptor binding.

Other heterocyclic 1,4-DHP fused analogues analogous to (7) have be reported to retain

potent receptor affinity as either antagonists or agonists.[59] The most common feature of

these derivatives is the retention of the 1,4-DHP as a part of a relatively planar bicyclic ring system (7). Isoxazoline analogues of 1,4-dihydropyridines were prepared by Taylor and have been used to study conformational effects at the calcium channel receptor,[60] where they revealed that saturating the ring juncture lead to more pronounced puckering of the DHP ring, and a lessened biological effect.

While the possible combinations of the isoxazole connected to the DHP are far from exhausted,in this account we will primarily focus on the study of the type (4) IDHPs (Figure 1, Structure (4)), which have been the emphasis of the work in our own laboratories.

1.6 Brief overview of the Synthesis and elaboration of IDHPs

For unhindered isoxazole aldehydes the classic Hantzsch synthesis works easily and effectively (Figure 2),[26, 27, 35] however, in the course of our studies to challenge the frontiers of conformationally encumbered structures, we found it necessary to conduct the reaction in a pressure vessel for optimal results.
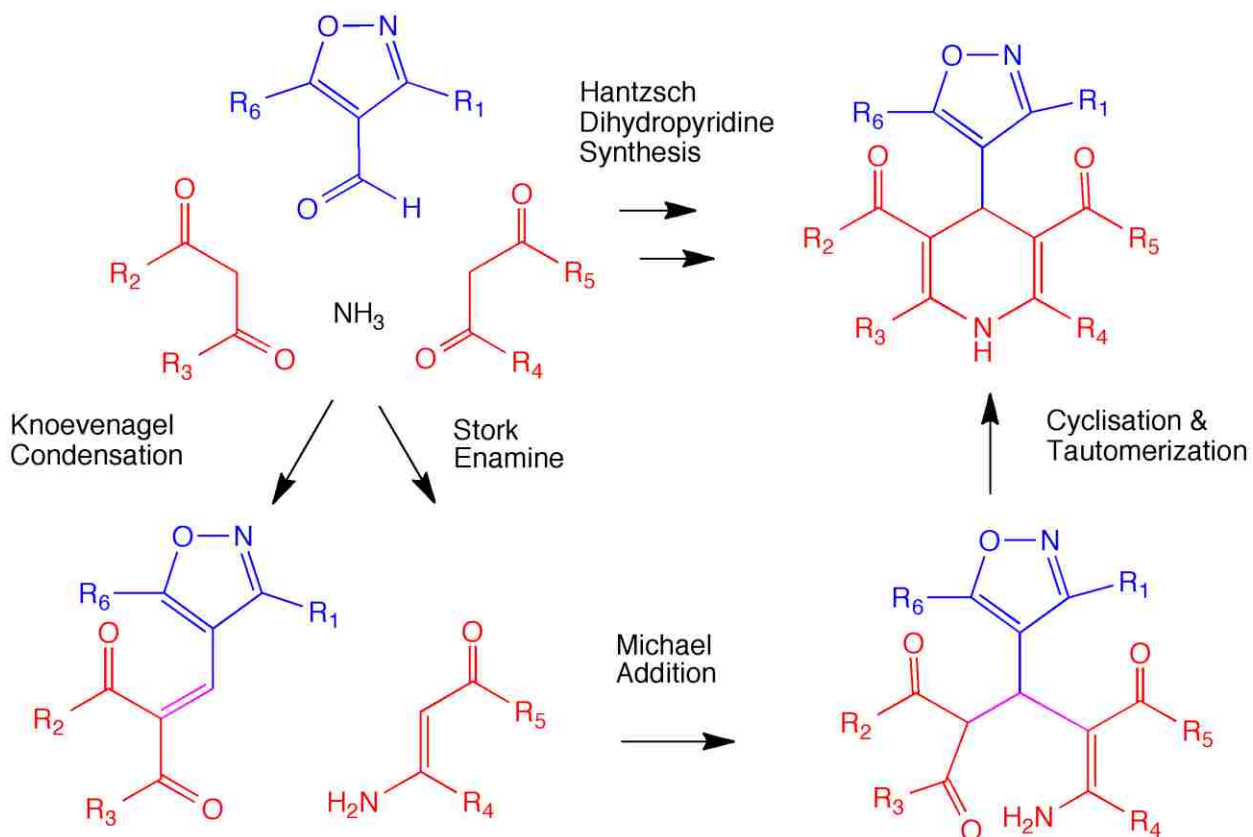
Figure 1.2. The Isoxazole version of the Hantzsch pyridine synthesis.

To address issue of conformationally diverse structures, our main entry into highly

substituted isoxazoles involved primarily (1) the nitrile oxide cycloaddition (exemplified

in the work of Mirzaei, Figure 4.C.) and/or (2) lateral metalation and electrophilic

quenching (Figure 3).

One method we have developed for regioselectively elaborating the functionality

of isoxazoles is lateral metalation and electrophilic quenching (LM & EQ), [24, 47-51, 53]

which has provided many of the branched isoxazoles useful for probing SAR (Figure 3).

The metalation of isoxazoyl-oxazolines was acomplished with n-butyl lithium, and clean

mono-incorporation of electrophiles can be obtained in excellent yields (Figure 3). the

deprotection is accomplished by N-methylation of the oxazoline nitrogen, followed by

hydride reduction, which after mild aqueous hydrolysis affords the aldehyde. The

Hantzsch synthesis is best performed under pressure when the groups on the isoxazole are large.
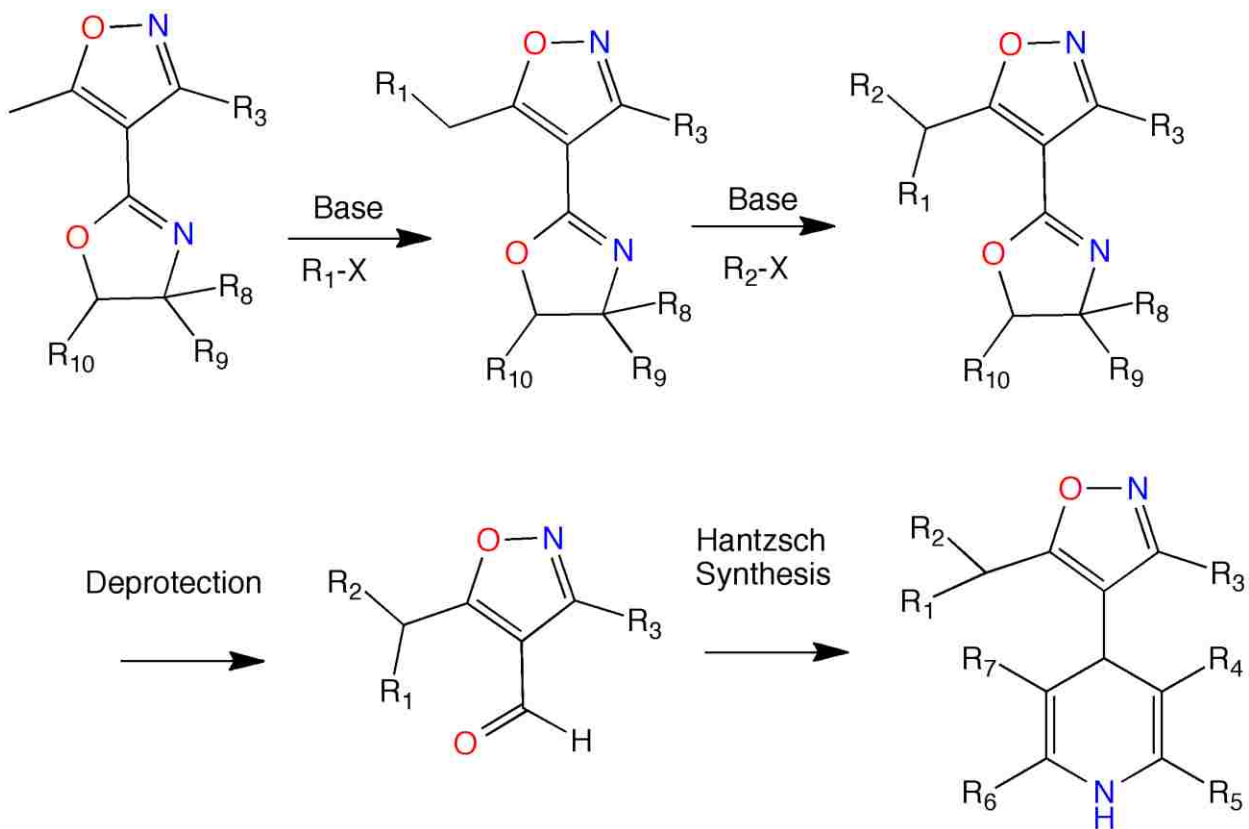
Figure1.3. Lateral Metalation and Electrophilic quenching is a selective route to substituted isoxazoles, and hence IDHPs. [24, 46-51, 53]
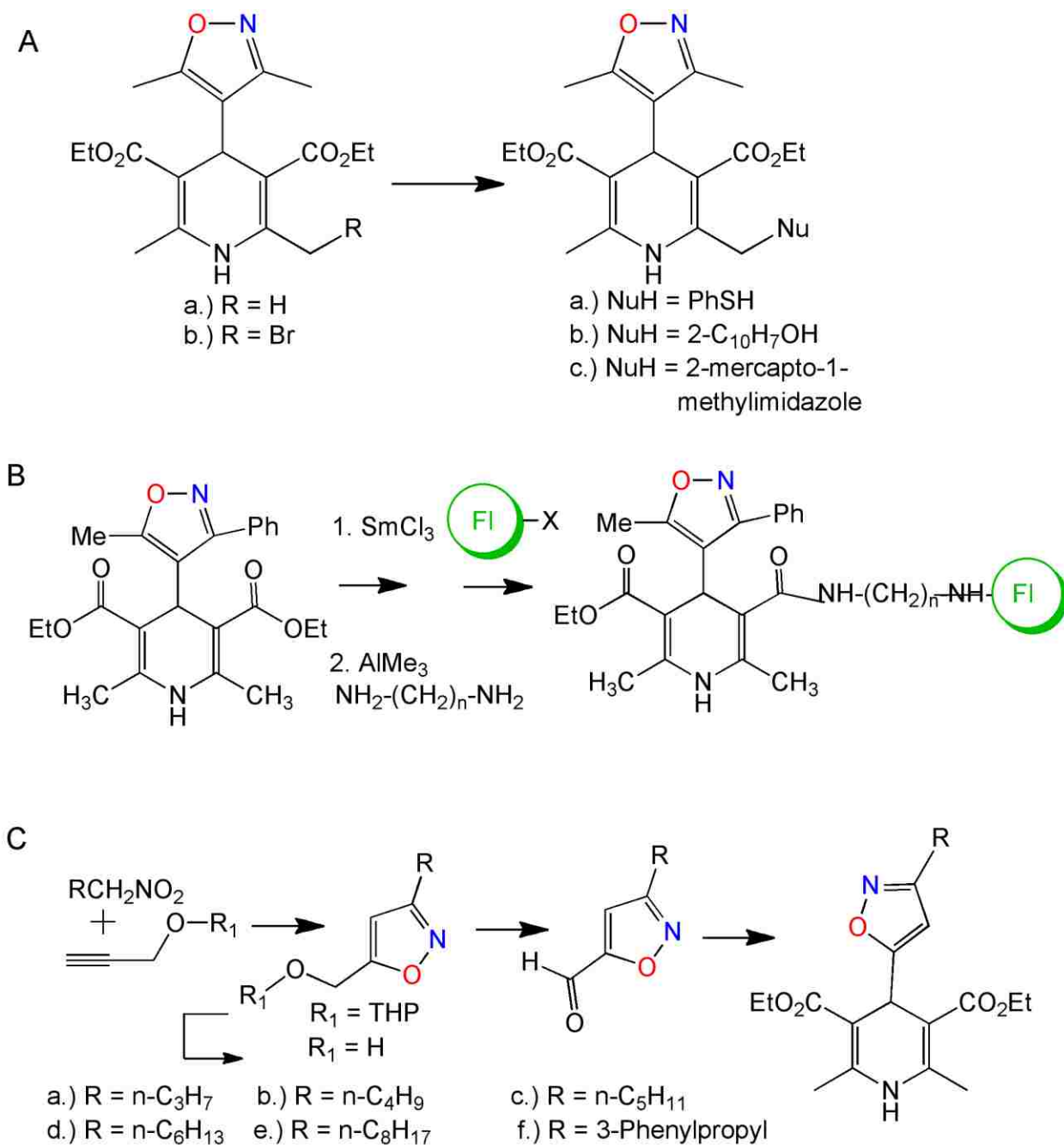
Figure 1.4. A. Mirzaei route to IDHP C-2 functionalized products, analogous to amlodipine. B. Lanthanide double activation amidation of Hantzsch esters. Compound 4-18 in Table 2 is n=8, Fl = Dansyl [54]. C. Mirzaei's example of a NOC *click* route to isoxazole carbaldehydes [57].

Mirzaei's group brominated the DHP moiety selectively as an entry into IDHP analogs similar to amlodipine (Figure 4.A) [57]. The 3- and 5- esters of the DHP are cross-conjugated vinylogous urethanes, and hence quite unreactive. We found it was necessary to apply our lanthanide accelerated Weinreb amidation to obtain amides (Figure 4.B), which were then further functionalized to allow for the attachment of fluorophores.[54]

Among the common methods for regioselective isoxazole synthesis is the nitrile oxide cycloaddition (NOC), which Folkin and Sharpless included among "Click" reactions,[61, 62] and is the subject of several excellent reviews.[19-22, 63] The use of the NOC is exemplified in Mirzaei's approach to IDHP (5) (Figure 4.C.), from isoxazole-5-carbaldehydes.[57]

1.7 **Conformational Analysis of IDHPs**

Conformational correlations from small molecule crystallography have proved of interest in scaffold hopping,[64] and serve as a useful starting point for understanding the biological efficacious topology. The sweep volume of rotation about the bond between the heterocyclic rings in isoxazol-4'-yl DHPs (Figure 8) is dramatic, and one of the main contrasts with the corresponding 4-aryl DHPs. As the groups on the C-3' and C-5' position of IDHP (4) are substituted with branched or progressively larger aromatic rings, the trend in the single crystal structure is for the larger group to orient over the DHP ring in the unit cell (Table 1, entries 4-4 through 4-12), so that the plausibility that this more compact arrangement arises from crystal packing forces must be considered. Therefore we have examined solution nuclear Overhauser effects, and variable temperature studies

12

to ascertain the presence of rotation at the heterocyclic ring juncture, and estimated the

energy of this process using a variety of computational methods.
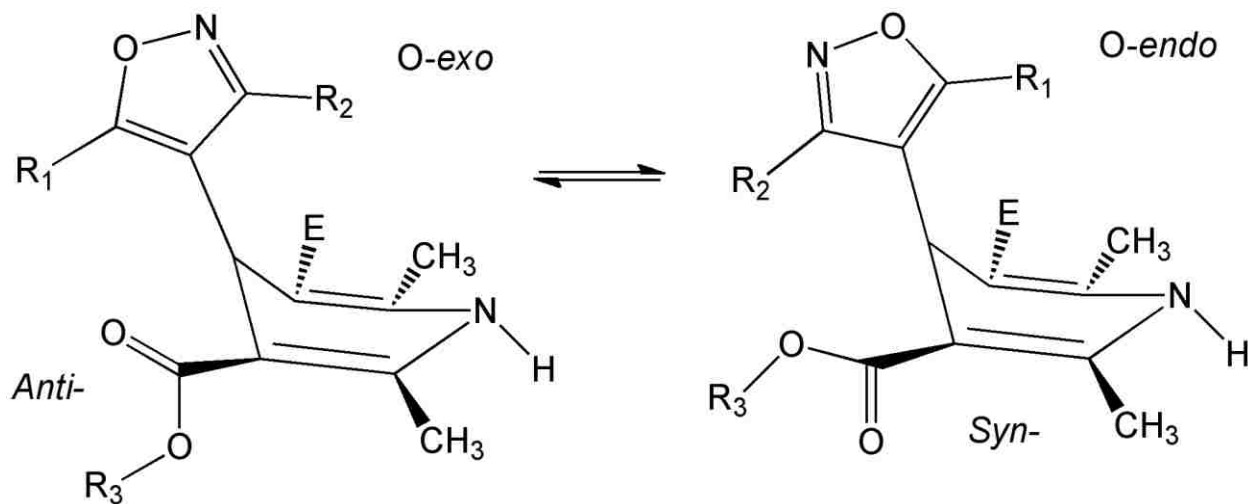
Figure 1.5. Conformation dynamics in type 4 IDHP. The numbering for R_1, R_2 and R_3 are

used in Table 1. E represents an ethoxycarbonyl group.
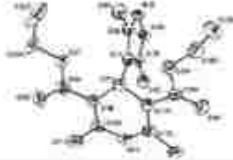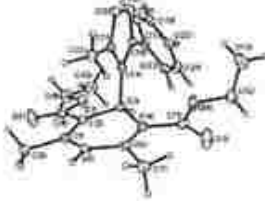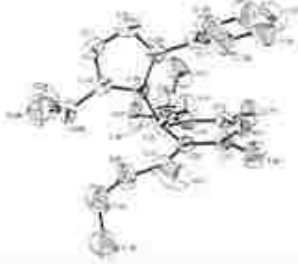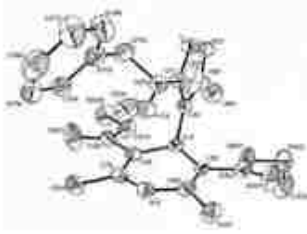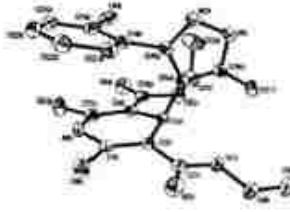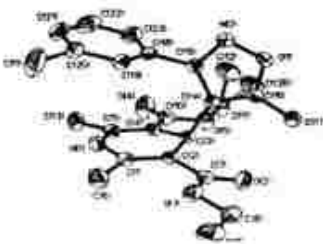
The IDHP 4-1 [35] crystallizes in the O-*endo*, and *syn-* ester conformation (Table

1) [42], however, nOe studies demonstrated that both conformations occur in solution at

room temperature, and MM2 calculations suggested a barrier to rotation on the order of

the cyclohexane chair to chair interconversion. Substitution of the C-3' methyl for a

phenyl (4-2), and the C-5' methyl for ethyl (4-3) resulted in similar O-*endo* solid state

conformers, however, branching at C-5' in the form of an isopropyl resulted in

conformational flip at the juncture of the heterocycles to O-*exo* (4-4).
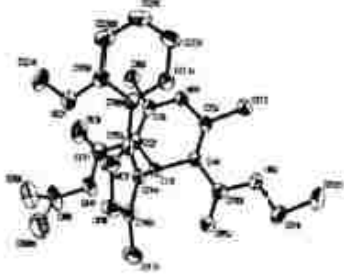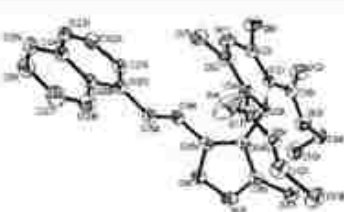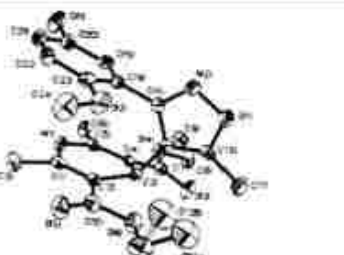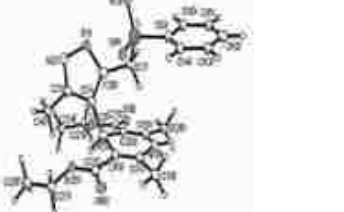
With further substitution on the C-3' aryl (entries 4-6 to 4-9, 4-11), or branching at C-5'

containing an aryl moiety (entries 4-5, 4-10, 4-12), crystallography has revealed that

compact packing in the solid state, where the larger group on the isoxazole orients above

the DHP, appears to be the major factor influencing conformation. Together with Palmer

and Andersen, [45] our group examined the solution dynamics at the heterocyclic ring for 4-8 and related IDHPs, and the barrier for rotation was found to be below the temperature attainable at physiological conditions.

The fluorophore IDHP conjugate (4-18) was found to exist almost exclusively as a folded conformation after chromatographic isolation, as evidenced by NOE. Variable temperature studies indicated that the conformation equilibrated to an extended conformation on warming, and that this conformation persisted.

JDHP	R₃	R₅	R₄	Ring junction	Ester conformer	[?]₀	VGCC K_i (nM)	VGCC patch clamp (µM)	ORTEP	Ref.
4-1	Me	Me	Et	O-endo	sp,sp	65.5	27.1	8.1		[45]
4-2	Me	Ph	Et	O-endo	sp,sp	65.7	13.9	–		[39]
4-3	Et	Ph	Et	O-endo	sp,sp	45.4	–	–		[41]
4-4	i-Pr	Ph	Et	O-exo	ap,sp	72.6	417*	–		[41]
4-5	1-Ph-2-yl-Pr	Me	Et	O-endo	sp,sp	–	(+) 3.7 (-) 210	–		[44]
4-6	Me	2-Cl-Ph	Et	O-exo	sp,sp	63.4	–	9.68		[51]
4-7	Me	3-Cl-Ph	Et	O-exo	sp,ap	56.7	–	1.98		[53]

IDHP	R₁	R₂	R₃	Ring junction	Ester conformer	[O]p	VGCC K_i (nM)	VGCC patch clamp (μM)	ORTEP	Ref.
4-8	Me	4-F-Ph	Me	O-exo	sp,sp	66.9	–	2.7		[44]
4-9	Me	2-OCH₃-Ph	Et	O-exo	sp,ap	60	–	17.1		[55]
4-10	1-naphth-CH₂CH₂	Me	Et	O-endo	sp,sp	71.5	4.1	0.47		[47]
4-11	Me	2-MeO,5-Cl-Ph	Et	O-exo	sp,ap	–	–	6.86		[57]
4-12	PhSO₂CH₂	Me	Et	O-endo	sp,sp	–	1000	–		[48]

*Weak vasodilator in the Langendorff perfused heart assay.
*Lacked nifedipine's negative inotropic activity in Langendorff assay.
ap: Antiperiplanar to the dihydropyridine double bond with respect to carbonyl group; DHP: bisacyloyl-dihydropyridine; sp: Synperiplanar to the dihydropyridine double bond with respect to carbonyl group; VGCC: Voltage gated calcium channel.

Table 1.1: Crystal structrues of IDHPs

1.8 Antagonists at the Voltage Gated Calcium Channel

Triggle had enumerated several germane issues in the SAR of the VGCC which suggested that the IDHPs could be of advantage. [28, 30] Therefore, once we had IDHPs in hand, we sought to examine their solid state structure to determine whether they had the required stereoelectronic characteristics. The IDHPs adopt a shallow boat conformation in the solid state often associated with robust calcium antagonists. The substitution at the 3'- and 5'- position of the isoxazole gives rise to dramatically different topologies arising from rotation at the bond connecting the heterocyclic rings, and represented an opportunity to explore conformational and configurational aspects of SAR.

1.9 Aryl DHPs and their SAR at the Calcium Channel

The 1,4-DHPs have been utilized in general medical practice to treat cardiovascular disease. Nifedipine was the first calcium channel antagonist approved for clinical use as an antihypertensive. The success of nifedipine led to its use as a lead compound and in turn gave rise to an increased interest in the DHP class of molecules. Using nifedipine as the prototypical 4-Aryl-1,4-DHP the development of numerous derivatives have been produced that showed superior bioavailability, a slower onset and longer duration of action. [65] The SAR which has developed in this area, as summarized in several excellent reviews by Triggle and colleagues, is useful due to its power to predict drug activity.[66-68] Optimal antagonist activity is obtained when C3 and 5 positions of the DHP are substituted by ester groups. The C4 position is optimally occupied by a phenyl ring with a *meta-* or *ortho-* electron withdrawing groups, with 2,3-disubstitution tolerated and which can be incorporated as part of heteroaromatic rings. [69]

The 1,4-DHP ring itself is essential as N-substitution, reduction to the piperidine, or oxidation to the pyridine ring system will greatly decrease or completely abolish activity, *via* removing the potential hydrogen bonding interaction with the calcium channel. Additional modification to the C3 and 5 substitution also can modulate activity and tissue selectivity. It has been observed that electronic features of the oxygen of the carboxyl ester influenced biological activity, due to the likely event that the carbonyl oxygen participates in hydrogen bonding with the calcium channel receptor.[70] The preferential orientation that is adopted is in the plane of the DHP ring itself with smaller variations being observed between $30\text{-}60^0$ from planarity. Additionally the syn or anti periplanar orientation of the carbonyl groups is another key factor for activity it has been suggested that syn-periplanar carbonyl groups might be a common feature of DHP calcium channel antagonists,[12, 71-73] and an anti-periplanar conformer associated with agonist activity.[59,70] When there are non-identical esters at the C3 and 5 position the C4 carbon is then chiral, and chirality of the DHP is one of the key distinguishing factors between antagonist and agonist activity. The (S) enantiomers are activators and bind the open state of the channel, where the (R) enantiomers are antagonists and bind the inactive state of the channel.[74-77]

1.10 IDHPs and their SAR at the Calcium Channel

The attachment of an isoxazole onto the DHP introduced a number of structural features that diverge from the 4-Aryl-1,4-DHPs,[12, 28-31, 78,79] yet presented the opportunity to weigh the importance of stereoelectronic effects in the SAR. The combination of the isoxazole scaffold with the DHP has been shown to give rise to robust activity at the VGCC, while lacking pronounced negative ionotropic activity of some DHPs. [38, 40, 42]

Similar to the 4-aryl DHP, the 1,4-IDHP system requires the DHP ring for activity, and the relative conformation of the 4-aryl substituents in significant. Roynyak, Andersen and co-workers[80], Goldman and Geiger [81] and Berntsson and Carter [82] performed NMR investigations which supported a preferred solution equilibrium conformation in which 4-aryl substituent is in a pesudoaxial orientation perpendicularly bisecting the plane of the 1,4-DHP. We have referred to the conformation at the juncture between the DHP and 4-isoxazolyl substituent as O-endo and O-exo (Figure 8), to readily distinguish this conformational feature, and groups at the 3'-and 5'- of the isoxazole describe a large sweep volume as rotation takes place about the 4,4' ring juncture. While in several cases the 3'- aryl or 5'-arylethyl group on the isoxazole crystallized with the aryl group over the DHP (Table 1), in each case studied by NMR it was revealed that facile rotation about the heterocyclic ring juncture was present. With studies on 1,3-benzothiazocines Baldwin et al [83] convincingly ruled out boat to boat interconversion for DHPs, and favored the exo geometry of the 4-aryl substituent with respect to the DHP moiety. Examination of over 30 crystal structures of DHPs lead to two molecular features that highly correlated with biological activity. These are termed $\sum |\rho| \square$ and $\sum |\tau|$, which refer to the extent of 1,4-DHP ring pucker as measured by the sum of the six intraring torsional angles, and the forward presentation of the 4-aryl ring, respectively. As observed in single crystal X-ray diffractometry, the more active IDHPs usually possessed extremely flat boats, and the subsequent forward presentation of groups in the 3'- or 5'- isoxazole position was greatly accentuated.

At the time we initiated our studies it was recognized that unsymmetrical ester groups in DHP calcium antagonists, which gave rise to a chiral center at C(4) of the DHP,

exhibited pronounced enantioselectivity of action. We set out to determine if chirality at the isoxazole would have the same effect. The (+)-1-phenylprop-2-yl group, assigned as (R)-, was indeed the eutomer with a pronounced eudisimic ratio (R/S 56.7), and was a robust antagonist with single digit nanomolar binding affinity (3.7 nM) [43]. These results were emerging as additional information became available about the calcium channel's primary sequence, and our initial modeling of the DHP binding subunit lead to a prediction of a potential lipophilic pocket, and exploration of a series of analogs to test that hypothesis [46]. The appearance of Mackinnon's landmark single crystal structure of the potassium channel allowed for homology modeling (Figure 9A), and a rational explanation for the unique SAR of IDHPs [52] (Figure 9B). An interesting issue described in this study is that docking of the IDHPs in the conformation found in the small molecule x-ray gave no SAR distinction, and VT NMR indicated that ready conformational adaptation to the receptor must occur.
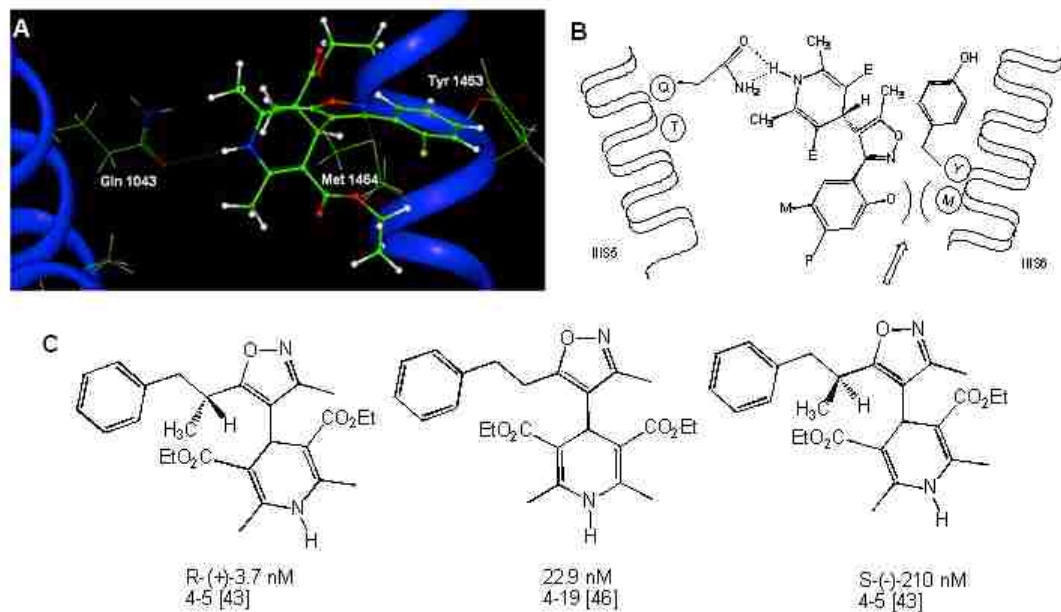
Figure 1.6. A. Homology model of the VGCC with docked IDHP, based on the MacKinnon potassium channel single crystal structure, pdb accession 1BL8 [52,84]. B.

Schematic summary of the unique SAR of IDHPs [52]. C. The methyl effect in SAR of

IDHPs (4)

1.11 Multidrug resistance

Chemotherapy is often complicated by drug efflux from tumor cells. One major

factor is the multidrug resistance transporter, known to be over expressed in several

tumor cell types. DHPs have been known for some time to be either competitive alternate

substrates or inhibitors of MDR-1, which in either case can give rise to reduced efflux of

cancer chemotherapeutics. Intensive efforts continue to be directed towards DHP

modification, as resistance is a serious problem. The MDR-1 is a large and complicated

protein with multiple documented and postulated binding sites for xenobiotics. We

considered the possibility that the chemistry we had developed for selective

functionalization of isoxazoles could be applied to enhance MDR selectivity at the

expense of the VGCC. There have been a number of compounds that have been identified

as MDR1 inhibitors.[32-34] The majority of these novel compounds that are known to

inhibit MDR1 have not yet advanced to being utilized in the clinic due mainly to severe

side effects and lack of selectivity. Nevertheless, reversal of multidrug resistance is of

widespread clinical interest and multidrug-resistance reversers (MDRR) are currently

under intensive investigation. Given MDR1's involvement in MDR it is a viable drug

target for the reversal of MDR.

First-generation inhibitors such as cyclosporin A, and verapamil suffered from

unacceptable high toxicity, and were dropped as potential inhibitors after phase II clinical

trials . The second-generation agents: valspodar, and biricodar have better toxicity

profiles, but showed cross reactivity and unpredictable pharmacokinetic interactions with

other transporter proteins . Third-generation inhibitors such as tariquidar (XR9576), zosuquidar (LY335979), laniquidar (R101933), and ONT-093 have high potency and specificity for MDR1. The structures for the known inhibitors of MDR1 are shown in Supplementary Material Figure SM-1. The pharmacokinetic studies to date have shown no significant interactions with CYP450 3A4 drug metabolism and no clinically significant drug interactions with common chemotherapy agents . The prevalence of MDR1 expression in several tissues is proving to be a major issue when considering side effects of potential inhibitors. It is for this reason that most MDR1 inhibitors have had sub-optimal results in clinical trials.

1.12 DHPs and Current treatment in MDR

With Verapamil being used as the first calcium channel blocker to advance to clinical trials for its ability to reverse MDR [85], with the compounds failing out due to high cardio toxicity and unsatisfying clinical outcome [86]. Further exploration in this area resulted in Nifedipine going through clinical trials. Clinical trials failed for similar reasons to verapamil, with response being poor and high toxic cardiovascular side effects being the main reason for not proceeding through clinical trials.

With suboptimal result being observed in clinical trials, leads to the development of new DHP derivatives with the expressed goal to first increase the MDR reversing activity and second to decrease the significant of the calcium channel blocking activity. While there are a number of variations that can be introduced to the DHP structure the most promising modification are the eudismic ratio that is seen in calcium channel SAR. The distomeric enantiomer of the DHP has been shown to have the same MDR reversing activity, while the calcium channel blocking effect are much weaker [87]. Further research

in this area confirms that MDR1 inhibition is independent of the calcium channel activity, where the enantiomers of niguldipine exhibit varying calcium antagonism but showed similar MDR activity [88-89]. Thus, structural modifications can be made to produce a more active MDR revering agent. The independent action of MDR reversing action and the calcium channel activity allow for more refinement of structure to produce more active compounds, making the DHP one of the most appropriate ring system to develop around to produce more active MDR reversing activity with minimum adverse effects.

To this end, the examination of derivatives of DHP has been shown to be effective MDR reversing agents, with some compounds currently in clinical trials. Most of the more successful compound that are being reported are compounds that have common structural features, with the addition of pyridyl groups on the C3 and 5 positions being a common theme. [90-91] With other studies making modification to the C3 and C5 removing the ester functionality, thus reducing calcium channel activity and maintain MDR activity [92]. The C4 position is another potential site of modification, heterocyclic aryl have been shown to both reduce calcium channel activity and increase MDR activity, but also introduced toxic side effects in animal models[93-94].

Zhou, Coburn and Morris chose to take existing lead compound such as dexniguldipine and make derivatives based on structure optimization for MDR1 and breast cancer resistance protein MDR. [95-97] In an effort to improve on the concept our research group have made novel 1,4-IDHP derivatives and have had promising results concerning MDR1 inhibition [53, 54]. The research in this area is developing and the implementation of the known privileged structures has been prevalent, and has become a useful strategy for drug development. 4- Isoxazolyl-1,4-dihydropyridines (IDHP) have

23

been known to bind L-type voltage gated calcium channels, and dihydropyridines

(DHPs) have been in general medical practice for use as anti-hypertensive agents for

decades[97], and as such the DHPs has been recognized as a privileged scaffold found in

medical chemistry [98]. More recently however, the DHP scaffold has been recognized as

a substructure to design around to produce MDRRs.[32, 93, 100-102] Given that the clinically

used DHPs such as nicardipine and niguldipine are known ligands for MDR1. [102-103]
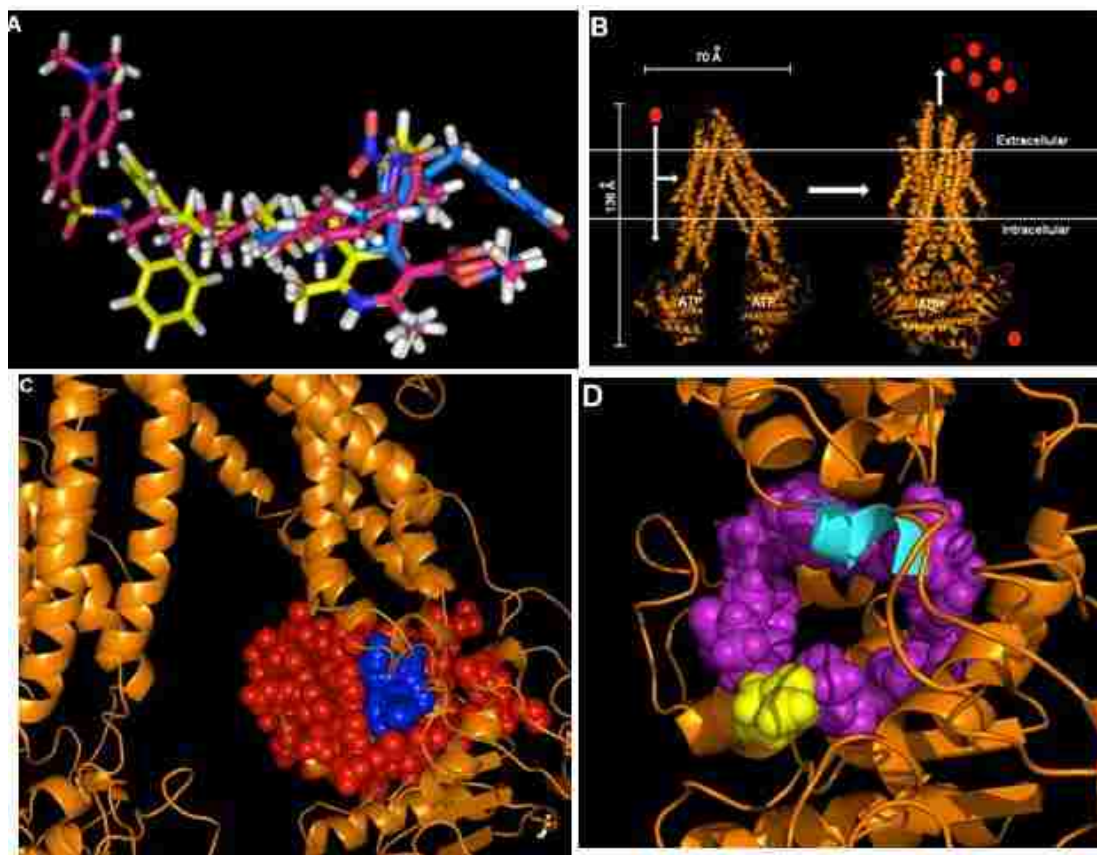
Figure 1.7.A.: An overlay of minimized niguldipine (gold) and novel IDHPs, containing a

branched C-5 (4-16) (blue) and tethered dansyl (4-18) (salmon), indicating analogous

functionality and topology [53, 54]. **B**. Left is our homology model based on the open

conformer of MDR1, based on *Mus musculus* pdb accession 3G5U, on the right is our

human homology thread with sav1866 pdb accession 2ONJ. The binding sites of interest

are known as the DHP binding site resides near the NBDs (Labeled with ATPs). This is

thought to be the general area in which the putative IDHP binding site is located. The

horizontal lines represent the approximant position of the lipid bi-layer. **C,** the DHP

photoaffinity binding site (red) and the Q-site predicted binding site (blue), **D.** The

overlapping amino acid sequence (purple) from the photoaffinity binding site and the Q-

site binding site. The location of Q475 (gold) a Mg^{2+} binding residue proximal to the

ATP binding and hydrolysis sequences. The sliding helix 2 sequence (F904 - L910)

shown in cyan is critical to MDR conformational dynamics in xenobiotic efflux.

The constructionof a common pharmacophore model (Figure 11) to visualize

common structure features to direct synthetic efforts towards more valid analogs. Figure

11 shows clinically used 1,4- dihydropyridine niguldipine (pink), and two IDHPs. The

spatial conservation of the function groups is apparent, the most apparent difference

being the conformationally unique structure that the isoxazole moiety imparts to the

IDHP. The IDHP allows for novel and structurally divergent compounds to expand the

library of compounds which have previously been studied, which in turn could

potentially allow for corresponding divergent and novel pharmacology.

To further study the effect of IDHPs as MDRRs on MDR1 and to aid in further

analog development a binding box for IDHP was needed as a working hypothesis. Given

that MDR1 has a large number of potential substrates we chose to focus our efforts on

initial characterization of the IDHP binding site. The characterization of the DHP site

was first attempted by using domain mapping experiments [104]. Domain mapping studies

in combination with immunoprecipitation were utilized to identify the DHP binding site

25

[104]. Other studies[106] have been performed with photo labeled DHP derivatives, the studies showed binding at two major regions, one in each half of the protein[108]. This suggested that the DHP derivatives bind to both NBDs.

To define the DHP binding site a niguldipine was chemically modified with a photoaffinity label which replaced the nitro group of niguldipine with an azido group. Photolysis of the modified DHP was carried out in the presence of MDR1. The protein was then identified via PAGE-SDS gels and purified via lectin affinity chromatography [107]. Western Blot analysis was carried out using monoclonal anti-MDR1 antibody C219. The pooled samples of niguldipine bound protein were then analyzed via Matrix-assisted laser desorption/ionization (MALDI). Edman degradation combined with MS revealed the amino acids that compose the labeled site. The final localization of the niguldipine binding site in MDR1 was found to be correspond to the sequence 468-527, this is in agreement with the previous immunoprecipitation experiments that showed the dexniguldipine binding site in the N-terminal or the cytoplasmic half of MDR1 [109]. In other proposed structural model of MDR1 the niguldipine binding site is also in the cytoplasm assigned to the sequence 491-526 [110]. The results suggest that this region is near the N-terminal NBD this indicates that the chemo sensitizer binding site and ATP binding domains interacts with each other. It is known that the drug binding site and ATP hydrolysis are coupled [111]. Observing that both sequences are closely related to one another is evidence that this is a reasonable consensus binding sequence.

Many studies have attempted to localize the drug-receptor binding site and key amino acid residues responsible for the interaction of MDR with its ligands. Studies of

ligand–ligand interactions on MDR1 revealed that some ligands interact as single

molecules, whereas others show cooperativity [112].

As mentioned above MDR1 contains multiple sites, distinct sites for transport of

rhodamine 123 (R-site) in addition to a modulatory site for prazosin and progesterone [113,

114]. Binding of ligands at one of these transporters site enhances the interaction at the

others. Equilibrium binding studies on MDR1 provided evidence for three sites for

transported ligands (vinblastine, pacitaxel, and rhodamine), which can interact with

ligand in the absence of externally added nucleotides, in addition to a modulatory site for

niguldipine/GF120918 [115]. The observation that there could be similarities in both the R-

site and the DHP binding site, which could allow for this cooperation and communication

to occur that could cause the conformational changes and allow MDR1 to function. Given

the previous research on the binding of DHP a computer model was used to produce a

refined ligand binding box.

1.13 IDHPs and MDR: towards a working hypothesis

To generate a testable hypothesis for binding at the DHP binding site, computer

modeling was employed. At the time that we initiated out studies an MDR1 human

crystallographic structure did not exist, so a homology model was constructed from the

published X-ray crystal structure *Mus musculus* (pdb accession number: 3G5U) a close

homolog of the human ABC transporter MDR1. A sequence homology was then

performed between the known human MDR1 sequence and the 3G5U followed by

threading of the known human MDR1 sequence into the published X-ray crystal

structure. As explained above the binding site for the DHP has been broadly defined as

the resides 468-527.To avoid any bias in further defining the DHP binding site, the

MDR1 human homology model was submitted as the entire MDR1 transporter to the Q-

site finder online server .
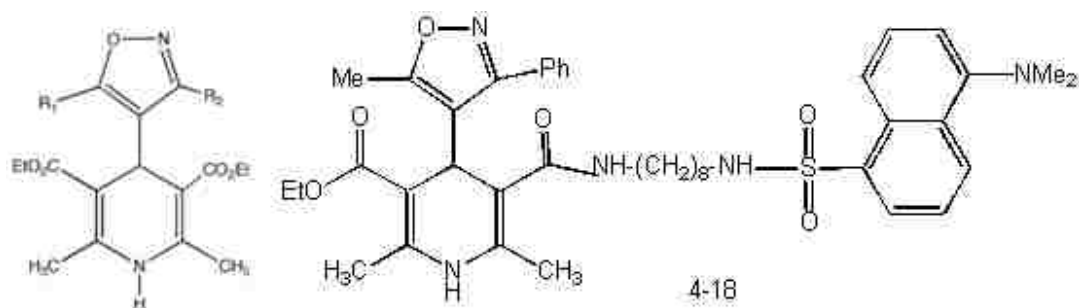
Figure 1.8.General Structure of IDHPs used for Table 2.

IDHP	R_1	R_2	MDR1 (% inh.)	Reference
4-2	CH_3	C_6H_5	48.9	53
4-4	i-Pr	C_6H_5	38.4	53
4-6	CH_3	o-Cl-C_6H_4	10.9	53
4-7	CH_3	m-Cl-C_6H_4	26.8	53
4-9	CH_3	o-MeO-C_6H_4	32.8	53
4-10	1-naphthyl CH_2CH_2	CH_3	19.0	53
4-11	CH_3	2-MeO-5-Cl- C_6H_3	15.0	53
4-13	CH_3	p-Cl-C_6H_4	11.7	53
4-14	$C_6H_5CH_2CH_2$	C_6H_5	27.6	53
4-15	p-Biphenyl- CH_2CH_2	CH_3	18.6	53
4-16	m-Br-$C_6H_4CH_2$	CH_3	61.2	53

	(CH$_3$)CH			
4-17	1-naphthyl CH$_2$(CH$_3$)CH	CH$_3$	38.3	53
4-18	CH$_3$	C$_6$H$_5$	63	54

Table 1.2 IDHP activity at MDR-1, data provided by NIMH PDSP.

MDR1 screening and the establishment of MDR1 inhibition activity was performed by the Psychoactive Drug Screening Program (PDSP) of the NIMH. The assay was performed using live Caco-2 cells, a cell line derived from human colonic epithelium cell that express MDR-1[39]. The assay uses Calcein-AM which passively diffuses in to the cell, after which it is hydrolyzed turning the compound fluorescent and adding a negative charge thus trapping the compound in the cell. Calcien-AM can be effluxed out of the cell via MDR-1, thus MDR-1 inhibition is a function of the fluorescence that is observed. Fluorescence is measured using a FlexStation II fluorimeter in a 96 well plate after preincubation with the given IDHP (50µM for 30min). After which calcein-AM was then added to a final concentration of 150 µM. Fluorescence was then monitored over 4 minutes, with each assay performed in quadruplicate, with 25 µM cyclosporine used as a control. The value of untreated control cells where taken as 0% inhibition and the slope of the fluorescene is normalized taking the value of cyclosporine at 100%.

With MDR binding data in hand, the IDHP structures were drawn and energy minimized using the Sybyl modeling program[54]. Ligand-receptor ensemble structures were virtually docked into an *in silico*-activated MDR1 human homology model, followed by energy minimization, molecular dynamics, and a final energy minimization simulation,, using the program GOLD and scored using GOLD Score with default

settings. Aggregates for molecular dynamics and minimization simulations were defined as residues within 6 Å from the ligand. Binding was localized near the GLN 475, one of the amino acids also at the interface of the overlapping photoaffinity binding (red in Figure 7.C) and the Q-site finder amino acids (R467, I470, G471, V472, V473, S474, Q475, E476, P477, V478, L479, F480, Y490, G491, blue in Figure 7.C). From this analysis three binding site cohorts were defined from the library of IDHPs in Table 2.

The low affinity cohort consisted of compounds 4-6, 4-11 and 4-13 that were bound on the outside of the overlap region of the photoaffinity site and Q-site finder calcualtion, in the vicinity of the Nucleotide binding domain (Shown in Figure 7.D), and never achieved more than 15% MDR-1 inhibition (Table 2). We have termed the medium affinity cohort the compounds 4-10, 4-15 and 4-17. Compounds 4-10 and 4-15 were bound in the same location adjacent to the edge of the consensus binding box and never achieved more than 19% MDR-1 inhibition (Table 2). The branched 4-17 on the other hand, bound bridging the high affinity cohort, this would explain the relatively high 38% MDR-1 inhibition that was observed. We have termed the high affinity cohort compounds 4-2, 4-7, 4-9, 4-14 and 4-16, which are predicted to bind esentially in the Q-site finder domain. Compounds bound in this location had robust MDR-1 activity with a range from 27% to 61% MDR1 (Table 2). Most notably, compound 4-16 was the most active compound in our initial series, giving credence to the computational model as a predictive tool. To aid in further development of future generation MDRRs, 4-16 was selected and all interactions were examined in a 6 Å radius around the IDHP structure. The binding box interactions were then divided into regions to classify the overall interactions that permit robust binding, the purple amino acids that are shown in Figure

7.D represent the overlapping amino acids from the photoaffinity study (red) and Q-site (blue). The low, medium and high affinity cohorts are illustrated in more detail in supplementary material (Figure SM-2).
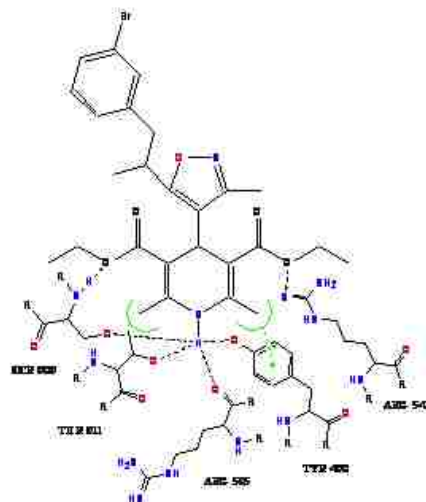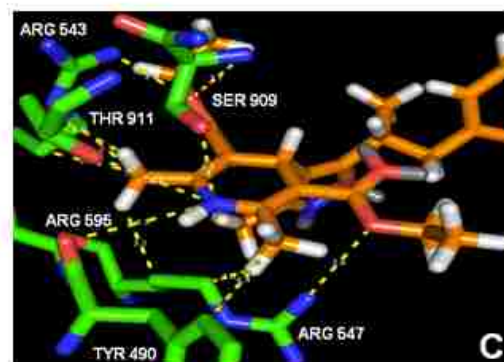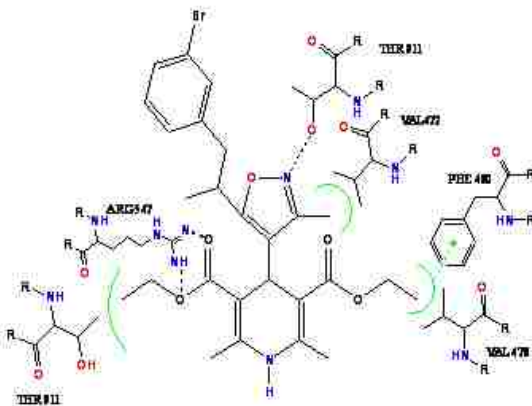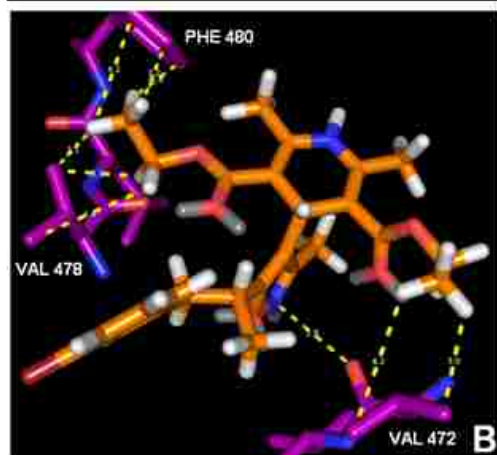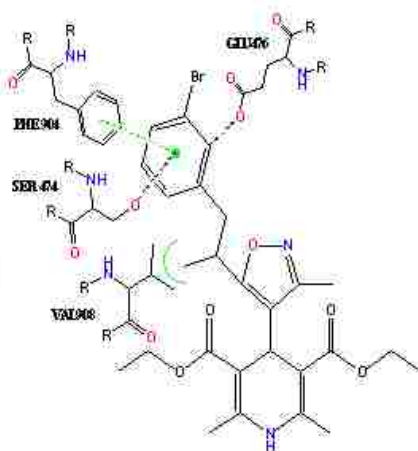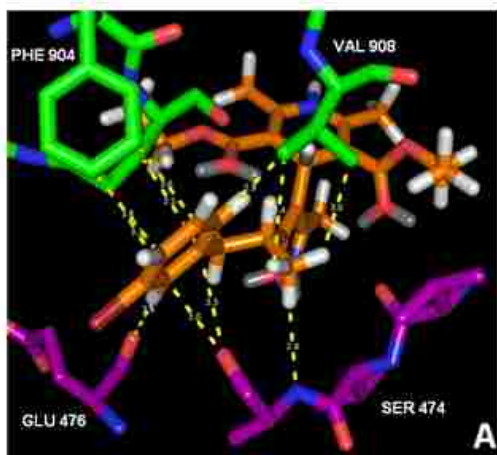
Figure 1.9. Generating a hypothesis: Homology model of human MDR-1 bound to IDHP ligand 4-16.A, Region 1 binds the C-5 isoxazole functional group of 4-16. B, Region 2 of Compound 4-16 includes an interaction with the isoxazole, C, 4-16 interactions with the DHP and esters.

Our homology model for MDR and docking studies with the IDHPs has generated our current working hypothesis, and is summarized in Figure **9**. A shows region 1 of compound 4-16 the majority of the interactions are lipophilic from Phe 904, Arg 905 and Val 908. There is also polar interaction that where are observed with the π cloud of the phenyl ring with residues Glu 476, Ser 474, and Val 472

Figure 9, B show region 2 of compound 4-16 there are lipophilic interactions on both the methyl groups by residues Phe 480, Val 478 and a polar interaction with Val 472 with the isoxazolyl.

Figure 9, C shows region 3 of compound 4-16 there are multiple interactions with the DHP nitrogen with the residues Ser 909, Thr 911 and Tyr 490, with additional polar interactions involving Ser 909, Arg 547 and Arg 543. This region also highlights a key anchoring point for the compound, the 1, 4-dihydropyridine substructure has been shown to be key in binding MDR1. Further analog development will be focused on conserving the 1,4-dihydropyridine substructure while altering other key structural factors in the series. In addition to the isoxazole anchoring interactions at the receptor, the spatial arrangement that is conferred via the inclusion of the isoxazolyl is novel and as such will be conserved in later analog development. The future IDHP analog development will focus on the modification of the topology of groups organized by the isoxazole.

1.14 Concluding remarks

Whether one terms the association of the isoxazole and DHP rings bioisosteric replacement, or scaffold hopping, substitution at the C-5 of the isoxazole gives rise to dramatically enhanced biological activity. In the case of the VGCC, a strategically placed methyl group produced a signifcant change with (R)-(+)-1-phenyl-prop-2-yl (3.7 nM) > Phenethyl (22.9 nM) > (S)-(-)-1-phenyl-prop-2-yl (210 nM), a eudismic ration of 56.7. This appears to be a classic example of the methyl [116] or methylation [117] effect. In the MDR-1 arena branching at the C-5 of the isoxazole produced an increase of binding of 25% (shown in Table 2), and replacing the DHP C-3 ester with a functionalized amide also lead to a dramatic increase in binding affinity. The lesson for the future is that a number of the isoxazoles in general medical practice bears an unfunctionalized methyl group, these are drugs with highly diverse molecular targets: sulfisoxazole, sulfamethoxazole, the oxacillins, glisoxepid, isocaboxazide, and paracoxib among others [123]. That an unadorned methyl is optimum for all biomolecular targets appears to be extremely unlikely, and it seems apparent that addition of even one methyl *in the correct critical position* should enhance activity in many cases. Our work represents an example of following the structure-based design path, even though that route was not always easy [123], and required improvement of existing methods and development of new chemistry. We suggest that numerous other opportunities for combined scaffolds, and strategically placed branching - including examples containing IDHPs - are waiting to be discovered in the future: because new biology is driven by new chemistry.

1.15 Future Perspective

Several distinctive features have emerged in delineating IDHP selectivity for MDR-1 verses VGCC, and these general trends (Figure 10) are illustrative of how a combination of scaffolds could be used to optimize selectivity. (1) While a 4-aryl or 4-heteroaryl is a requirement for the VGCC, alkyl groups have been tolerated at MDR-1. (2) The size of the 4-aryl at the VGCC has strict limits, for example *para*-substitution is known to lower activity whereas branching for MDR-1 dramatically enhances activity, and the limits of substitution here have only been touched on in studies to date, it is likely that additional lipophilic interactions are available at the transporter. (3) Esters of limited size are tolerated at the "Port" side of the VGCC, where amide substitution with a linked lipophilic group enhance MDR-1 activity. (4) Stereochemistry is critical at the VGCC, with R>>S in most cases, where the efflux pump - as expected - is not particularly picky. This opens the possibility for the use of the VGCC *distomer to enhance selectivity at the MDR-1*. (5) Substitution at the DHP nitrogen or oxidation to the pyridine is well recognized to abolish VGCC activity, whereas either is tolerated at MDR-1. Finally, it was established by Triggle [118] that dimerization of DHPs did not give rise to an increase in VGCC activity, while both the groups of Andrus [119] and Hrycyna and Chmielewski [120-122] have established that dimerization of MDR-1 substrates often produces more active inhibitors. A combination of these factors could well give selectivity that presently is unknown, and open the door for better theranostic candidates for multidrug resistance.

VGCC: Branching or Aryl Activity R > S

MDR1: Branching or Aryl Activity expected to show little or no stereochemical preference

VGCC: Aryl >> Alkyl

MDR1: Aryl ~ Alkyl

VGCC: Stereochemical Preference R > S for DHPs

MDR1: No Sterochemical Preference in DHPs

VGCC: Oxidation to pyridine abolishes activity

MDR1: Oxidation to pyridine shows no reduction of activity

VGCC: ester linkage to heterocycle is preferred, ester > amide

MDR1: amide linkage increases activity

Figure 1.10. Emerging SAR that allows for improvements in the Future Medicinal

Chemistry of IDHPs

1.16 Executive Summary

Introduction

- Privileged Structures or scaffolds include isoxazoles and 1,4-dihydropyridines

- The isoxazole structure was discovered by Claisen, and later found in nature and useful in drug design

- The 1,4-dihydropyridine (DHP) structure known since the work of Hantzsch is well recognized as the scaffold for the antihypertensives of the nifedipine class

- Representative connections of the heterocyclic rings in IDHPs

- 4',4-IDHP s and their intriguing conformational dynamics

IDHPs and their SAR at the Calcium Channel

- Triggle has described the SAR of Aryl DHPs

- Aryl DHP conformation likely relates to Ca^{2+} Channel activity

- IDHPs have characteristic conformational dynamics which significanty affect their topology

- We have developed a homology model for Ca^{2+} Channel activity of IDHPs which explains their unique SAR

IDHPs and MDR: towards a working hypothesis

- Current efforts to develop treatment for MDR are intensive

- Aryl DHPs and the attempts at MDR modulation have provided useful SAR insights

- IDHPs bind MDR and we have developed a homology model as our current working hypothesis

Future Perspective

- Reduction of VGCC activity in IDHPs in favor of MDR1 activity can be driven by known and emerging SAR

- Among intriguing factors is stereochemistry, VGCC usually have a pronounced eutomer, where MDR-1 is not particularly stereoselective, therefore the VGCC distomer could be used to select for the MDR-1.

- Current literature in dimers and MDR1 modulators suggests another promising avenue for future study

1.17 References

1. Silverman RB, *Organic Chemistry of Drug Design and Drug Action*, 2nd Edition, Academic Press, New York, (2004).

2. Brown N, Editor, *Bioisosteres in Medicinal Chemistry,* Mannhold R, Kubinyi H, Folkers G, Series Editors, Methods and Principles in Medicinal Chemistry, Vol. 54, Wiley-VCH, 2012.

3. Evans B, Rittle K, *et al*, Hirshfieldt J. Methods for Drug Discovery: Development of Potent, Selective, Orally Effective Cholecystokinin Antagonists. *J. Med. Chem.* 31(12), 2235-2246 (1988).

4. Bemis G, Murcko M. The properties of known drugs. 1. Molecular frameworks. *J. Med. Chem.* 39(15), 2887-2893 (1996).

5. Bemis G, Murcko M. Properties of known drugs. 2. Side chains. *J. Med. Chem.* 42(25),5095-5099 (1999).

6. Kelekota J, Roth F. Chemical substructures that enrich for biological activity. *Bioinformatics.*24(21), 2518-2525 (2008).

7. Hajduk P, Bures M, Praestgaard J, Fesik S. Privileged molecules for protein binding identified from NMR-bases screening. *J. Med. Chem.*43(18), 3443-3447 (2000).

8. Klabunde T, Hessler G. Drug design strategies for targeting G-Protein-coupled receptors. *Chembiochem.* 3(10), 928-944 (2002).

9. Matter H, Baringhaus KH, Naumann T, Klabunde T, Pirard B. Computational approaches towards the rational desing of drug-like compound libraries. *Comb. Chem. High Throughput Screen.* 4(6), 453-475 (2001).

10. Brown N, editor, *Scaffold Hopping in Medicinal Chemistry*, Mannhold R, Kubinyi H, Folkers G, Series Editors, Methods and Principles in Medicinal Chemistry, Vol. 58, Wiley-VCH, 2013.

11. Boehm H-J. Scaffold Hopping. *Drug Discovery Today: Technol.* 1(3), 217-224 (2004).

12. Triggle J. 1,4-Dihydropyridines as calcium channel ligands and privileged structures. *Cell Mol Neurobiol.* 23(3), 293-303 (2003).

13. Jacobson, K.; Kim, Y.; King, F. In search of selective P2 receptor ligands: interaction of dihydropyridine derivatives at recombinant rat $P2X_2$ receptors. *J. Auton. Nerv. Syst.* 81(3), 152-157 (2000).

14. Pevarello P, Amici R, Brasca MG, Villa M, Varasi M. Recent applications of isoxazole ring in medicinal chemistry. *Targets Heterocycl. Syst.* 3, 301 (1999)

15. Kubinyi H, Muller G, editors. *Chemogenomics in Drug Discovery: A Medicinal Chemistry Perspective*, Wiley, 2004, Figure 1.6, page 19.

16. Claisen L, Lowman O. Zur Kenntniss des Benzoylacetones. *Chem. Ber.* 21, 1149 (1888).

17. Hantsch A, Ueber die Einwirkung des Natriums auf auf Isobuttersaureather. *Justus Liebigs Ann. Chem.* 1, 249 (1888).

18. Baumann M, Baxendale IR, Ley SV, Nikbin N. An overview of the key routes to the best selling 5-membered ring heterocyclic pharmaceuticals. *Beilstein J. Org. Chem.* 7, 442–495 (2011).

19. Kochetkov NK, Sokolov SD. Chemistry of Heterocyclic Compounds: Isoxazoles, Part 1. *Adv. Het. Chem.* 49 (2)365 (1963).

20. Wakefield BJ, Wright DJ. *Adv. Het. Chem.*, 25, 147 (1979).

21. Lang SA, Lin Y-i. Comprehensive Heterocyclic Chemistry. Potts, K. T., Ed. Pergamon Press, NY 6, 1 (1984);

22. Grunanger P, Vita-Finzi P. "Isoxazoles", John Wiley & Sons, Inc. New York, 1990.

23. Pinho e Melo, TMVD. Recent Advances on the synthesis and reactivity of isoxazoles. *Current Org. Chem*. 9(10), 925-958 (2005)**.**

24. Natale NR, Mirzaei YR. The Lateral Metalation of Isoxazoles. A Review. *Org. Prep. Proced. Int*. 25(5),515-556 (1993)**.**

25. Hantzsch, A. Justus Liebigs. *Ann. Chemie*. 215, 1–82 (1882).

26. Eisner U, Kuthan J. Chemistry of dihydropyridines. *Chem. Rev.* 72 (1), 1–42 (1972).

27. Stout DM, Meyers AI. Recent advances in the chemistry of dihydropyridines. *Chem. Rev.* 82 (2), 223–243 (1982).

28. Triggle DJ. The 1,4-dihydropyridine nucleus: A pharmacophoric template. *MiniRev. Med. Chem.*3(3), 166–175 (2003).

29. Zamponi, G. *Voltage-Gated Calcium Channels*, Landes Bioscience, New York, 2005.

30. Triggle DJ, Langs DA, Janis, RA. Ca+2 channel ligands: Structure-function relationship of the 1,4-dihydropyridines. *Med. Res. Rev.* 9(2), 123-180 (1989).
This comprehensive review summarizes the SAR and stereoelectronic effects of the Calcium Channel activity of DHPs, and stands as a classic in the field

31. Natale NR. Learning from the Hantzsch Synthesis, *Chemical Innovation.* 30(11), 22-28 (2000).

32. Nogae I, Kohno K, *et al,* Gottesman M. Analysis of structural features of dihydropyridine analogs needed to reverse multidrug resistance and to inhibit

photoaffinity labeling of P-glycoprotein. *Biochem. Pharmacol.* 38(3), 519–527 (1989).

33. Gottesman M, Fojo T, Bates SE. Multidrug resistance in cancer: role of ATP-dependent transporters. *Nat. Rev. Cancer.* 2(1), 48-58 (2002).

It is difficult to select a single entry from Gottesman's monumental accomplishments in the MDR field, but this is a highly cited representative example

34. Gillet JP, Gottesman M. Mechanisms of Multi-drug resistance in cancer. Chapter 4 in Multi-drug Resistance in cancer. Methods in Molecular Biology, vol 596. Zhou J, Editor. Humana Press, 2010; 47-76.

35. Natale NR, Quincy DA, Neutral Dichromate Oxidations. Preparation and Utility of Isoxazole Aldehydes. *Synth. Commun.* 13, 817-822 (1983).

36. Shafu B, Amini M, Akbarzadeh T, Shafiee A. Synthesis and Antitubercular Activity of N3,N6 –Diaryl1-4-(5-arylisoxazol-3-yl)-1,4-dihydropyridine-3,5-dicarboxamide. *J. Sci. Islamic Republic of Iran.* 19, 323-328(2008).

37. Daryabari N, Akbarzadeh T, Amina M, Miri R, Mirkhani H, Shafiee A. Synthesis and Calcium channel antagonist activities of new derivatives of dialkyl 1,4-dihydro-2,6-dimethyl-4-(5-phenylisoxazol-3-yl)pyridine-3,5-dicarboxylates. *J Iran Chem Soc.* 4(1), 30-36 (2007).

38. Schauer CK, Anderson OP, Quincy, DA, Natale NR. Structure of 3,5-Dicarboethoxy-2,6-dimethyl-4-(3'-Phenyl-5'methyl-isoxazol-4'-yl)-1,4-dihydropyridine, A Calcium Antagonist. *Acta Crystallogr., Sect. C, Cryst. Struct. Commun. C42,* 884-886 (1986)

39. Knerr GD, Quincy DA, McKenna JI, Natale NR. The Mass Spectral Fragmentation of Isoxazolyl-Dihydropyridines. *J. Heterocycl. Chem. 24,* 1429-1433 (1987)

40. McKenna JI, Schlicksupp L, Natale NR, Maryanoff BE, Flaim SF, Willett, RD. Cardioactivity and Solid State Structure of Two 4-Isoxazolyl-Dihydropyridines Related to the 4- Aryldihydropyridine Calcium Channel Blockers. *J. Med. Chem. 31(2),* 473-6 (1988). [PMID: 3339618].

41. Kovacic P, Edwards WD, Natale NR, Sridhar R, Kiser P. Structure Calculations on Calcium Channel Drugs: Is Electron Transfer Involved Mechanistically? *Chem. Biol. Interactions.75(1)*, 61-70 (1990) [PMID: 2364458].

42. Natale NR, Triggle DJ, Palmer RB, Lefler BJ, Edwards WD. 4-Isoxazolyl-Dihydropyridines: Biological, Theoretical and Structural Studies. *J. Med. Chem. 33(8)*, 2255-2259 (1990) [PMID: 2142737].

43. Mirzaei YR, Simpson BM, Triggle DJ, Natale NR. Diastereoselectivity in the Lateral Metalation and Electrophilic Quenching of Isoxazolyl- Oxazolines. *J. Org. Chem. 57*, 6271-6279 (1992)

Chirality at the C-5 of the isoxazole in an IDHP exhibits a significant eudismic ratio

44. Balasubramaniam TN, Natale NR, Electrophilic Quenching of Dianions of 4-[5'-sulfonylmethylIsoxazolyl]-1,4-dihydropyridines. A Direct Route to Functionalized Hantzsch Esters. *Tetrahedron Lett. 34(7)*, 1099-1102 (1993).

45. Palmer RB, Andro TM, Natale NR, Andersen NH. Conformational Preferences and Dynamics of 4-Isoxazolyl-1,4-dihydropyridine Calcium Channel Antagonists as Determined by Variable Temperature NMR and NOE Experiments. *Magnetic Resonance Chem. 34*, 495-504 (1996)

46. Natale NR, Rogers, ME, Staples R, Triggle DJ, Rutledge A. Lipophilic 4-Isoxazolyl-1,4-Dihydropyridines: Synthesis and Structure Activity Relationship. *J. Med. Chem. 42(16),* 3087-3093 (1999) [PMID: 10447952].

47. Natale, NR, Niou C-S, A Facile Synthesis of Functionally Complex Isoxazole Derivatives. *Tetrahedron Lett*., 3943-3946 (1984)

48. Natale NR, McKenna JI, Niou C-S, Borth M, Hope H, Metalation of Isoxazolyloxazolines, A Facile Route to Functionally Complex Isoxazoles: Utility, Scope and Comparison with Dianion Methodology. *J. Org. Chem.*, **1985**, *50,* 5660-6.

49. Niou C-S, Natale NR. Synthesis, Metalation and Electrophilic Quenching of Alkyl-Isoxazole-4-tertiary carboxamides. A Critical Comparison of Three Isoxazole Lateral Metalation Methods, *Heterocycles*.*24,*401-12 (1986)

50. Schlicksupp L, Natale NR, Regioselectivity in Lateral Deprotonation of an Isoxazole Carboxamide of (S)-Prolinol. Conformational Correlation by Crystal Structure, Solid State and Solution ^{13}C NMR . *J. Heterocycl. Chem. 24,*1345-8 (1987)

51. Campana C, Mirzaei J, Koerner C, Gates C, Natale N.R. 3-(1,3-Diphenylpropan-2-yl)-4-methyl-6-phenylisoxazolo[3,4-*d*]pyridazin-7(6*H*)-one, *Acta Cryst., E69,* 1680-1681(2013)

52. Zamponi G, Stotz SC, Staples RJ, Rogers TA, Nelson JK, Hulubei V, Blumenfeld A, Natale NR. Unique Structure Activity Relationship of 4-Isoxazolyl-1,4-dihydropyridines. *J. Med. Chem\.46(1)*, 87-96 (2003) [PMID: 12502362].

53. Hulubei V, *et al*, Steiger SA, Natale NR. 4-Isoxazolyl-1,4-dihydropyridines exhibit binding at the multidrug resistance transporter. *Bioorg. Med. Chem. 20(22),* 6613-6620 (2012). [PMID: 23063517].

Our first indication that IDHP will be useful for probing MDR activity

54. Szabon-Watola MI, Ulatowki SV, George KM, Hayes, CD, Steiger SA, Natale NR. Bioorg. *Med. Chem. Lett.* 24, 117-121 (2014)

55. Baldwin J, Halczenko W, Hartman G, Philips B. 4-Heteroaryl-1,4-dihydropyridines-3,5-dicarboxylates, useful as calcium channel blockers. US Patent: US4735956A (1988)

56. Philips B, Hartman G. Preparation and reaction of isomeric formyl-2,1-benzisoxazoles. *J. Het. Chem.* 23(3), 897-899 (1986).

57. Mirzaei Y.R., Samed T, Majid G, Hasan N, Laden E, Facile Synthesis of Isoxazole-4 and 5-Carbaldehydes and their Conversion to Isoxazolyl-1, 4-Dihyropyridines. *Org. Prep. Proced. International. 35,* 207-214 (2003)

58. Hamama WS, Ibrahim ME, and Hanafi H. Zoorob Efficient Regioselective Synthesis and Potential Antitumor Evaluation of Isoxazolo[5,4-**b**]pyridines and Related Annulated Compounds. *Arch. Pharm. Chem. Life Sci*. *345*, 468–475 (2012), and cited references.

59. Laurent S, Kim D, Smith T W, Marsh J D. Inotropic effect, binding properties, and calcium flux effects of the calcium channels agonist CGP 28392 in intact cultured embryonic chick ventricular cells. *Circ. Res.* 56(5), 676-682 (1985).

60. Taylor M, Himmelsbach R, Kornberg B, Quin J, Lunney E, Michel A. 1,3-Dipolar cycloaddition of nitrile oxides with 1,4-dihydropyridines and conformational analysis of isoxazolo[5,4-b]pyridines. *J. Org. Chem.* 54, 5585-5590 (1989).

61. Heaney F. Nitrile Oxide/Alkyne Cycloadditions – A Credible Platform for Synthesis of Bioinspired Molecules by Metal-Free Molecular Clicking. *Eur. J. Org. Chem.* 3043–3058 (2012)

62. Hansen TV, Wu P, Folkin VV. One pot Copper(I)-catalyzed synthesis of 3,5-disubstituted isoxazoles. *J. Org. Chem.* 70, 7761-7764 (2005).

63. Himo F, *et al,* Sharpless KB, Folkin VV. Copper(I) –catalyzed synthesis of azoles. DFT study predicts unprecedented reactivity and intermediates. *J. Am. Chem. Soc. 127*, 210-216 (2005).

64. Maass P, Schulz-Gasch T, Stahl M, Rarey M**.** Recore: A Fast and Versatile Method for Scaffold Hopping Based on Small Molecule Crystal Structure Conformations. *J. Chem. Inf. Model.* 47, 390**-**399 (2007).

65. Furuta T, Shibata S, Kadama I, Yamada K. Cardiovascular effects on FR34235, a new dihydropyridine slow channel blocker, in isolated rabbit myocardium and aorta. *J. Cardiovasc Pharmacol.* 5(5), 836-841(1983).

66. Coburn R, Wierzba M, Suto M, Solo A, Triggle A, Triggle D. 1,4-Dihyropyridine antagonist activities at the calcium channel: a quantitative structure-activity relationship approach. *J. Med. Chem.* 31, 2103-2107 (1988).

67. Triggle D. 1,4-Dihydropyridine calcium channel ligands: selectivity of action. The role of pharmacokinetics, state-dependent interactions, channel isoforms, and other factors. *Drug Devel. Research.* 58, 5-17 (2003).

68. Triggle D. Calcium channel ligands. *Ann. Rev. Pharmacol. Toxicol.* 27, 347-369 (1987).

69. Mohajeri A, Hemmateenejad B, Mehdipour A, Miri R. Modeling calcium channel antagonistic activity of dihydropyridine derivatives using ATMS indices analyzed by GA-PLS and PC-GA-PLS. *J. Mol. Graph Model.* 26 (7), 1057-1065 (2008).

70. Mahmoudian, M, Richards W. A conformational distinction between dihydropyridine calcium agonists and antagonists. *Chem. Commun.* 10, 739-741 (1986).

71. Mojarrad J, Miri R, Knaus E. Design and synthesis of methyl 2-7,7-dihalo-5-phenyl-2-azabicyclo[4.1.0]hepta3-ene-4-carboxylates with calcium channel antagonist activity. *Bioorg. Med. Chem.*12, 3215-3220 (2004).

72. Bechem M, Goldmann S, Gross R, *et al.* A new type of Ca-channel modulation by a novel class of 1,4 dihydropyridines. *Life Sci.* 60 (2), 107-18 (1997).

73. Zheng W, Stoltefuss J, Goldmann S, Triggle J. Pharmacologic and radioligand binding studies of 1,4-dihydropyridines in rat cardiac and vascular preparations: stereoselectivity and voltage dependence of antagonist and activator interactions. *Mol Pharmacol.* 41(3), 535-541 (1992).

74. Handrock R, Herzig S. Stereoselectivity of Ca+2 channel block by dihydropyridines: no modulation by the voltage protocol. *Eur. J. Pharmacol.* 309(3), 317-321 (1996).

75. Mahmoudian M, Richards W. QSAR of binding of dihydropyridine-type calcium antagonists to their receptor on ileal smooth muscle preparations. *J. Pharm. Pharmacol.* 38(4), 272-276 (1986).

76. Goldmann S, Stoltefuss J, Born L. Determination of the absolute configuration of the active amlodipine enantiomer as (-)-S: a correction. *J Med Chem.* 35(18), 3341-3344 (1995).

77. Goldmann S, Stoltefuss J. 1,4-Dihydropyridines: effects of chirality and conformation on the calcium antagonist and agonist activities. *Angew. Chem. Int. Ed.* 30 (12), 1559–1578 (1991).

   The classic observation of the pronounced eudismic ratio for the antihypertensive activity of DHPs

78. Janis R. A, Silver P J, Triggle D. J. Drug action and cellular calcium regulation. *Adv. Drug Res.*16, 309-591 (1987).

79. Janis R. A, Triggle D. J. New developments in calcium ion channel antagonists. *J. Med. Chem.*26(6), 775-785 (1983).

80. Rovnyak G, Andersen N, Gougoutas J, *et al.* Studies directed towards ascertaining the active conformation of 1,4-dihydropyridine calcium entry blockers. *J. Med. Chem.*31(5), 936-944 (1988).

81. Goldman S, Geiger W. Rotational barriers of 4-aryl-1,4-dihydropyridines (Ca antagonists) *Angew. Chem., Int. Ed. Engl.* 23, 301-302 (1984).

82. Berntsson P, Carter R. E. Determination of the conformation of felodipine by 1H NMR spin lattice relaxation time measurements. *Acta Pharmaceutica Suec.* 18, 221-226(1981).

83. Baldwin J J, Claremon DA, Lumma P K, *et al*. Diethyl 3, 6-dihydro-2, 4-dimethyl-2, 6-methano-1, 3-benzothiazocine-5, 11-dicarboxylates as calcium entry antagonists: new conformationally restrained analogs of Hantzsch 1, 4-dihydropyridines related

to nitrendipine as probes for receptor-site conformation *J. Med.Chem.* 30(4), 690-695 (1987).

84. Cosconati S, Marinelli L, Lavecchia A, Novellino E . Characterizing the 1,4-Dihydropyridines Binding Interactions in the L-Type Ca2+ Channel: Model Construction and Docking Calculations. *J. Med. Chem.* 50(7), 1504-1513 (2007), and cited references.

85. Tsuruo T, Lida H, Yamashiro M, Tsukagoshi S, Sakurai Y. Enhancement of vincristine- and adriamycin-induced cytotoxicity by verapamil in P388 leukemia and its sublines resistant to vincristine and adriamycin. *Cancer Res.*31(19), 2905-2910 (1983).

86. Miller T, Gorgan T, Dalton W. P-glycoprotein expression in malignant lymphoma and reversal of clinical drug resistance with chemotherapy plus high-dose verapamil. *J. Clin. Oncol.* 9(1), 17-24 (1991).

87. Hollt V, Kouba M, Dietel M, Vogt G. Steroisomers of calcium antagonists which differ markedly in their potencies as calcium blockers are equally effective in modulating drug transport by P-glycoprotein. *Biochem. Pharmacol.* 43(12), 2601-2608 (1992).

88.Teodori E, Dei S, Scapecchi S, Gualtieri F. The medicinal chemistry of multidrug resistance (MDR) reversing drugs. *II Farmaco.* 57(2), 385-415 (2002).

89. Tolomeo M, Gancitano R, Musso M, *et al.* Effects of R-enantiomer(GR66234A) and L-enantiomer (GR66235A) of telupidine, a newer dihydropyridine derivative, on cell line displaying the multidrug resistant phenotype. *Haematologica*. 79(4), 328-333 (1994).

90. Tasaka S, Ohmori H, Gomi N, *et al*. Synthesis and structure-activity analysis of novel dihydropyridine derivatives to overcome multidrug resistance. *Bioorg. Med. Chem. Lett.* 11(2), 275-277 (2001).

91. Bazargan L, Fouladdel S, Shafiee A, Amini M, Ghaffari S, Azizi E. Evaluation of anticancer effects of newly synthesized dihydropyridine derivatives in comparison to verapamil and doxorubicin on T47D parental and resistant cell lines in vitro. *Cell Biol. Toxicol.* 24(2), 165-174 (2008).

92. Saponara S, Ferrara A, Gorelli B, *et al*. 3,5-dibenzoyl-4-(3-phenoxyphenyl)-1,4-dihydro-2,6-dimethylpyridine (DP7): a new multidrug resistance inhibitor devoid of effects on Langendorff-perfused rat heart. *Eur. J. Pharmacol.* 563(1), 160-163 (2007).

93. Mehdipour A, Javidnia K, Hemmateenejad B, Amirghofran Z, Miri R. Dihydropyridine derivatives to overcome atypical multidrug resistance: design, synthesis, QSAR studies, and evaluation of their cytotoxic and pharmacological activities. *Chem. Biol. Drug. Des.* 70(4), 337-346 (2007).

94. Mohajeri A, Hemmateenejad B, Mehdipour A, Miri R. Modeling calcium channel antagonistic activity of dihydropyridine derivatives using QTMS indices analyzed by GA-PLS and PC-GA-PLS. *J. Mol. Graph Model.* 26(7), 1057-1065 (2008)

95. Zhou X, Coburn R, Morris M. Effects of new 4-aryl-1,4-dihydropyridines and 4-arylpyridines on drug efflux mediated by multidrug resistance-associated protein 1. *J. Pharm. Sci.*94(10), 2256-2265 (2005).

96. Zhou X, Yang X, Wang Q, Coburn R, Morris M. Effects of dihydropyridines and pyridines on multidrug resistance mediated by breast cancer resistance protein: in

vitro and in vivo studies. *Drug Metab. Dispos.*33(8), 1220-1228 (2005).

97. Zhou X, *et al*, Coburn R, Morris M. New 4-aryl-1,4-dihydropyridines and 4-arylpyridines as P-glycoprotein inhibitors. *Drug. Metab Dispos.*33(3), 321-328 (2005).

98. Mary A, Zamponi G. Voltage-dependent inactivation of voltage gated calcium channels. *Landes Bioscience*. 90(1), 48-46 (2005).

99. Welsch M, Snyder S, Stockwell B. Privileged scaffolds for library design and drug discovery. *Current opinion in chemical biology.* 14(3), 347-361 (2010).

100. Miri R, Mehdipour A. Dihydropyridines and atypical MDR: A novel perspective of designing general reversal agents for both typical and atypical MDR. *Bioorg. Med. Chem*. 16(18), 8329–8334 (2008).

101. Shah A, Bariwal J, Molnár J, Kawase M, Motohashi N. Advanced Dihydropyridines as Novel Multidrug Resistance Modifiers and Reversing Agents. *Top. Heterocycl. Chem*. 15, 201–252 (2008).

102. Zhou F, Shao O, Coburn A, Morris E. Quantitative structure-activity and quantitative structure-pharmacokinetics relationship of 1,4-dihydropyridines and pyridines as multidrug resistance modulators. *Pharm. Res*. 22(12), 1989-1996 (2005).

103. Nobili S, Landini I, Giglioni B, Mini E. Pharmacological Strategies for Overcoming Multidrug Resistance. *Current Drug Targets.* 7(7), 861-879 (2006)

104. Borchers C, Boer R, Klemm K, *et al*. Characterization of the Dexniguldipine binding site in the multidrug resistance-related transport protein P-Glycoprotein by photoaffinity labeling and mass spectrometry. *Mol. Pharm.* 61(6), 1366-1376 (2002).

105. Safa A. Photoaffinity labels for characterizing drug interaction sites of P-glycoprotein. *Methods Enzymol.* 292, 289-307 (1998).

106. Greenberg M. Identification of drug interaction sites in P-glycoprotein. *Methods Enzymol*. 263, 307-317 (1998)

107. Bruggemann P, German A, Gottesman M, Pastan I. Two different regions of P-glycoprotein are photoafffinty-labeled by azidopine. *J Biol Chem*. 264(26), 15483-15488 (1989).

108. Boer R, Ulrich W, Haas S, *et a*l. Interaction of cytostatics and chemosensitizers with the dexniguldipine binding site on P-glycoprotein. *Euro. J. Pharmacology*, 295(2), 253-260 (1996).

109. Ferry R, Russel A, Cullen H. P-glycoprotein possesses a 1,4-dihydropyridine-selective drug acceptor site which is allosterically coupled to a Vinca alkaloid-selective binding site. *Biophys Res Commun*, 188(1), 440-445 (1992).

110. Ramachandra M, Ambudkar V, Chen D, Hrycyna A, Dey S, Gottesman M, Pastan I. Human P-glycoprotein exhibits reduced affinity for substrates during a catalytic transition state. *Biochemistry*, 37(14), 5010-5019 (1998).

111. Ayesh S, Shao M, Stein D. Co-operative, competitive and non-competitive interactions between modulators of P-glycoprotein, *Biochim. Biophys. Acta (BBA)-Molecular Basis of Disease.* 1316(1), 8–18 (1996)

112. Shapiro A, Ling V. Positively cooperative sites for drug transport by P-glycoprotein with distinct drug specificities. *Eur. J. Biochem*. 250(1), 130–137 (1997)

113. Shapiro A, Fox K, Lam P, Ling V. Stimulation of P-glycoprotein-mediated drug transport by prazosin and progesterone. Evidence for a third drug-binding site. *Eur.*

J. Biochem. 259(3), 841–850 (1999).

114. Van Veen W, Marqolles A, Muller M, Higgins F, Konings N. The homodimeric ATP-binding cassette transporter LmrA mediates multidrug transport by an alternating two-site (two-cylinder engine) mechanism, *EMBO J.* 19(11), 2503–2514 (2000).

115. Martin C, Berridge G, Higgins F, Mistry P, Charlton P, Callaghan R. Communication between multiple drug binding sites on P-glycoprotein, *Mol. Pharmacol.* 58(3), 624–632 (2000)

116. Leung CS, Leung SS, Tirado-Rives J, Jorgensen WL. Methyl effects on protein-ligand binding. *J Med Chem.* 55(9), 4489-500 (2012). [PMID: 22500930]

117. Barreiro EJ, Kummerle AE, Fraga, CAM. The Methylation Effect in Medicinal Chemistry. *Chem. Rev.* 111(9), 5215–5246 (2011).

118. Joslyn AF, Luchkowski E, Triggle DJ. Dimeric 1,4-dihydropyridines as calcium channel antagonists. *J. Med. Chem.*31(8), 1489-1492 (1988).

119. Sauna ZE, Andrus MB, Turner TM, Ambudkar SV. Biochemical basis of polyvalency as a strategy for enhancing the efficacy of P-glycoprotein (ABCB1) modulators: stipiamide homodimers separated with defined-length spacers reverse drug efflux with greater efficacy. *Biochemistry.* 43(8), 2262-2271 (2004).

120. Namanja HA, *et al*, Hrycyna CA, Chmielewski J. Toward Eradicating HIV Reservoirs in the Brain: Inhibiting P-Glycoprotein at the Blood-Brain Barrier with Prodrug Abacavir Dimers. *J. Am. Chem. Soc*. 134(6), 2976–2980 (2011).

121. Pires MM, Emmert D, Hrycyna, CA, Chmielewski J. Inhibition of P-Glycoprotein-Mediated Paclitaxel Resistance by Reversibly Linked Quinine Homodimers. *Mol*

Pharmacol. 75 (1),92–100 (2009).

122. Pires MM, Hrycyna CA, Chmielewski J. Bivalent Probes of the human multidrug Transporter P-glycoprotein. *Biochemistry.* 45(38), 11695-11702 (2006).

123. Lemke TL, Williams DA, Roche VF, Zito SW, editors. *Foye's Principles of Medicinal Chemistry,* 7th Edition. Lippincott Wiliiams and Wilkins, NY 2013.

124. Tsukamoto T. Tough Times for Medicinal Chemists: Are We to Blame? *ACS Med. Chem. Lett.* 4(4),369–370 (2013)

This paper was published in Acta Cyst C.

Chapter 2

The effect of bromine scanning around the phenyl group of 4-phenyl-hexahydroquinolone derivatives

2.1 Synopsis

In three quinolone compounds, the 1,4-dihydropyridine (1,4-DHP) rings adopt flat boat conformations which are bisected by the plane of the pseudo-axial brominated aryl ring. The cyclohexanone rings adopt envelope conformation. The packing of all the three compounds are linked through intermolecular N—H…O hydrogen bonds.

2.2 Abstract

Three quinolone compounds were synthesized and crystalized in an effort to study the calcium channel antagonists structure-activity relationship. In all three quinolones, ethyl 4-(4-bromophenyl)-2,7,7-trimethyl-5-oxo-1,4,5,6,7,8-hexahydroquinoline-3-carboxylate (I), ethyl 4-(3-bromophenyl)-2,7,7-trimethyl-5-oxo-1,4,5,6,7,8-hexahydroquinoline-3-carboxylate (II), and ethyl 4-(2-bromophenyl)-2,7,7-trimethyl-5-oxo-1,4,5,6,7,8-hexahydroquinoline-3-carboxylate (III), common structural features such as the flat-boat conformation of 1,4-dihydropyridine (1,4-DHP) ring, the envelop conformation of the fused cyclohexanone, and the bromophenyl ring at pseudo-axial position and orthogonal to the 1,4-DHP ring are retained. However, due to different packing interactions in each compound, halogen bonds are observed in compounds (I) and (III). Compound (III) was crystalized with two enantiomers in one asymmetric unit. All of the prepared derivatives satisfy basic structural requirements to have moderate activity as calcium channel antagonists.

2.3 Introduction

The 1,4-dihydropyridine (1,4-DHP) heterocycle comprises a large family of medicinally important compounds. The substructure has garnered the most attention as calcium channel antagonists working as slow calcium channel blockers, which have been used in the treatment of angina pectoris and hypertension. The examination of Hantzsch 1,4-dihydropyridine ester derivatives have produced more active and longer acting agents than the prototypical nifedipine molecule. Many other derivatives have been synthesized to yield compounds as calcium agonists or antagonists (Martin-Leon *et al.*, 1995; Rose, 1990, 1992). A fused cyclohexanone ring is one of the modifications on 1,4-DHP compounds, which have been shown to have moderate calcium antagonistic activity, as well as modest anti-inflammatory and stem cell differentiation properties, and have been implicated in slowing neurodegeneration disorders. Thus, further understanding of the structure activity relationship will allow for the determination of off target activity and the reduction of side effect. It has been proven that the flattened boat conformation of the 1,4-DHP ring is one factor that lead to higher calcium channel activity. The N1 and C4 atoms of the DHP ring can be marginally displaced from the mean plane of the boat (Linden *et al.*, 2002). An aryl group in the 4-position of 1,4-DHP is essential for optimal activity. A study showed that the aryl ring with halogen or other electron-withdrawing groups exhibited higher receptor-binding activity (Takahashi *et al.*, 2008). On 1,4-DHP ring, ester groups are usually substituted on 3- and 5- positions. It is suggested that at least one *cis-* ester is required for the calcium antagonistic effect and H-bonding to the receptor (Fossheim, 1986). In an effort to find more active calcium channel antagonists in the 1,4-DHP genre, we synthesized a series of 1,4-DHP fused-ring derivatives –

hexahydroquinolones. In this paper, we report three structures which have bromine substituted on the para- meta- and ortho- positions on the phenyl moiety attached to the 1,4-DHP ring.
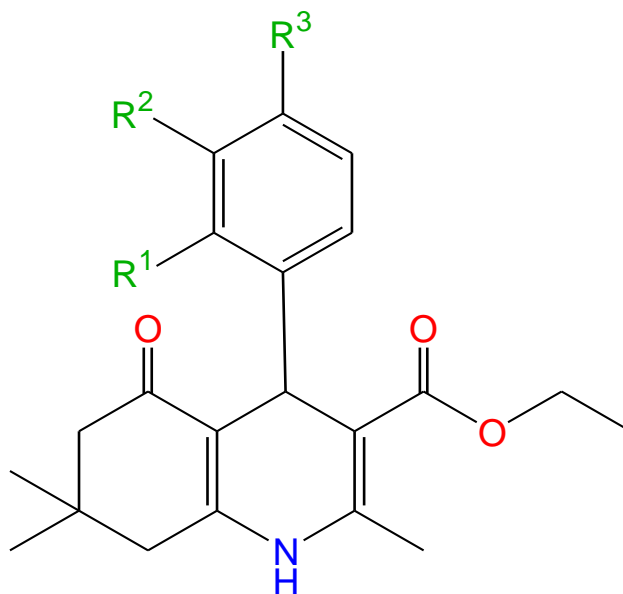
I. $R^1 = R^2 = H$, $R^3 = Br$
II. $R^1 = H$, $R^2 = Br$, $R^3 = H$
III. $R^1 = Br$, $R^2 = R^3 = H$

Figure 2.1: General structure of the examined compounds

2.4 Synthesis and crystallization

An oven-dried 100 mL round bottom was charged with 0.757 g of dimedone, 0.703 g of ethyl acetoacetate, 0.170 g of ytterbium (III) trifluoromethanesulfonate and a magenetic stir bar. The mixture was then taken up in 13.5 mL of absolute ethanol, capped and put under an inert atmosphere of argon, after which the solution was allowed to stir at room temperature for 20 min. Homologues 1.0 g (5.405 mmol) of bromo-benzaldehyde and 0.419 g of ammonium acetate were added to the stirring solution, the solution was

allowed to stir at room temperature for 48 hr. Reaction progress was monitored via TLC. Once the reaction was complete, excess solvent was removed via rotary evaporation. The solution was then purified via a silica column chromatography. The product was re-crystallized into white to light yellow crystalline solids with hexane and ethyl acetate [Compound (I) = 1.91 g, 4.57 mmol, 84.00%] [Compound (II) = 1.86 g, 4.45 mmol, 82.30%] [Compound (III) = 1.45 g, 3.466 mmol, 63.76%].

2.5 Characterization information

Melting points were determined in open capillary tubes with a Mel-Temp melting point apparatus (200watts) and are uncorrected. Structures were confirmed with ^{1}H and 13C NMR, and mass spectroscopy. H NMR spectra were obtained in chloroform-d_1 using a Bruker AMX-400 MHz spectrometer. Chemical shifts are reported as p.p.m. relative to the tetramethylsilane (TMS). LC-MS (liquid chromatography-mass spectrometry) were obtained using a Waters LCT Premier XE series spectrometer.

Ethyl 4-(4-bromophenyl)-2,7,7-trimethyl-5-oxo-1,4,5,6,7,8-hexahydroquinoline-3-carboxylate (I): **^{1}H NMR:** (CDCl$_3$) δppm 7.31 (d, J=8.28Hz, 2H), 7.20 (d, J=8.28Hz, 2H), 6.01 (bs, 1H), 5.02 (s, 1H), 4.05 (q, J=7.03Hz, 2H), 2.38 (s, 3H), 2.21 (s, 2H), 2.17(s, 2H), 1.20 (t, J=7.15Hz, 3H), 1.08 (s, 3H), 0.93 (s, 6H). **^{13}C NMR:** (CDCl$_3$) δppm 195.42, 167.19, 148.01, 146.07, 143.60, 130.96, 129.89, 119.82, 111.90, 105.72, 59.94, 50.69, 41.14, 36.33, 32.75, 29.44, 27.15, 19.49, 14.23. **HRMS:** calculated for C$_{21}$H$_{24}$NO$_3$Br, 418.1018; found, 418.1024. **MS:** m/z = 418 ([M^{+1}] 100), 419 ([M^{+2}] 10), 420 ([M^{+3}] 100). **MP:** 254-255°. **TLC:** SiO$_2$; Hexane:EtOAc 3:2 R$_f$ = 0.19.

Ethyl 4-(3-bromophenyl)-2,7,7-trimethyl-5-oxo-1,4,5,6,7,8-hexahydroquinoline-3-carboxylate (II): **^{1}H NMR:** (CDCl$_3$) δppm 7.41 (s, 1H), 7.26 (d, J=7.53Hz, 1H), 7.22 (d,

J=8.53Hz, 1H), 7.07 (t, J=7.78Hz, 1H), 6.09 (bs, 1H), 5.03 (s, 1H), 4.07 (m, J=7.15Hz, 2H), 2.38 (s, 3H), 2.31 (s, 2H), 2.22 (s, 2H), 1.21 (t, J=7.15Hz, 3H), 1.09 (s, 3H), 0.96 (s, 6H). ^{13}**C NMR:** (CDCl$_3$) δppm 195.39, 167.15, 149.30, 148.24, 143.79, 131.09, 129.17, 126.97, 122.10, 111.71, 105.60, 59.96, 50.69, 41.12, 36.64, 32.78, 29.40, 27.22, 19.51, 14.21. **HRMS:** calculated for C$_{21}$H$_{24}$NO$_3$Br, 418.1018; found, 418.0979. **MS:** *m/z* = 418 ([M^{+1}] 100), 419 ([M^{+2}] 90). **MP:** 235-236°. **TLC:** SiO$_2$; Hexane:EtOAc 3:2 R$_f$ = 0.12.

Ethyl 4-(2-bromophenyl)-2,7,7-trimethyl-5-oxo-1,4,5,6,7,8-hexahydroquinoline-3-carboxylate (III): ^{1}**H NMR:** (CDCl$_3$) δppm 7.44 (dd, J=7.91Hz, 1H), 7.37(dd, J=7.78Hz, 1H), 7.16 (tt, J=7.53Hz, 1H), 6.94 (tt, J=7.91Hz, 1H), 5.92 (bs, 1H), 5.37 (s, 1H), 4.08(m, J=7.15Hz, 2H), 2.32 (s, 3H), 2.30 (s, 2H), 2.19 (s, 2H), 1.18 (t, J=7.03Hz, 3H), 1.08 (s, 3H), 0.96 (s, 6H). ^{13}**C NMR:** (CDCl$_3$) δppm 195.30, 167.44, 148.04, 145.88, 143.22, 133.08, 132.03, 127.49, 126.97, 123.38, 111.74, 105.86, 59.84, 50.69, 41.29, 37.98, 32.58, 29.28, 27.38, 19.49, 14.36. **HRMS:** calculated for C$_{21}$H$_{24}$NO$_3$Br , 418.1018; found, 418.1037. **MS:** *m/z* = 417 ([M] 100), 418 ([M^{+1}] 100), 419 ([M^{+2}] 30). **MP:** 200-204°. **TLC:** SiO$_2$; Hexane:EtOAc 3:2 R$_f$ = 0.23.

2.6 Refinement

Crystal data, data collection and structure refinement details are summarized in Table 1. The methyl H atoms were constrained to an ideal geometry, with C – H = 0.98 Å and U_{iso}(H) = 1.5U_{eq}(C), and were allowed to rotate freely about the C – C bonds. The rest of the H atoms were placed in the calculated positions with C – H = 0.95 – 1.00 Å and refined as riding on their carrier atoms with U_{iso}(H) = 1.2U_{eq}(C). The positions of amine H atoms were determined from a difference Fourier maps and refined freely along with their isotropic displacement parameters. Two low-angle reflections of (I) and four of

(III) were omitted from the refinement because their observed intensities were much lower than the calculated values as a result of being partially obscured by the beam stop.

2.7 Results and discussion

Both ethyl 4-(4-bromophenyl)-2,7,7-trimethyl-5-oxo-1,4,5,6,7,8-hexahydroquinoline-3- carboxylate (I) (Fig. 1) and ethyl 4-(3-bromophenyl)-2,7,7-trimethyl-5-oxo-1,4,5,6,7,8-hexahydroquinoline-3- carboxylate (II) (Fig. 2) crystallize in the orthorhombic space group Pbcn with one molecule in the asymmetric unit. The asymmetric unit of ethyl 4-(2-bromophenyl)-2,7,7-trimethyl-5-oxo-1,4,5,6,7,8-hexahydroquinoline-3- carboxylate (III) (Fig. 3) is composed of two enantiomers of (III), which crystallize in the monoclinic space group P2$_1$/c. All three compounds have very similar structural conformations, which accommodate the requirements for calcium channel antagonists.

In all three structures, the 1,4-DHP ring is characterized by a shallow or flattened boat conformation, one factor that leads to higher calcium channel activity. The boat conformation can be quantified by the ring puckering parameters (Cremer & Pople, 1975). An ideal boat would have $\theta = 90°$ and $\varphi = n \times 60°$. In (I), the puckering parameters are $Q = 0.196$ (2) Å, $\theta = 106.5$ (6)°, and $\varphi = 5.2$ (8)° for the atom sequence N(1)-C(2)-C(3)-C(4)-C(10)-C(9). The corresponding parameters for (II) are $Q = 0.3014$ (17) Å, $\theta = 107.1$ (3)°, and $\varphi = 0.9$ (3)°. While for (III), two sets were obtained as $Q_A = 0.162$ (3) Å, $\theta_A = 67.3$ (10)°, and $\varphi_A = 197.5$ (10)° and $Q_B = 0.279$ (3) Å, $\theta_B = 106.9$ (6)°, and $\varphi_B = 3.9$ (6)° for molecules A and B, respectively. The shallowness of the boat conformation is indicated by the marginal displacements of N(1) and C(4) from the mean plane (the base of the boat) defined by the two double bonds [C(2)=C(3) and C(10)=C(9)]. The deviation

59

of the N(1) atom from the base of the boat is generally smaller , between 0.00 – 0.19 Å, while the deviation of C(4) is most frequently found around 0.3 Å (Linden *et al.*, 2004, 2005). These are also observed in our compounds: deviations of N(1) are 0.095(3) Å, 0.142(2) Å, 0.047(3) Å, and 0.134(3) Å for (I), (II), (III)A, and (III)B, respectively; and the deviations of C(4) are 0.235 (4) Å, 0.365 (2) Å, 0.207 (4) Å, and 0.336 (4) Å for (I), (II), (III)A, and (III)B, respectively. The sum of the absolute values of the ring internal torsion angles is also considered a quantitative measure of the "flatness" of the 1,4-DHP ring. With a flattened or unpuckered ring showing a 0° and 240° for an ideal boat conformation of the ring. Our compounds show 67.74° for (I), 104.39° for (II), 55.72° for (III)A and 96.52° for (III)B, indicating a flattened boat conformation, compared to the sum of angles being 72° for nifedipine, the known standard for the 1,4-DHPs.

The relationship between the 1,4-DHP pyridine ring and the aryl group attached to the C(4) position is another key factor of DHP structure activity relationship. It has been reported that the pseudo-axial position of the aryl ring is essential for pharmacological activity (Langs & Triggle, 1987). In our compounds, the bromophenyl rings are almost orthogonal to the base of the 1,4-DHP ring defined by atoms C(2), C(3), C(10), and C(9), with angles between mean planes [plane C(2), C(3), C(10), and C(9) to plane C(17), C(18), C(19), C(20), C(21), and C(22)] to be 86.32 (8)°, 88.46 (5)°, 99.37 (8)°, and 89.36 (9)° for (I), (II), (III)A, and (III)B, respectively. Another quantitative descriptive factor is the torsion angle between the N(1) – C(4) axis and the bond in the phenyl group right above the 1,4-DHP ring [C(17) – C(18) in compounds (I) and (II) and C(17) – C(22) in compound (III)]. The torsion angles defined by the N(1) – C(4) – C(17) – C(18) are 6.75 (19)° and 7.14 (12)° for (I) and (II), respectively. The corresponding

60

torsion angles in compound (III) showed even more orthogonal configuration as the values are 1.88 (18)° and 3.3 (2)° for (III)A and (III)B, respectively. The ortho-bromo group is placed in a synperiplanar orientation with respect to the C(4) – H bond. Such orientation has been observed in other ortho-substituted phenyl rings in 4-ary-1,4-DHP compounds (Linden *et al.*, 2004). It is worth noting that although meta-NO_2 substitution has been reported to be syn-periplanar to the H atom on C(4) carbon (Morales *et al.*, 1996), the meta-bromine in (II) is in anti-periplanar position. In the same manner as other reported ortho-substituted structures, compound (III) has the bromine pointing away from the DHP.

Due to the electron delocalization of the conjugate system, each ester group on the 1,4-DHP is coplanar and at *cis* orientation to the adjacent endocyclic double bond. The coplanes extend out through the ester chains in (I) and (II). However, in (III), because of different packing pattern, the end methyl group in (III)A curled up in the direction of aryl group. As a result, it pushed the aryl group slightly away from the orthogonal position, thus making the angle between 1,4-DHP and the aryl ring the most deviated from 90° – 99.37 (8)° in (III)A vs. 89.36 (9)° in (III)B.

Again, Cremer & Pople's ring puckering parameters are used to quantify the conformation of the fused cyclohexanone ring. In all three compounds, the cyclohexanone rings adopt the envelope conformation, which ideally would have $\theta = 54.7°$ (or $\theta = 125.3°$ in the case of absolute configuration change) and $\varphi = n \times 60°$. For compound (I), the puckering parameters are $Q = 0.447$ (3) Å, $\theta = 57.4$ (4)°, and $\varphi = 178.6$ (4)° for atom sequence C(5) – C(6) – C(7) – C(8) – C(9) – C(10). Correspondingly, for the same atom sequence in compound (II), (III)A, and (III)B, the puckering parameters

are Q = 0.4595 (18) Å, θ = 59.4 (2)°, and φ = 122.0 (3)°, Q = 0.462 (3) Å, θ = 122.5 (4)°,

and φ = 2.9 (4)°, Q = 0.477 (3) Å, θ = 59.4 (4)°, and φ = 183.4 (4)°, respectively. All

these parameters are very close to those of the ideal envelope conformation. Because of

the almost perfect envelope conformation, C(7) atom stands out from the plane formed by

the rest of the atoms in the ring and points to the same side as the C(4)-aryl ring. It is also

interesting that the axial methyl group on C(7) is almost syn-periplanar to the bond that

connects C(4) and the aryl ring. The relationship can be shown by the torsion angle of

C(11) – C(7) – C(4) – C(17), which is 13.86 (17)° for (I), 4.51 (13)° for (II), 16.2 (2)° for

(III)A and 5.5 (2)° for (III)B.

One feature, which has not been reported in this type of structures, is the

intermolecular halogen bonding between bromine and the ester carbonyl oxygen. A

halogen bond is defined as a short C – X ⋯ O – Y interaction, where the X ⋯ O distance

is less than or euqal to the sums of the respecetive van der Waals radii, 3.37 Å for Br ⋯

O in this case, with the C – X ⋯ O angle 165° and the X ⋯ O – Y angle 120°

(Auffinger *et al.*, 2004). Although (II) has a distance of 3.4837 (14) Å, which is only

slightly longer than the sum of van der Waals radii, the angles being 166.17 (13)° for

Br(1) ... O(2) -- C(14) and 77.24 (6)° for C(19) -- Br(1) ... O(2) are out of range for

halogen bonds. However, the Br ⋯ O distance is 3.1976 (18) Å in (I) with C(20) –

Br(1) ⋯ O(2) angle to be 152.24 (9)° and Br(1) ⋯ O(2) – C(14) angle 111.06 (15)°. Also

in (III), the distance is 3.1764 (18) Å between Br(1A) and O(2B) and the angles are

106.79 (16)° and 160.65 (8)° for Br(1A) ⋯ O(2B) – C(14B) and C(18A) – Br(1A) ⋯

O(2B), respectively. These numbers fall into the range for halongen bonds. Halogen

bonding has been known for decades and has been found in biological systems, where the

halogen acts as a Lewis acid and the interacting atom can be any electron-donating moiety. For example, in addition to the backbone carbonyl oxygen as the most prominent Lewis base involved in halogen bonds, hydroxyls and carboxyls in the side chain groups can also form halogen bonds in the protein binding sites (Wilcken *et al.*, 2013). The possibility of halogen bonding from bromine in these three compounds needs to be considered during the structure-activity relationship study.

In all three compounds, hydrogen bonds are formed between the N-H group and carbonyl O atom in cyclohexanone of another molecule (Table 2, 3, and 4). The hydrogen bonds link the molecules into extended chains running along *c* axis in both (I) and (II), but along *a* axis in (III) (Fig. 4, 5, and 6). In compound (I), the largest difference hole of -1.21 which is 0.68 Å away from Br(1) may indicate a slight disorder of Br atom. In conclusion, the structures reported here demonstrate that the conformational features have been conserved in cyclohexanone-fused 1,4-DHP derivatives. As a promising base structure for calcium channel antagonists, different substitutions and more structural modifications are being carried on in our group. The progress will be reported in due course.

For all structures: $C_{21}H_{24}BrNO_3$, $M_r = 418.32$, $Z = 8$. Experiments were carried out at 100 K with Mo $K\alpha$ radiation using a Bruker SMART BREEZE CCD diffractometer. Refinement was with 0 restraints. H atoms were treated by a mixture of independent and constrained refinement.

	(I)	(II)	(III)
Crystal data			

Crystal system, space group	Orthorhombic, *Pbcn*	Orthorhombic, *Pbcn*	Monoclinic, *P*2$_1$/*c*
a, b, c (Å)	18.0371 (4), 15.4309 (3), 14.2604 (3)	17.0813 (5), 15.4877 (5), 14.2544 (5)	14.5012 (18), 18.299 (2), 15.1952 (19)
α, β, γ (°)	90, 90, 90	90, 90, 90	90, 107.5262 (15), 90
V (Å^3)	3969.08 (14)	3771.0 (2)	3844.9 (8)
μ (mm^{-1})	2.09	2.20	2.16
Crystal size (mm)	$0.26 \times 0.18 \times 0.13$	$0.40 \times 0.21 \times 0.19$	$0.34 \times 0.16 \times 0.08$
Data collection			
Absorption correction	Multi-scan *SADABS* v2012/1 (Bruker AXS Inc.)	Multi-scan *SADABS* V2012/1 (Bruker AXS Inc.)	Multi-scan *SADABS* v2012/1 (Bruker AXS Inc.)
T_{min}, T_{max}	0.909, 1.000	0.839, 1.000	0.866, 1.000
No. of measured, independent and observed [$I > 2\sigma(I)$] reflections	35271, 4558, 3391	55070, 5055, 4278	45465, 8935, 6859
R_{int}	0.038	0.032	0.065
$(\sin \theta/\lambda)_{max}$ (Å^{-1})	0.650	0.684	0.653
Refinement			

$R[F^2 > 2\sigma(F^2)]$, $wR(F^2)$, S	0.042, 0.101, 1.04	0.032, 0.084, 1.03	0.036, 0.081, 1.02
No. of reflections	4558	5055	8935
No. of parameters	243	243	485
$\Delta\rho_{max}$, $\Delta\rho_{min}$ (e Å^{-3})	1.49, −1.21	1.31, −0.38	1.46, −0.47

Computer programs: Bruker *APEX2*, Bruker *SAINT*, *SHELXS* (Sheldrick, 2008),

SHELXL (Sheldrick, 2008), Olex2 (Dolomanov *et al.*, 2009).

Table 2.1: Crystal Structure data

D—H$\cdots A$	D—H (Å)	H$\cdots A$ (Å)	$D\cdots A$ (Å)	D—H$\cdots A$ (°)
N1—H1$\cdots$O1[i]	0.89 (3)	1.94 (3)	2.812 (2)	168 (3)

Symmetry code(s): (i) x, −y, z−1/2.

Table 2.2: Selected hydrogen-bond parameters for (I)

D—H$\cdots A$	D—H (Å)	H$\cdots A$ (Å)	$D\cdots A$ (Å)	D—H$\cdots A$ (°)
N1—H1$\cdots$O1[i]	0.86 (2)	2.05 (2)	2.8896 (19)	166 (2)

Symmetry code(s): (i) x, −y, z−1/2.

Table 2.3: Selected hydrogen-bond parameters for (II)

D—H$\cdots A$	D—H (Å)	H$\cdots A$ (Å)	$D\cdots A$ (Å)	D—H$\cdots A$ (°)
N1B—H1B$\cdots$O1A[i]	0.80 (3)	2.02 (3)	2.818 (3)	174 (3)
N1A—H1A$\cdots$O1B[ii]	0.83 (3)	2.07 (3)	2.884 (3)	165 (2)

Symmetry code(s): (i) −x+1, y−1/2, −z+1/2; (ii) −x, y+1/2, −z+1/2.

Table 2.4: Selected hydrogen-bond parameters for (III)
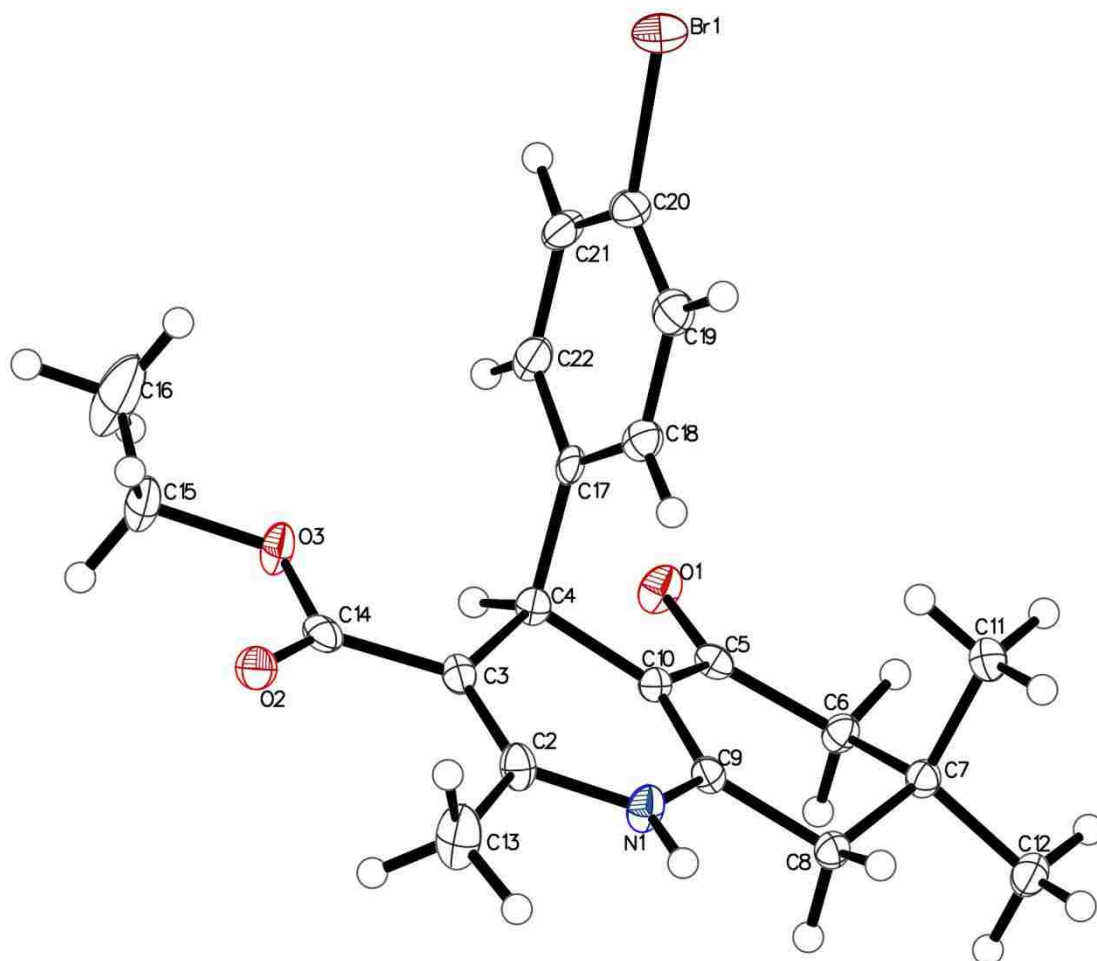
Figure 2.2 The asymmetric unit of (I), showing the atom-labelling scheme with

displacement ellipsoids at 50% probability level.
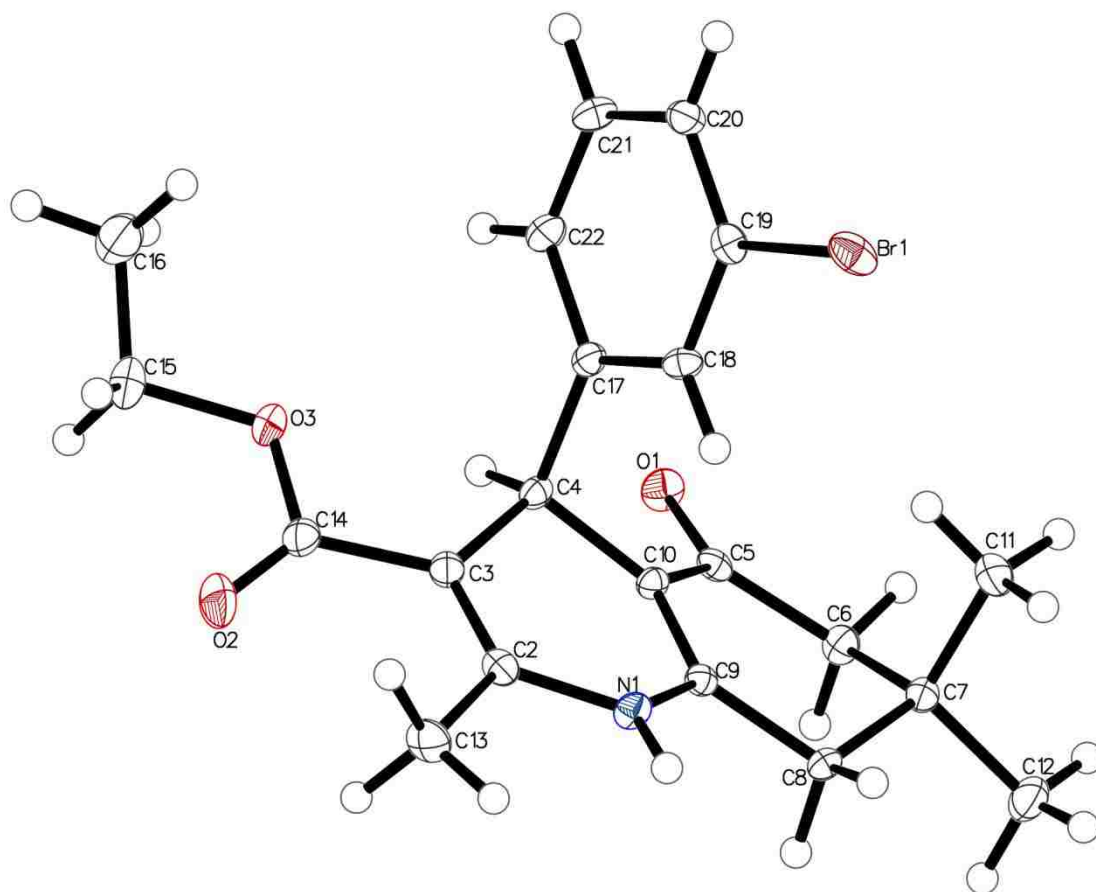
Figure 2.3 The asymmetric unit of (II), showing the atom-labelling scheme with displacement ellipsoids at 50% probability level.
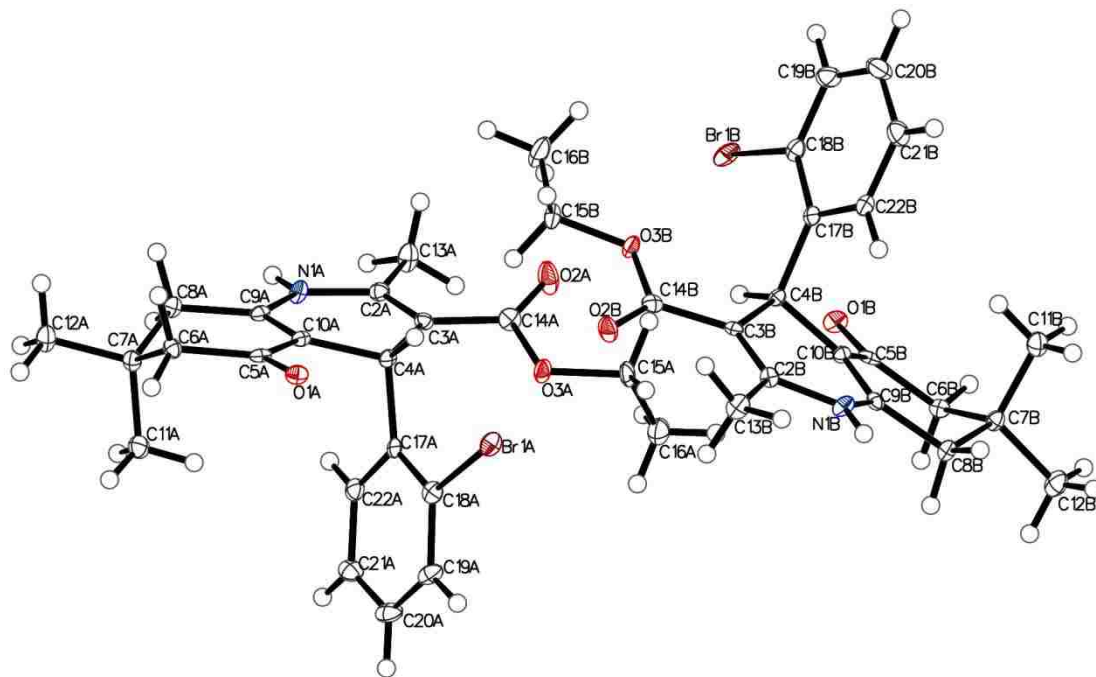
Figure 2.4 The asymmetric unit of (III), showing the atom-labelling scheme with

displacement ellipsoids at 50% probability level.
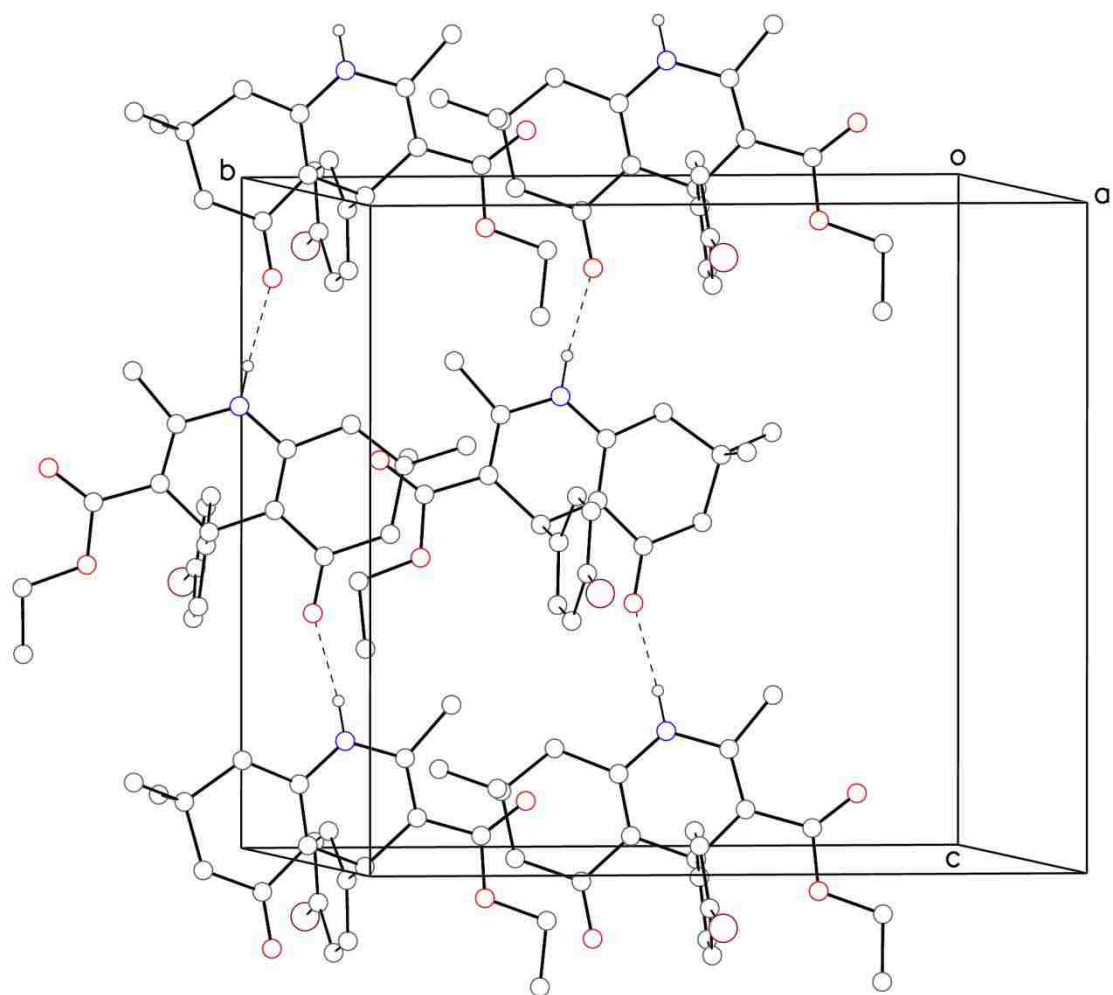
Figure 2.5 Part of the crystal structure of (I), showing the formation of chains of

molecules running along *c* axis. Hydrogen bonds are indicated by dashed lines. For the

sake of clarity, H atoms not involved in hydrogen bonding have been omitted.
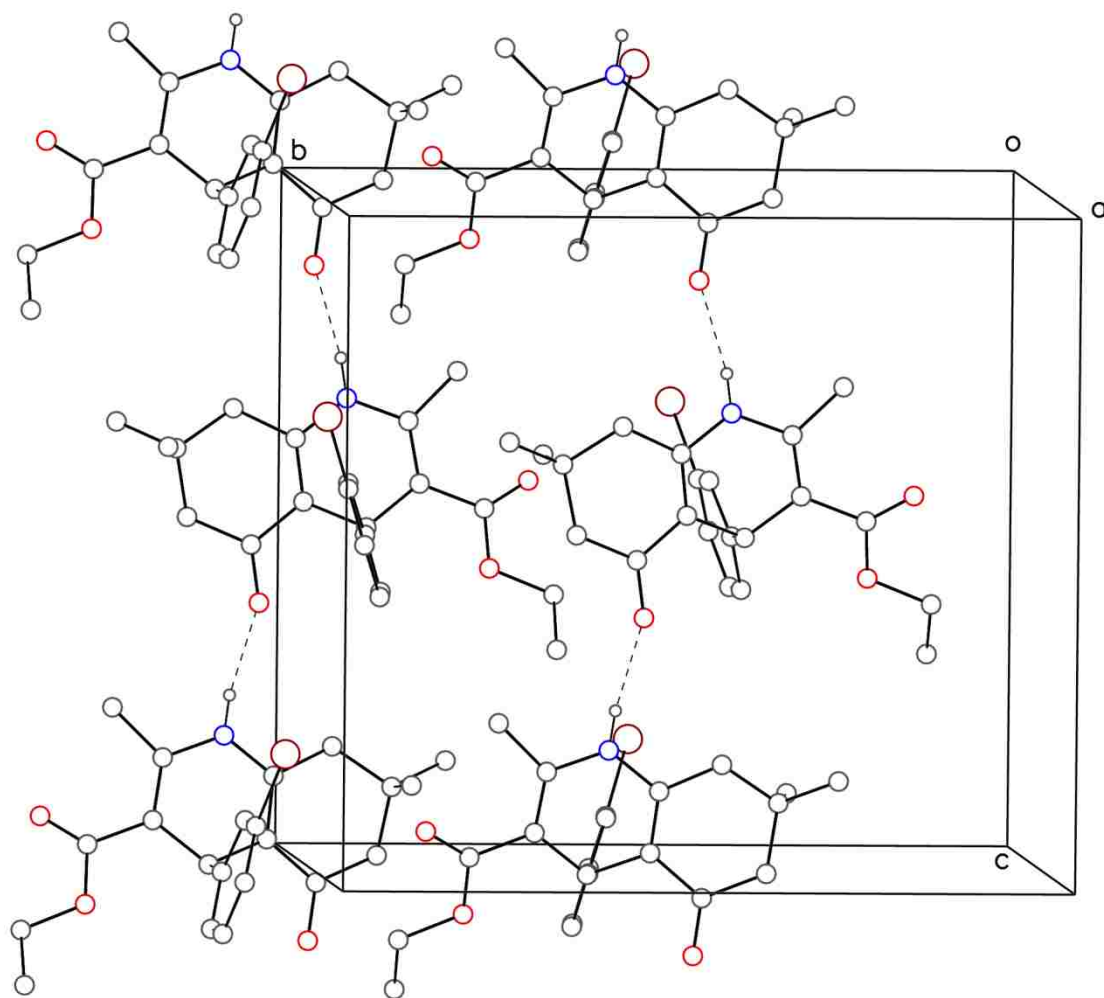
Figure 2.6 Part of the crystal structure of (II), showing the formation of chains of molecules running along *c* axis. Hydrogen bonds are indicated by dashed lines. For the sake of clarity, H atoms not involved in hydrogen bonding have been omitted.
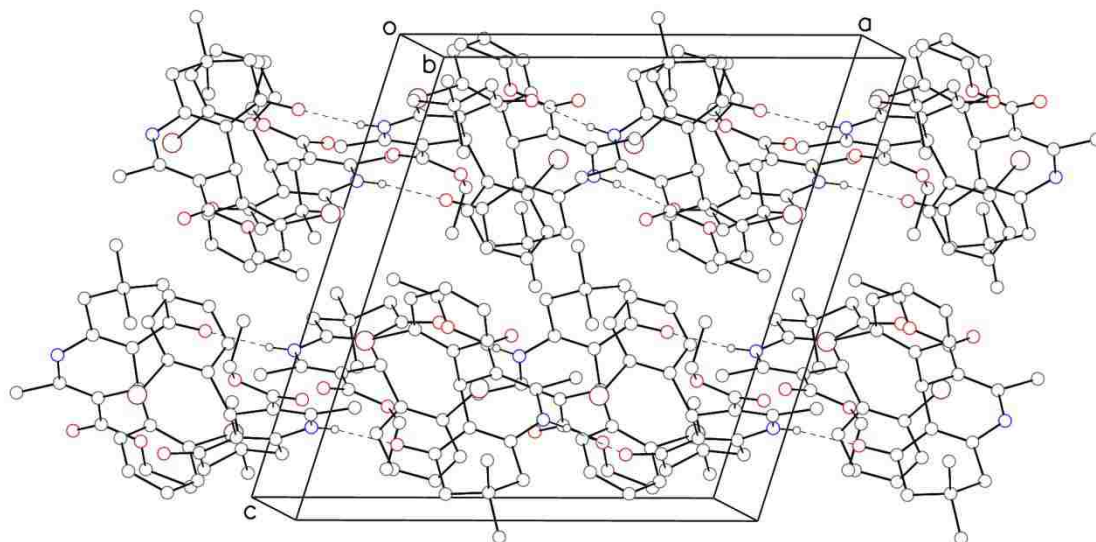
Figure 2.7 Part of the crystal structure of (III), showing the formation of chains of molecules running along *a* axis. Hydrogen bonds are indicated by dashed lines. For the sake of clarity, H atoms not involved in hydrogen bonding have been omitted.

2.8 References

Auffinger, P., Hays, F. A., Westhof, E. & Ho, P. S. (2004). *Proc. Natl Acad. Sci. USA*, **101**, 16789–16794.

Bruker (2008). *APEX2, SAINT and SADABS.* Bruker AXS ins., Madison, Wisconsin, USA.

Cremer, D. & Pople, J. A. (1975). *J. Am. Chem. Soc.* **97**, 1354-1358.

Dolomanov, O.V., Bourhis, L. J., Gildea, R. J., Howard, J. A. K. & Puschmann, H. (2009). *J. Appl. Cryst.* **42**, 339-341.

Fossheim, R. (1986). *J. Med. Chem.* **29,** 305-307.

Langs, D. A., Triggle, D. (1987). *Acta Cryst.* **C43,** 707-711.

Linden, A. Safak, C. & Aydin, F. (2004). *Acta Cryst.* C**60**, o711-713.

Linden, A., Simsek, R., Gunduz, M. & Safak, C. (2005). *Acta Cryst.* C**61**, o731-734.

Martin-Leon, N., Quinteiro, M., Seoane, C., Soto, J., Mora, A., Suarez, M., Ochoa, E., Morales, A. & Bosque, J. (1995). *J. Heterocycl. Chem.* **32**, 235-238.

Morales, A. D., Garcia-Granda, S., Navarro, M. S., Diviu, A., M. & Perez-Arquero, R. E. (1996). *Acta Cryst.* C**52**, 2356-2359.

Rose, U. (1990). *Arch. Pharm.* **323**, 281-286.

Rose, U. & Draeger, M. (1992). *J. Med. Chem.* **35**, 2238-2243.

Sheldrick, G. M. (2008). *Acta Cryst.* **A64**, 112-122.

Spek, A. L. (2009). *Acta Cryst.* **D65**, 148–155.

Takahashi, D., Oyunzul, L., Onoue, S., Ito, Y., Uchida, S., Simsek, R., Gunduz, M. G., Safak, C. &

Wilcken, R., Zimmermann, M. O., Lange, A., Joerger, A. C. & Boeckler, F. M. (2013). *J. Med. Chem.* **56**, 1363-1388.

This paper was published in Acta Cryst E.

Chapter 3

Diethyl 4-(biphenyl-4-yl)-1,4-dihydropyridine-3,5-dicarboxylate

3.1 Abstract

The titled compound, $C_{24}H_{25}NO_4$, has a flattened dihydropyridine ring and phenyl groups that are synclinal to one another. The calculated angle between the two planes of the phenyl groups is 49.82 (8)^o; the axis of the biphenyl rings [C(14)-C(23)] has an 81.05 (9)^o angle to the plane of the dihydropyridine ring [C(1)-C(2)-C(4)-C(5)]. The plane of the central phenyl ring [C(14)-C(15)-C(16)-C(17)-C(18)-C(19)] has 47.77 (8)^o angle from the N(1) and C(3) axis in the dihydropyridine ring. The packing of the molecule shows strong π-stacking interactions between intermolecular phenyl rings. Intermolecular hydrogen bonds are also observed.
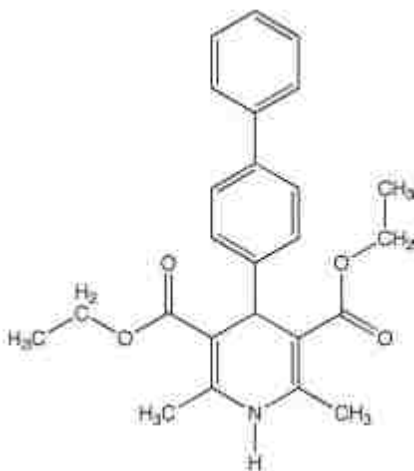
Figure 3.1: Strucure of the titled compound

3.2 Related Literature

For general structure-activity relationship study of 1,4-dihydropyridines (DHPs) on calcium channel, see: Bossert *et al.* (1981) and Triggle (2003). For the binding studies

of DHPs to multiple drug resistant protein 1 (MDR1), see: Abe *et al.* (1995), Cole *et al.* (1989), Tasaki *et al.* (1995), Vanhoefer *et al.* (1999), Tolomero *et al.* (1994), and Cindric *et al.* (2010).

3.3 Comment

Hantzsch 1,4-dihydropyridines (DHPs) are an extensively studied class of compounds that are known predominantly for their L-type voltage gated calcium channel modulation. (Bossert et al. 1981, Triggle 2003) There have been extensive structure-activity relationship (SAR) studies done on DHPs that have revealed the basic structural requirements for robust binding affinity to calcium channels. (Triggle 2003) Other studies in the field have shown that DHPs bind to multiple receptors, most notably the multiple drug resistant protein 1 (MDR1) (Abe et al. 1995, Cole et al. 1989, Tasaki et al. 1995, Vanhoefer et al. 1999, Tolomero et al. 1994, Cindric et al. 2010). Using established SAR more selective compounds can be designed for greater selectivity resulting in more clinically relevant compounds.

The title compound, $C_{24}H_{25}NO_4$, has very similar structural feature as other DHPs. Such features include a flattened boat conformation of the 1,4-DHP ring and two ester groups coplanar to the double bonds in the 1,4-DHP, with one carbonyl being cis and the other carbonyl being trans to the double bonds (Figure 1). Although the phenyl group attached at C(3) is still orthogonal to the bottom [C(1)-C(2)-C(4)-C(5)] of 1,4-DHP ring (81.05 (9)^o), it twists away from the N(1)-C(3) axis with the degree of 47.77 (8)^o. The next phenyl ring twists again, with 49.82(8)^o from the center phenyl group, and becomes almost orthogonal to the N(1)-C(3) axis [12.97(9)^o]. Upon anexpanded view, the π-π stacking between the biphenyl groups from two molecules can be easily seen (Figure

2). The distances from one biphenyl group to another are 6.771 (3) Å and 6.510 (3) Å for the two phenyl rings. The packing of this molecule also involves intermolecular hydrogen bonding between N(1)-H(1)-O(3) with a distance between H(1)-O(3) of 2.029 Å.

3.4 Synthesis and crystallization

An oven-dried 100 mL round bottom flask was charged with 1.90g of biphenyl-4-carbaldehyde, 2.86 g of ethyl acetoacetate, 2.49 mL of 14.8M ammonium hydroxide, and a magenetic stir bar. The mixture was taken up in 50mL of absolute ethanol, and the round bottom flask was fitted with a dean stark trap and heated until reflux while stirring. Reaction progress was monitored via TLC. Once the reaction was complete, excess solvent was removed via rotovap. The solution was then purified via a silica column. The product was re-crystallized into white to yellow crystalline clumps with hexane and dichloromethane (yield = 1.24g , 3.06 mmol, 29.31%).

3.4 Refinement

Crystal data, data collection and structure refinement details are summarized in Table 1. The methyl H atoms were constrained to an ideal geometry, with C -- H = 0.98 Å and U_{iso} (H) = 1.5 Ueq (C), and were allowed to rotate freely about the C -- C bonds. The rest of the H atoms were placed in the calculated positions with C -- H = 0.95 \~ 1.00 Å and refined as riding on their carrier atoms with U_{iso} (H) = 1.2 Ueq (C). The positions of amine H atoms were determined from a difference Fourier maps and refined freely along with their isotropic displacement parameters. One low-angle reflection was omitted from the refinement because its observed intensity was much lower than the calculated value as a result of being partially obscured by the beam stop.

Crystal data

C25H27NO$_4$	$\gamma = $ 73.530 (2)°
$M_r = $ 405.47	$V = $ 1031.25 (7) Å^3
Triclinic, P	$Z = 2$
$a = $ 7.3431 (3) Å	Mo $K\alpha$ radiation
$b = $ 10.6075 (4) Å	$\mu = $ 0.09 mm^{-1}
$c = $ 13.8449 (6) Å	$T = $ 100 K
$\alpha = $ 85.762 (3)°	0.15 × 0.14 × 0.13 mm
$\beta = $ 88.124 (3)°	

Data collection

Bruker SMART BREEZE CCD diffractometer	4752 independent reflections
Absorption correction: multi-scan SADABS V2012/1 (Bruker AXS Inc.)	2983 reflections with $I > 2\sigma(I)$
$T_{min} = $ 0.919, $T_{max} = $ 1.000	$R_{int} = $ 0.072
19956 measured reflections	$\theta_{max} = $ 27.6°

Refinement

$R[F^2 > 2\sigma(F^2)] = \underline{0.062}$	$\underline{0}$ restraints
$wR(F^2) = \underline{0.149}$	$\underline{\text{H atoms treated by a mixture of}}$ $\underline{\text{independent and constrained refinement}}$
$S = \underline{1.01}$	$\Delta\rho_{max} = \underline{0.43}$ e Å^{-3}
$\underline{4752}$ reflections	$\Delta\rho_{min} = \underline{-0.37}$ e Å^{-3}
$\underline{279}$ parameters	

Table 3.1: Crystal Data

D—H$\cdots A$	D—H	H$\cdots A$	$D\cdots A$	D—H$\cdots A$
C13—H13B$\cdots$O2	0.98	2.11	2.857 (3)	131.2
N1—H1$\cdots$O3^{i}	0.91 (3)	2.03 (3)	2.938 (3)	173 (2)

Symmetry code: (i) $x+1$, y, z.

Tabel 3.2 Hydrogen-bond geometry
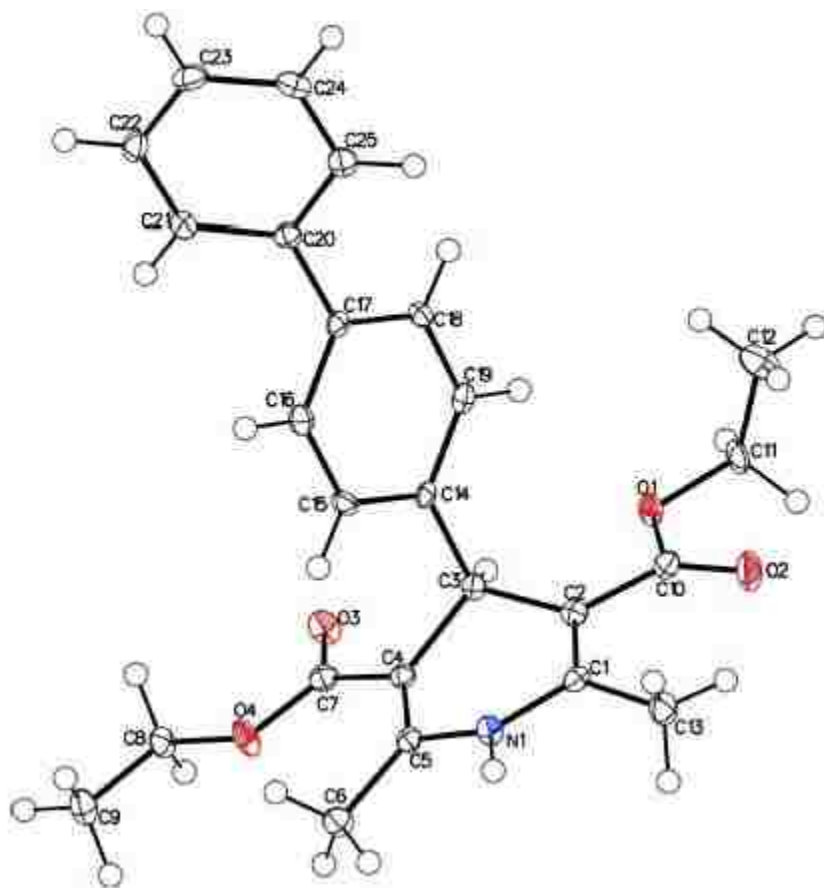
Figure 3.2 : Crystal structure of the title compound with labeling and displacement ellipsoids at the 50% probability level.
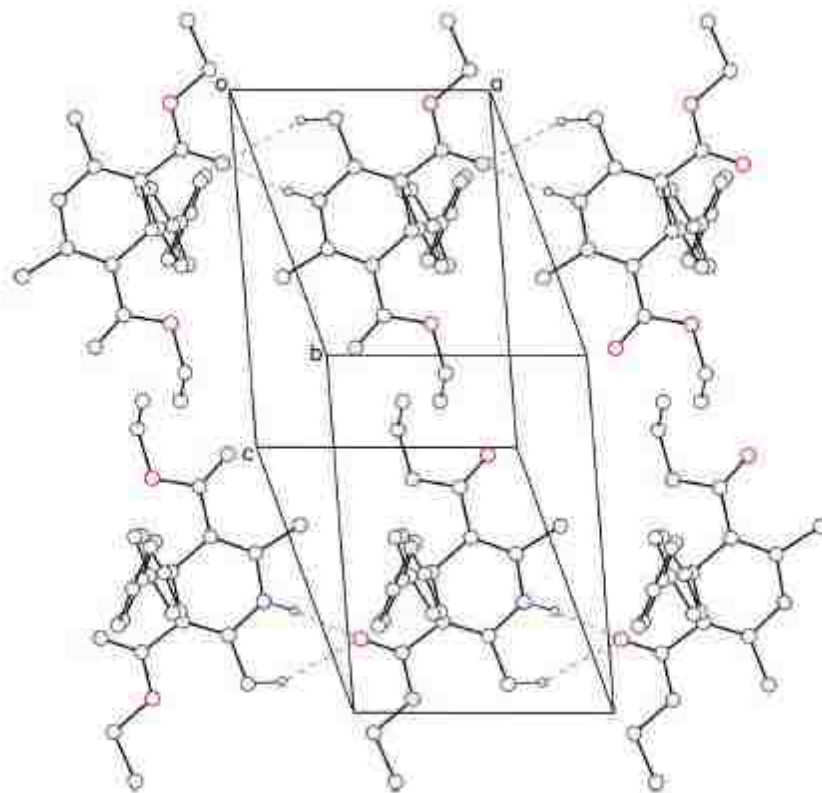
Figure 3.3: Packing diagram of the title compound, showing the intermolecular hydrogen bonds which form chain motifs running along the α axis. For the sake of clarity, H atoms that are not involved in H-bounds are removed.
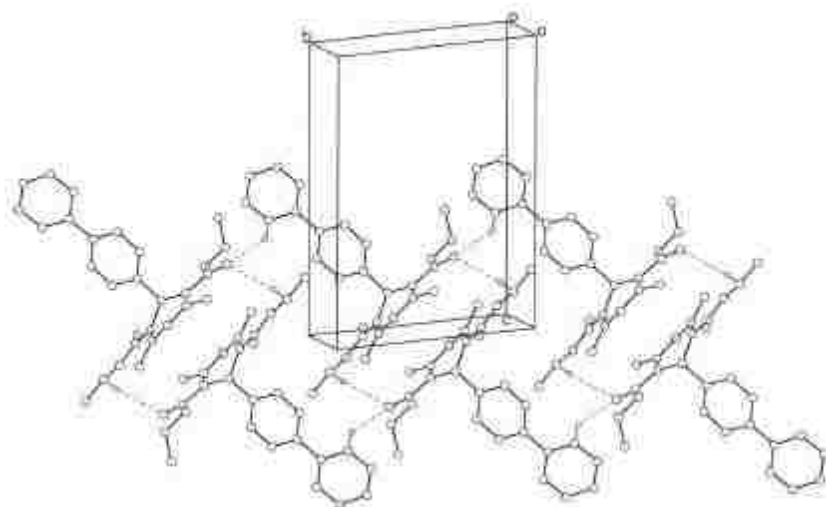
Figure 3.4: Packing diagrams of the title compound, showing intermolecular C-H ⋯ O interactions in dashed lines which cross link the molecules into a sheet motif running

slightly off the 110 plane. For the sake of clarity, H atoms not involved in the interaction are removed
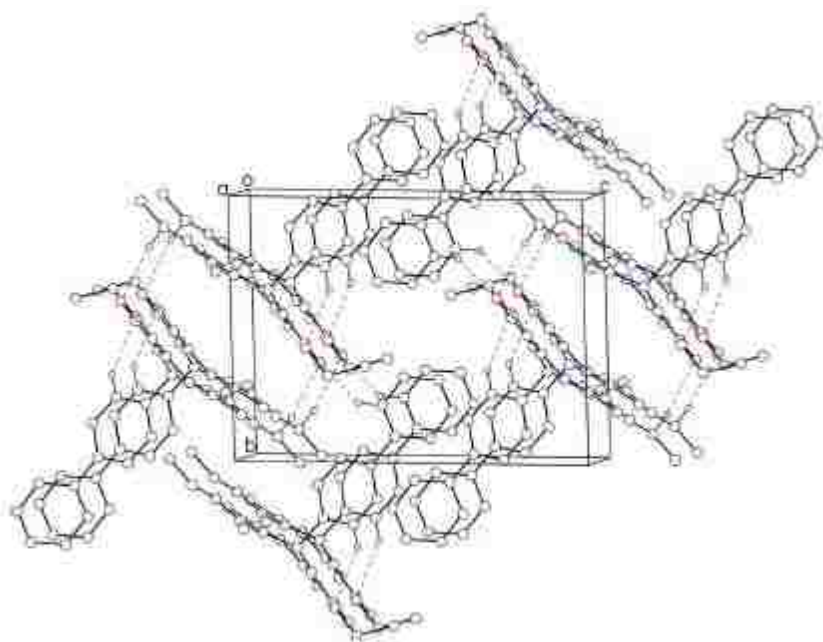
Figure 3.5: Packing diagram of the title compound. The intermolecular interaction from the three dimensional network in the crystal packing. For the sake of clarity, H atoms that are not involved in the interactions are removed.

3.5 References

Abe, T., Koike, K., Ohga, T., Kubo, T., Wada, M., Kohno, K., Mori, T., Hidaka, K. & Kuwano, M. (1995). *Br. J. Cancer.* **72**, 418-423.

Bossert, F., Meyer, H. & Wehinger, E. (1981). *Angew. Chem.* **20**, 762-769.

Bruker (2008). *APEX2*, *SAINT* and *SADABS*. Bruker AXS Ins., Madison, Wisconsin, USA.

Cindric, M., Cipak, A., Serly, J., Plotniece, A., Jaganjac, M., Mrakovcic, L., Lovakovic, T., Dedic, A., Soldo, I., Duburs, G., Zarkovic, N. & Molnar, J. (2010). *Anticancer Res.* **30**, 4063-4070.

Cole, S., Downes, H. & Slovak, M. (1989). *Br. J. Cancer.* **59**, 42-46.

Dolomanov, O. V., Bourhis, L. J., Gildea, R. J., Howard, J. A. K. & Puschmann, H. (2009). *J. Appl. Cryst.* **42**, 339-341.

Sheldrick, G. M. (2008). *Acta Cryst.* A**64**, 112–122.

Tasaki, Y., Nakagawa, M., Ogata, J., Kiue, A., Tanimura, H., Kuwano, M. & Nomura, Y. (1995). *J. Urol.* **154**, 1210-1216.

Tolomero, M., Gancitano, R., Musso, M., Porretto, F., Perricone, R., Abbadessa, V. & Cajozzo, A. (1994). *Haematologica.* **79**, 328-333.

Triggle, D. (2003). *Cell Mol Neurobiol.* **23**, 293-303.

Vanhoefer, U., Muller, M., Hilger, R., Lindtner, B., Klaassen, U., Schleucher, N., Rustum, Y., Seeber, S. & Harstrick, A. (1999). *Br. J. Cancer.* **81**, 1304-1310.

Chapter 4

Dimeric isoxazolyl-1,4-dihydropyridines inhibitors of the multidrug resistance

transporter-1 (MDR-1)

4.1 Dimeric Compounds Used as MDR1 Modulators

The multidrug resistance transporter-1's (MDR1's) role in altering the

uptake, distribution and bioavailability of xenobiotics is well known. MDR1 has

also been shown to be a major contributor to the development of MDR in cancer,

via preventing entry of therapeutically relevant drugs into the cancerous cell. As

such, MDR1 is highly investigated as a drug target both for controlling

absorption, distribution, metabolism and excretion (ADME) of clinically relevant

compounds and for the production of MDR inhibitors. However, the lack of

effective third generation inhibitors in clinical trials has cast doubt on the

usefulness of compounds that inhibit MDR in cancer treatment.[1,2,3] The

observation that dihydropyridines (DHPs) nicardipine[4] and niguldipine[5,6]

exhibit activity as inhibitors of MDR1[7] has stimulated renewed interest in DHPs

as MDR1 inhibitors and is currently being investigated by multiple groups.[8,9,10]

A relatively new approach in drug design and one that is being utilized

here, is the development of bivalent compounds.[11] Pharmacophore modeling for

MDR-1 indicates several common features for inhibitors,[12,13] notably at least two

aryl pockets, and a tether of approximately 3-5 methylenes, leading to another

functional group that possesses H-bond donor and lipophilic groups.[14] This is in

agreement with previous indications that point to the existence of at least two

spatially distant substrate binding sites inside the nucleotide binding domain

84

(NBDs).[15,16] Two distinct binding sites provide the opportunity to inhibit MDR1 in two sites at the same time and as an affect exert twice the inhibitory activity. Designing multivalent inhibitors that interact at both potential binding sites is an attractive opportunity for the synthetic chemist to design MDR1 inhibitors.

In the vein of building on this research, some groups have prepared dimeric inhibitors that have shown improved inhibitory activity verses their monomer counterparts. Chmielewski's group used quinine and quinidine as a starting point (known compounds that are transported by MDR1) and observed that dimeric derivatives have been shown to have inhibitory activity at MDR1.[17][18] Andrus's group has designed stipiamide homodimers that have shown robust MDR1 inhibitory activity.[19] The synthesized dimers were cross linked with hydropholic polyethylene glycol (PEG) based tethers and found an optimum inhibitor of MDR1 with a tether length of approximately 35 Å.[19] Early work with dimers experimented with different tether compounds include emetine, abacavir, quinine and quetiapine and have shown overall increased activity.[20,21]

Our hypothesis is that developing dimeric isoxazole-DHPs (IDHPs) should have an increase in activity, based on the existing precedent that dimers have a general trend in the literature of showing increased activity due to the possibility that MDR1 can simultaneously bind two ligands.[22,23] Thus, a polyvalent inhibitor would bind more tightly to MDR1 and thus be an effective inhibitor. Additionally, dimeric compounds may introduce an element of selectivity. In his study of dimeric tethered DHPs at the voltage gated calcium channel (VGCC), Triggle found that analogs possessing a second 1,4-DHP

nucleus or possessing an inactive pyridine were less active, leading to the

conclusion that such dimers likely do *not* bridge adjacent VGCC subunits. We

reasoned we could use this observation, together with other known VGCC

structure-activity relationships (SAR), to design greater selectivity for MDR1 into

the IDHPs. With this general goal, we employed computational modeling as a

guide to direct our synthetic efforts.
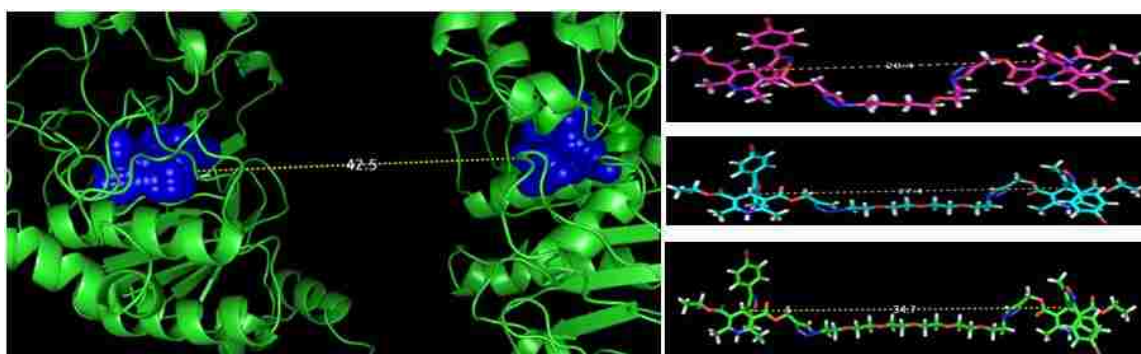
Figure 4.1: (left)The calculated distance between the Q-Site binding sites residing proximal to the nucleotide binding domains in the non-ATP bound state(apo) of MDR-1. (right) The calculated distance between the C4 position of the IDHP and the variation in the distance as the tether length increases.

Figure 4.1 shows the non-ATP bound state of MDR1 and the calculated distance

between the two NDBs. The calculated distance of 42.5 Å represents the open to the

inside conformation of MDR1 and as such will be the maximum distance that the NBDs

will be separated. The NBDs will move towards each other after ATP hydrolysis and the

42.5Å distance will become substantially shorter as a result, reaching the minimum

distance in the open-to-outside conformation of 12.7Å. Using our model of the apo state,

we used this as a guide to direct and synthesize bivalent IDHPs with a tether of 34.7Å.

This is consistent with work done by Andrus, his study utilizing stimpiamide dimers

showed that MDR1 inhibition dramatically increases with dimers that were around 20Å.

Thus, the proposed bivalent IDHPs should be an ideal substrate for MDR1 and will trap

MDR1 in an intermediate inactive state. The direct measurement of the binding affinity of MDR1 for these compounds is useful in evaluating the computer model and predicting the overall performance of other potential inhibitors. Additionally, the use of these divalent IDHP adducts can provide some valuable information on the size of the substrate-binding pocket and it ability to accommodate multiple drugs.

Our research group has previously prepared divalent DHP-fluorophore conjugates which were linked by hydrocarbon tethers,[24] but we wish to explore the potential advantages of longer PEG based tethers in this study. Due to the calculated distances between our putative targets we wanted to utilize a PEG tether due to the longer distances we wish to span, since our previous study experimented with hydrocarbon tethers, wherein folding by hydrophobic collapse was a concern. With a PEG tether we propose that a PEG won't undergo hydrophobic collapse in the binding cavity, and as such can be used as a bridge between the two DHP binding sites. This will potentially allow for both DHP sites to be blocked at the same time, without the issue of the tether folding. The end result will be halted function of MDR1.
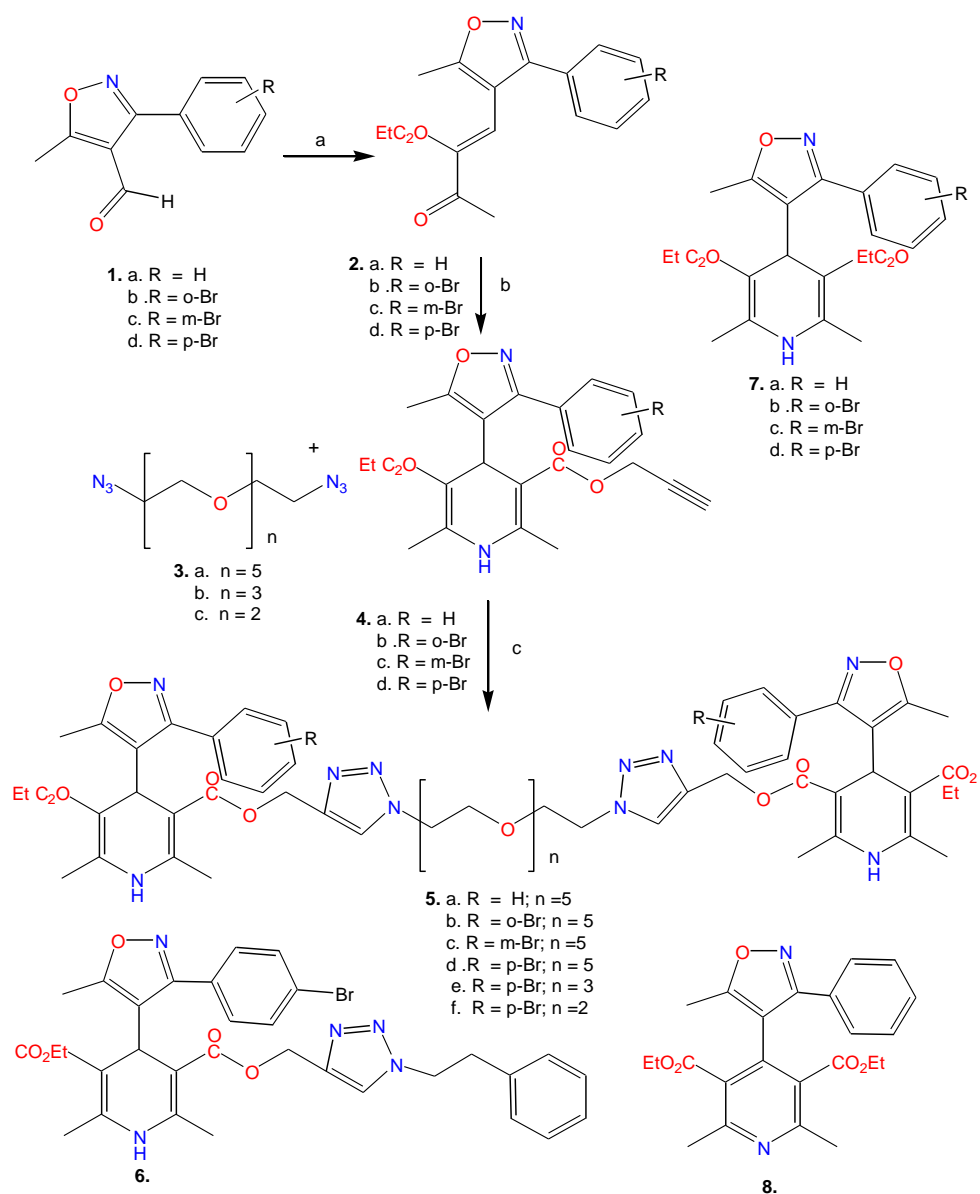
Figure 4.2: Synthetic route for synthesis dimeric IDHPs

The synthesis of a library of compounds such as this is difficult and requires

multiple synthetic steps to achieve the target compounds. The DHP substructure is

synthesized from commercially available Bromobenzaldehydes as starting materials. The

aldehyde is converted to an oxime, and followed by conversion to a

bromobenzohydroximinoyl chloride *via* reaction with N-Chloro succinimide (NCS).

Ethyl acetoacetate was used to perform a cycloaddition in the presence of sodium

88

ethoxide.[25] After the cycloaddition the carboxyl group is reduced to the hydroxyl via

Lithium Aluminum hydride (LAH) reduction.[26] The resulting hydroxyl is then oxidized

via Pyridinium Chlorochromate (PCC) to produce the isoxazolyl aldehydes (**1a-d**). *While*

these steps have been described previously, it should be noted that the isoxazole

aldehydes (1) in Scheme 4-2 were not commercially available. The isoxazole aldehydes

(**1 a-d**) were then reacted with ethyl acetoacetate in a Knoevenagel condensation reaction

to produce half of the desired IDHP(**2a-d**).[27] To produce the other half of the

unsymmetrical IDHP, boronic acid catalyzed transesterification of ethyl acetoacetate with

propargyl alcohol is used to produce prop-2-yn-1-yl 3-oxobutanoate (not shown).[28]

Prop-2-yn-1-yl 3-oxobutanoate is then reacted with the Knoevenagel product (2a-d) to

finish the Hantzsch pyridine synthesis and achieve the desired DHP substructures (**4a-**

d).[29] To attach the PEG tether to the synthesized DHP(**4a-d**)we utilized click

chemistry.[30]A commercially available diol was used as a starting material for the PEG

tether substructure. The diol was mesylated via the reaction with methanesulfonyl

chloride and a PEG dimesylate results. The dimesylate was then reacted with sodium

azide, to provide the diazides (**3a-c**). The diazide was then reacted with the

unsymmetrical DHP (**4a-d**) *via* a copper catalyzed click reaction, forming a triazole ring

in the process (**5a-d**).[31] Compound **6** was synthesized in a similar matter, utilizing the

unsymmetrical DHP(**4d**) and clicking it with an azide formed from the commercially

available phenethyl alcohol, initially envisioned as a triazole control (*vide infra*). By

varying tether lengths as well as conducting a bromine scan around the 3-isoxazolyl-

phenyl group allows us to examine SAR factors for this series of compounds.

4.2 Single Crystal X-ray Diffractometry of 7.c

The conformation of DHPs is important to their structure activity relationships, and IDHPs have particularly pronounced divergent topologies dependent on rotation about the bond joining the heterocyclic rings. In the VGCC arena, several parameters have been found to correlate with biological activity: the conformation of the esters at C-3 and C-5 of the DHP, and the sum of the six intraring torsion angle in the flattened boat conformation of the DHP. We had earlier postulated that the heterocyclic ring juncture could well adapt divergent conformations dependent on the biomolecular target. We have found single crystal x-ray diffractometry useful to help inform our computational studies on rotational barriers and drug-receptor modeling.
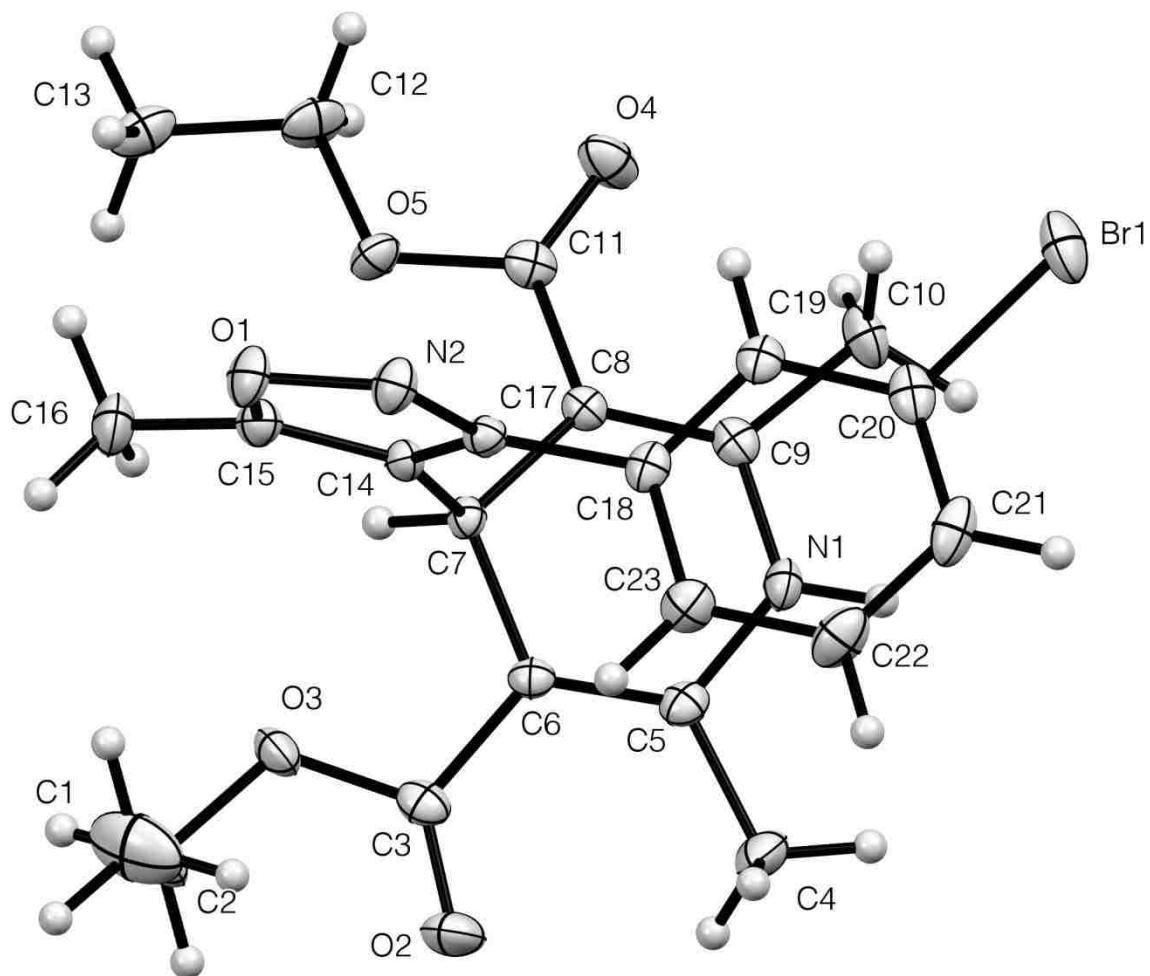
Crystal data

$C_{23}H_{25}BrN_2O_5$	
$M_r = \underline{489.36}$	$D_x = \underline{1.459}$ Mg m^{-3}
Monoclinic, $\underline{C2/c}$	Melting point: ? K
$a = \underline{17.6211\ (9)}$ Å	? radiation, $\lambda = \underline{0.71073}$ Å
$b = \underline{15.3041\ (8)}$ Å	Cell parameters from $\underline{323}$ reflections
$c = \underline{17.9370\ (9)}$ Å	$\theta = \underline{3.4}$–$\underline{28.4}°$
$\beta = \underline{112.8770\ (6)}°$	$\mu = \underline{1.88}$ mm^{-1}
$V = \underline{4456.7\ (4)}$ Å^3	$T = \underline{100}$ K
$Z = \underline{8}$	Prism, clear pale yellow
$F(000) = \underline{2016}$	$\underline{0.52} \times \underline{0.51} \times \underline{0.24}$ mm

Data collection

? diffractometer	$\underline{4567}$ independent reflections
Radiation source: ?	$\underline{4179}$ reflections with $I > 2\sigma(I)$
? monochromator	$R_{int} = \underline{0.021}$
Detector resolution: $\underline{8.3333}$ pixels mm^{-1}	$\theta_{max} = \underline{26.4}°$, $\theta_{min} = \underline{1.8}°$
Absorption correction: numerical SADABS V2012/1 (Bruker AXS Inc.)	$h = \underline{-22}\ \ \underline{21}$
$T_{min} = \underline{0.41}$, $T_{max} = \underline{0.66}$	$k = \underline{-19}\ \ \underline{19}$
$\underline{24782}$ measured reflections	$l = \underline{-22}\ \ \underline{22}$

Refinement

Refinement on $\underline{F^2}$	Secondary atom site location: ?
Least-squares matrix: full	Hydrogen site location: inferred from neighbouring sites
$R[F^2 > 2\sigma(F^2)] = \underline{0.035}$	H-atom parameters constrained

$wR(F^2) = \underline{0.098}$	$w = 1/[\sigma^2(F_o{}^2) + (0.0521P)^2 + 9.9351P]$ where $P = (F_o{}^2 + 2F_c{}^2)/3$
$S = \underline{1.07}$	$(\Delta/\sigma)_{max} = \underline{0.002}$
<u>4567</u> reflections	$\Delta\rho_{max} = \underline{1.46}$ e Å^{-3}
<u>285</u> parameters	$\Delta\rho_{min} = \underline{-0.45}$ e Å^{-3}
<u>80</u> restraints	Extinction correction: <u>none</u>

Tables containing the Fractional atomic coordinates and isotropic or equivalent isotropic

displacement parameters (Å^2), Atomic displacement parameters (Å^2), and Geometric

parameters (Å, °) are given in the **Experimental Section.**

<u>4.3</u> Important Intermolecular interactions of 7c.

There is a plausible Halogen bond in the sc-xrd, as defined by the Br1 to O3'

distance of 3.363Å and halogen to nucleophile angle of 143.1°, which are within the

tolerances for a moderate strength halogen bond according to the criteria suggested by

Auffinger [32], and Wilcken.[33] The distance of the amine is another predicted key factor

for the activity of both the VGCC and MDR. The distance of the hydrogen bound in the

structure is 0.880 Å. The crystal structure shows hydrogen bounding interactions with the

oxygen of an adjacent isoxzaole, O1 with the hydrogen bound to N1 of the DHP. This

interaction could be indicative of key hydrogen bounding interactions with a given

receptors.

<u>4.4</u> Biological Activity: Comparison of binding at MDR1, the VGCC and mGluR.

While testing at the VGCC is used to establish reactivity with a known binding

receptor for DHPs, the mGluR5 binding was used to establish general off target binding.

mGluR5 is a 7HTM and as such it shares general receptor topology and binding at other

ubiquitous 7HTM receptors. As such, mGluR5 binding can be seen as a general measure of promiscuous off target binding.

Structure	R	n	VGCC (nM)	mGluR$_5$ (nM)	MDR-1 (%)
7.a	H	0	13.9	ND	48.9[5]
7.b	o-Br	0	909	1,524	59.6
7.c	m-Br	0	208	>10,000	82.1
7.d	p-Br	0	36	>10,000	62.3
5.a	H	5	>10,000	>10,000	49.2
5.b	o-Br	5	>10,000	4,858	78.9
5.c	m-Br	5	3,766	8,638	146.6
5.d	p-Br	5	2,706	193	130.1
5.e	p-Br	3	516	546	30.4
5.f	p-Br	2	603	933	102.9
6	p-Br	0	127	1,972	202.7
8	H	0	>10,000	>10,000	102.4

Table 4.1: Summary of biological evaluation of Dimer IDHPs and relevant controls.

As a general statement, increased activity is observed with the inclusion of a triazole, as seen by both the activity of the dimers (5a-f) and with the click control (8), when comparing them to the monomers (7a-d) and the pyridine (8). The monomeric IDHPs(7a-d) exhibit robust calcium antagonist activity; and given Natale's previous work in the field this would be expected. The relationship of activity to substitution at the 3-aryl-isoxazole position is as followed *p*-(7d) > *m*-(7c) > *o*-(7b) and is consistent with previous observations. However, the range is more pronounced for the Br series, with the *p*-(7d) over 25 times more potent than the *o*-, which may be attributed to the halogen bonding evidenced in the sc-xrd. The relationship for substitution at the isoxazole 3-aryl is maintained in both monomers(7a-d) and dimers(5a-f), with the activity following a trend of m-Br > p-Br > o-Br > H, however, the m-Br (5c) and p-Br (5d) dimers have significantly more binding potency at MDR1.

The purpose of testing against three different receptor types is to examine selectivity factors that structural variations can have an effect on. The isoxazolyl-pyridine, (8) shows the greatest level of selectivity with regards to MDR1. Oxidation to the pyridine removes the potential hydrogen bound interactions from of the 1,4-dihydropyridne nitrogen, this would be predicted to abolish VGCC activity. This was found to be the case, essentially abolishing the activity at both the VGCC and mGluR$_5$, however its binding at the MDR1 was comparable to the cyclosporine A control. The effect of dimerization on the other hand is dramatic when considering selectivity. The effect of differing tether lengths presents a potential factor to engineer selectivity into compounds, with longer tethers being more selective for MDR1, and shorter tether showing more polypharmacology. Contrasting monomeric (7a-d) and dimeric (5a-f) compounds VGCC activity is essentially abolished for the dimer. The most active MDR1 inhibitor in the series,(6) shows a good deal of poly pharmacology which is consistent with the observation of shorter tethered compounds in the series. A more in-depth examination of the compound and the factors that contribute to its activity will be examined with computational modeling.

4.5 Computational Model for the most efficacious IDHP 6 at MDR1.

The mammalian MDR1 homology model that was engineered previously is utilized again here to explore the SAR function of the best compound.[34] The proposed binding box that was established in our previous work is the site that was used to localize binding calculations. The best MDR1 inhibitor, compound **6**, was calculated to bind in the previously defined, medium affinity cohort with the tethered end of the compound

extending into the high affinity cohort. The position of the compound as a whole is in

agreement with previous generations of tethered compound development.
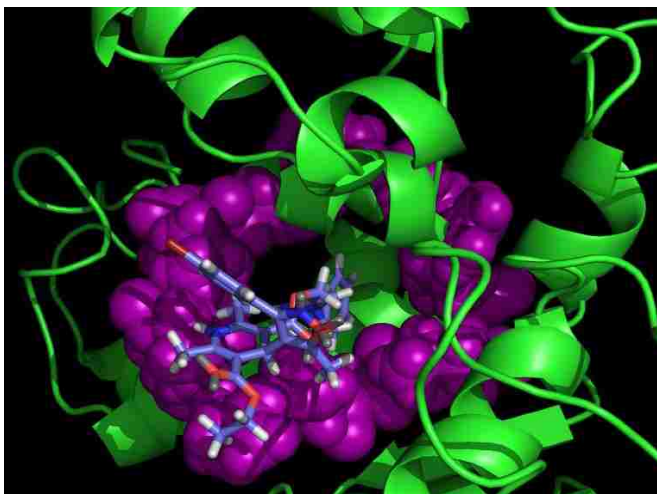
Figure 4.3: Binding calculations of the best binder in the series, compound **6** Table 4-1.
Amino acid residues highlighted in purple are the overlap between the DHP covalent
affinity site and the calculated binding site predicted by Q-site finder (Chapter 1, *op cit*).

A 6Å sphere around compound **6** was then examined to establish close contacts

and construct an SAR. The process taken to establish close contacts and develop an SAR

is identical to that taken in the first generation of compound development (Chapter 1). As

such, the process for this generation of SAR development is truncated and simplified, by

comparison. To simplify the close contact interactions to a manageable amount of data

compound **6** was broken done into three defined binding regions.
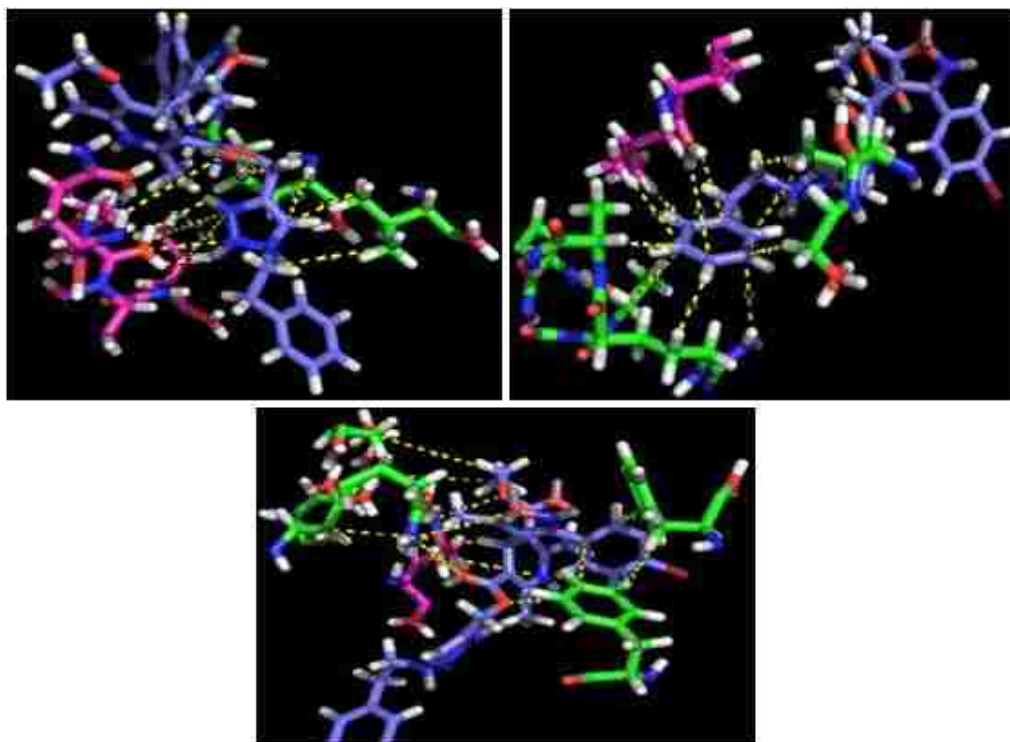
Figure 4.4: Predicted close contact interactions of compound 6.

Close contact interactions were then consolidated into a single figure (Figure 4.4), to produce an SAR. The majority of interactions new to this series are consolidated on the triazole substructure along with defined anchoring interaction on the phenethyl portion of the compound. This is in addition to the interactions that anchor the IDHP substructure, resulting in a logical increase in binding affinity.

The dimeric compounds were also examined by computational modeling. The compounds where found to have a number of binding interactions with the PEG tether clustered in the vicinity of the ATP binding site of MDR1. Thus, the enhanced binding of dimers my simply arise from the sum of both IDHPs which cluster on the edge of the site, in addition to the PEG interactions with polar amino acid residues in the ATP site.

The improved activity is another positive trend when comparing drug development generations. The central pharmacophore of the first generation compounds, the 3-phenyl-

5-methyl-IDHP, exhibited an inhibitory activity of 48.9% versus cyclosporine A. The

currently most active compound **6** exhibited an inhibitory activity of 202.7%, twice as

efficacious as the cyclosporine A control, a substantial and significant improvement.

Given that cyclosporine A inhibition is known to be around 800-900 nMol[35] at MDR1,

and that compound **6** shows roughly twice the inhibition of cyclosporine A. Thus,

compound **6** can then be assigned as a sub mMol inhibitor.
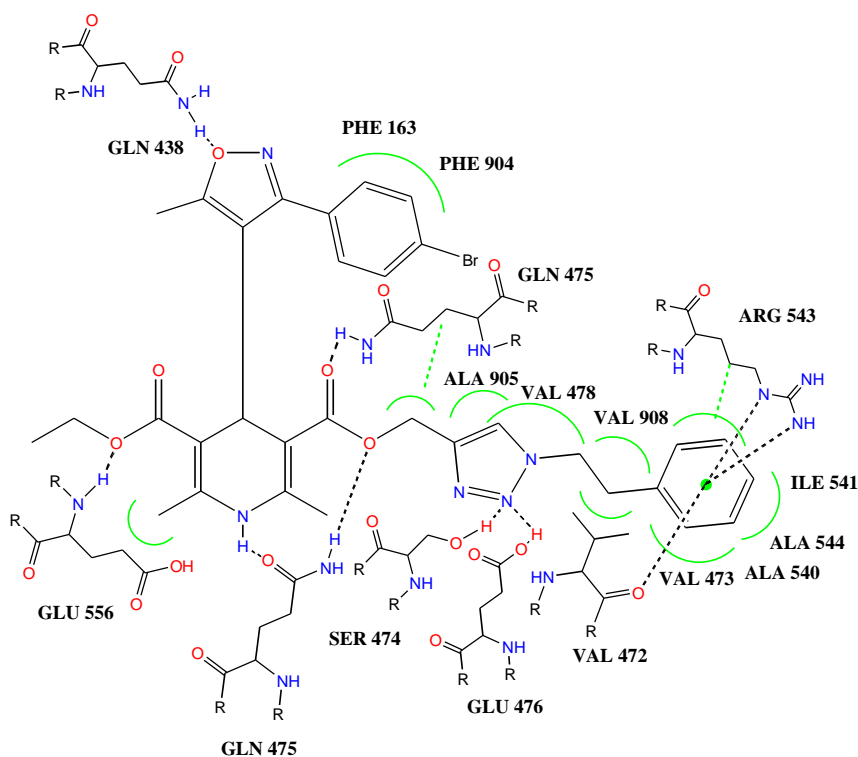
Figure 4.5: Computational Drug-receptor interaction for the most active compound at
MDR1.

    With the general trend for this generation of compound showing that dimerization

increases activity, we want to further explore selectivity factors that we can introduce

with synthetic modifications. The next generation of compound development (*vide infra*,

Chapter 5) will focus on increasing selectivity factors while retaining our present level of

inhibitory activity. With our lead compound **6** being more inherently "drug like" than the

dimer compound (based primarily on the MW guidelines of Lipinski) our focus will be

directed at modifications to the compound **6** core structure. With this in mind, we examined the aspects that the previous generations have established and what aspects of the SAR we can leverage to increase selectivity. The continued examination and progress to this goal will be elaborated on in future chapters.

4.6 **Experimental**

Synthesis of 1-Azido-2-[2-(2-{2-[2-(2-azido-ethoxy)-ethoxy]-ethoxy}-ethoxy)-ethoxy]-ethane. (3.a.) An oven dried round bottom flask (10mL) was charged with 1.0g of hexaethylene glycol (0.282 mmol), 0.717g of Et$_3$N, and 6.0mL of CH$_2$Cl$_2$ with a magnetic stir bar at room temperature. The round bottom was then capped with a rubber septa placed under an argon atmosphere. A solution of CaCl$_2$ and water (25g/200mL) was then made and placed in an insulated container. The round bottom was then placed in the CaCl$_2$/water solution and dry ice was added, the solution was then allowed to reach -25°C. 0.830mL of MsCl was then added via gas-tight syringe. The reaction was then kept at -25°C for two hours. The reaction yielded a white-cream solution. Excess solvent was then removed via rotovap. The same 10mL round bottom was then charged with 8mL of EtOH and 0.464g of NaN$_3$ at room temperature. The round bottom was fitted with a condenser and was then heated to reflux (79-80°C) for an hour. The reaction yielded an orange solution. The solution was then extracted with EtOAc and brine three times, and dried over NaSO$_4$. The solution was then contracted *via* rotovap yielding yellow-gold oil. (1.187g, 3.52 mmol, 98%)

^{1}H NMR: (CDCl$_3$) δ 3.54 (bs 16H), 3.26 (bs 4H), 1.5 (s 4H)

^{13}C NMR: (CDCl$_3$) δ 70.51, 69.88, 50.33

MS: *m/z* = 332.18 (m+ 1 ,100% rel. intensity) 333.156 (100), 373.24(70)

TLC: SiO_2; EtOAc; R_f = 0.49

1-Azido-2-{2-[2-(2-azido-ethoxy)-ethoxy]-ethoxy}-ethane (3.b.)

¹H NMR: (CDCl₃) δ 3.54 (bs 8H), 3.25(bs 4H), 1.46 (s 4H)

¹³C NMR: (CDCl₃) δ 71.23, 68.75, 51.02

TLC: SiO_2; EtOAc 4:1 R_f = 0.36

1-Azido-2-[2-(2-azido-ethoxy)-ethoxy]-ethane (3.c.)

¹H NMR: (CDCl₃) δ 3.53 (bs 4H), 3.25(bs 4H), 1.27(bs 4H)

¹³C NMR: (CDCl₃) δ 70.83, 68.36, 50.56

TLC: SiO_2; EtOAc 4:1 R_f = .46

General synthesis of 4-Bromo-benzaldehyde oxime. An oven dried round bottom (250mL) was charged with 4.3g of 4-bromobenzaldhyde, 3.012g of NH₂OH*HCl, and 5.27g of NaCH₃CO₂. A mixture of THF:EtOH:H₂O(2:1:1) was made (60mL) and added at room temperature to the round bottom along with a magnetic stir bar. The round bottom was then capped and allowed to stir for 72 hours. The reaction yielded a white-cream color solution. The solution was then extracted with CHCl₃ and Brine three times, and dried over NaSO₄. The solution was then concentrated via rotovap yielding a white solid. (4.24g, 21.692 mmol, 99%)

¹H NMR: (CDCl₃) δ 8.08 (d 1H J = 2.20Hz), 7.51 (d 2H J = 0.01Hz), 7.46 (d, 2H J = 0.01), 2.18 (s 1H)

¹³C NMR: (CDCl₃) δ 149.41, 132.04, 130.78, 128.44, 124.33

MS: *m/z* = 199 (M+, 100% rel. intensity), 240 ([M+]+CH₃CN, 100)

TLC: SiO_2; Hexane:EtOAc 9:1 R_f = 0.22

mp: 112°C (dec.)

2-Bromo-benzaldehyde oxime

^{1}H NMR: (CDCl$_3$) δ 8.54 (s 1H), 7.58 (d 2H J = 0.01Hz), 7.26 (d 2H J = 0.01), 2.15 (s 1H)

^{13}C NMR: (CDCl$_3$) δ 149.83, 133.18, 131.26, 127.62, 127.45, 123.86

TLC: SiO$_2$; Hexane:EtOAc 9:1 R$_f$ = 0.32

mp: 94°C (dec.)

3-Bromo-benzaldehyde oxime

^{1}H NMR: (CDCl$_3$) δ 8.10 (s 1H), 7.74 (s 1H), 7.52 (q 1H J = 0.01Hz), 7.50 (q 1H J = 0.01Hz), 2.13 (s 1H)

^{13}C NMR: (CDCl$_3$) δ 149.06, 133.87, 132.99, 130.30, 129.79, 125.69, 122.93

TLC: SiO$_2$; Hexane:EtOAc 9:1 R$_f$ = 0.52

mp: 58°C (dec.)

General synthesis of Bromobenzohydroximinoyl chloride. An oven dried round bottom (250mL) was charged with a magnetic stir bar, 2.78g (0.556 mmol) of 4-bromobenzaldehyde oxime, 2.07g (0.276 mmol) of NCS, 0.188 g of pyridine, and 13.2mL of CHCl$_3$ at room temperature. A mineral oil bath was then heated to 40°C and the round bottom was then placed in the bath for five hours. The reaction yielded a light yellow solution. The solution was then extracted with CH$_2$Cl$_2$ and brine three times with 50mL, and dried over NaSO$_4$. The solution was then contracted via rotovap yielding a white-cream solid. (3.139 g; 13.477 mmol; 96.95%)

^{1}H NMR: (CDCl$_3$) δ 7.70 (d 2H J = 9.23Hz), 7.55 (d, 2H J = 9.65Hz), 2.21 (s 1H)

^{13}C NMR: (CDCl$_3$) δ 164.24, 130.24, 131.26, 132.51, 125.67

MS: m/z = 232(M+,100% rel. intensity) 231.94 (M+1, 100), 273 ([M+]+CH$_3$CN 60)

mp: 80.5°C (dec.)

TLC: SiO$_2$; Hexane:EtOAc 10:1 R$_f$ = 0.36

General synthesis of 3-(4-Bromo-phenyl)-5-methyl-isoxazole-4-carboxylic acid ethyl ester. An oven dried round bottom(500mL) was charged with 5.069g (1.188 mmol) of 4-Bromobenzohydroximinoyl chloride, and left under the high vacuum over night. Another oven dried round bottom (500mL) was charged with 274.99mL of EtOH, and a magnetic stir bar, the round bottom was then capped with a rubber septum and placed under an argon environment. 1.29g (0.030 mmol) of Na was then weight out and placed in the EtOH, the solution was then stirred and the Na was allowed to dissolve. The round bottom with 4-Bromobenzohydroximinoyl chloride was then removed from the high vacuum and 7.32 g (0.953 mmol) of ethyl acetoacetate was added. The round bottom was then capped with a rubber septum and placed under an argon environment. The Na/EtOH mixture was then added to the 4-Bromobenzohydroximinoyl chloride/ ethyl acetoacetate mixture at room temperature. The round bottom was then capped with a rubber septum and placed under an argon environment. The solution was then stirred for three hours. The solution was then extracted with CHCl$_3$ and Brine three times with 50 mL, and dried over NaSO$_4$. The solution was then concentrated via rotovap yielding a yellow oil. The solution was then purified *via* a silica column. The purification compound yielded a white solid (2.109g, 6.80 mmol, 45.43%)

^{1}H NMR: (CDCl$_3$) δ 7.55 (d 2H J = 8.56Hz), 7.50 (d 2H J = 8.56Hz) 4.25 (q 2H J = 7.09Hz), 2.71 (s 3H), 1.24 (t 3H J = 7.09Hz)

^{13}C NMR: (CDCl$_3$) δ 176.06, 161.72, 161.63, 131.19, 131.04, 127.42, 124.27, 108.29, 60.85, 29.71, 14.06, 13.66

MS: m/z = 309 (M+, 100% rel. intensity) 311.02(M+2, 100), 350.78 ([M+]+CH$_3$CN, 50)

TLC: SiO$_2$; Hexane:EtOAc 10:1 R$_f$ = 0.33

mp: 71-72°C (dec.)

3-(2-Bromo-phenyl)-5-methyl-isoxazole-4-carboxylic acid ethyl ester

^{1}H NMR: (CDCl$_3$) δ 7.63 (d 1H J = 7.34Hz), 7.36 (s 1H), 7.32 (s 1H), 7.31 (s 1H), 4.12 (q 2H J = 6.36Hz), 2.74 (s 1H), 1.05 (t 3H J = 5.87Hz)

^{13}C NMR: (CDCl$_3$) δ 170.42, 157.30, 156.77, 127.66, 126.19, 126.06, 122.29, 188.82, 104.95, 55.84, 8.45

TLC: SiO$_2$; Hexane:EtOAc 10:1 R$_f$ = 0.26

3-(3-Bromo-phenyl)-5-methyl-isoxazole-4-carboxylic acid ethyl ester

^{1}H NMR: (CDCl$_3$) δ 7.79 (s 1H), 7.59 (q 2H J = 7.83Hz), 7.31 (t 1H J = 7.83Hz), 4.26 (q 2H J = 6.85Hz), 2.73 (s 3H), 1.25 (t 3H J = 6.85Hz)

^{13}C NMR: (CDCl$_3$) δ 171.51, 156.96, 156.46, 127.97, 127.68, 125.70, 124.75, 123.32, 117.10, 103.62, 56.13, 8.84

TLC: SiO$_2$; Hexane:EtOAc 10:1 R$_f$ = 0.38

General synthesis of [3-(Bromo-phenyl)-5-methyl-isoxazol-4-yl]-methanol. An oven dried 100ml 2-neck round bottom was charged with 0.434g (1.40mmol) and a magnetic stir bar and the vessel was sealed and placed under a vacuum. A oven dried condenser was then attached to the 2 neck round bottom and the system was seal and placed under a vacuum and flushed with argon, this process was performed three times. The 2-neck round bottom was then placed in an ice bath and was allowed to reach 0°C. Freshly

distilled THF (10ml) was then added to the 2-neck round bottom and the solution was again allowed to reach 0ºC. 0.065g (0.0025 mmol) of LiAlH$_4$ was then added in potions to the solution, there was slight foaming that was observed. The reaction was then left to react and was allowed to come to room temperature. Reaction progress was checked by TLC, after the reaction was completed the mixture was quenched with sodium sulfate decahydrate (1g), foaming was observed. The solution was then purified *via* filtering it threw a silica plug with Et$_2$O, the resulting solution was then concentrated *via* rotovap yielding a yellow oil. (0.283g, 1.06mmol, 75.5%)

^{1}H NMR: (CDCl$_3$) δ 7.70 (d 1H J = 6.85Hz), 7.61 (d 2H J = 8.07), 7.48 (d 2H J = 8.07Hz), 7.38 (d 1H J = 6.85Hz), 4.43 (s 1H), 4.39 (s 2H), 2.34 (s 3H)

^{13}C NMR: (CDCl$_3$) δ 168.75, 161.62, 132.09, 129.84, 128.01, 124.26, 112.69, 53.73, 11.17

MS: *m/z* = 266.98 (M+, 80% rel. intensity), 307.24([M+]+CH$_3$CN, 70), 533.84(M$_2$+ 30)

TLC: SiO$_2$; Hexane:EtOAc:CH$_2$Cl$_2$ 3:1:1 R$_f$ =.086

[3-(2-Bromo-phenyl)-5-methyl-isoxazol-4-yl]-methanol

^{1}H NMR: (CDCl$_3$) δ 7.64 (s 1H), 7.43 (s 1H), 7.35 (s 1H), 7.30 (s 1H), 4.35 (s 2H), 2.47 (s 3H)

^{13}C NMR: (CDCl$_3$) δ163.52, 157.58, 128.20, 126.99, 126.35, 122.76, 118.16, 109.70, 49.22, 6.63

TLC: SiO$_2$; Hexane:EtOAc:CH$_2$Cl$_2$ 3:1:1 R$_f$ =.12

[3-(3-Bromo-phenyl)-5-methyl-isoxazol-4-yl]-methanol

^{1}H NMR: (CDCl$_3$) δ 7.96 (s 1H), 7.73 (s 1H), 7.56 (s 1H), 7.44(s 1H), 7.31 (s 1H), 4.35 (s 2H), 2.44 (s 3H)

^{13}C NMR: (CDCl$_3$) δ 164.15, 156.55, 127.98, 126.39, 125.63, 122.15, 118.09, 108.12, 48.56, 6.63

TLC: SiO$_2$; Hexane:EtOAc:CH$_2$Cl$_2$ 3:1:1 R$_f$ =.11

(5-Methyl-3-phenyl-isoxazol-4-yl)-methanol

^{1}H NMR: (CDCl$_3$) δ 7.73 (d 2H J = 9.54Hz), 7.36 (d 2H J = 9.54Hz), 7.22 (s 1H), 4.40 (s 1H), 2.29 (s 3H)

^{13}C NMR: (CDCl$_3$) δ 168.76, 162.50, 129.76, 128.81, 128.24, 113.10, 53.04, 10.93

TLC: SiO$_2$; Hexane:EtOAc:CH$_2$Cl$_2$ 3:1:1 R$_f$ =0.08

General synthesis of 3-(4-Bromo-phenyl)-5-methyl-isoxazole-4-carbaldehyde. (1.d.)

An oven dried 200ml round bottom was charged with 0.283g (1.06mmol) of [3-(4-Bromo-phenyl)-5-methyl-isoxazol-4-yl]-methanol, 15ml of dichloromethane, 2.04g of anhydrous magnesium sulfate and a magnetic stir bar. .415g of pyridinium chlorochromate was then added and the vessel was sealed and allowed to react for 2 hours. Reaction progress was checked by TLC, once the reaction was complete excess solvent was removed via rotovap. The solution was then purified via a silica column. The purification yielded yellow oil. (.277g 1.04 mmol, 98%)

^{1}H NMR: (CDCl$_3$) δ 9.95 (s 1H), 7.65 (d 2H J = 7.84Hz), 7.61(d 2H J = 7.84Hz), 2.79 (s 3H)

^{13}C NMR: (CDCl$_3$) δ 183.87, 177.40, 161.16, 132.18, 130.51, 126.07, 125.19, 115.04, 12.94

MS: *m/z* =264.97 (M+, 70% rel. intensity), 306.81 ([M+]+CH$_3$CN,60), 530.09 (M$_2$+ 30)

TLC: SiO$_2$; Hexane:EtOAc 4:1 R$_f$ =0.18

3-(2-Bromo-phenyl)-5-methyl-isoxazole-4-carbaldehyde. (1.d.)

¹H NMR: (CDCl₃) δ 9.68 (s 1H), 7.72 (d 1H J = 7.83Hz), 7.46 (d 2H J = 5.38Hz), 7.39 (s 1H), 2.79 (s 3H)

¹³C NMR: (CDCl₃) δ179.55, 170.72, 157.22, 128.54, 127.06,, 124.43, 122.99, 118.26, 8.31

TLC: SiO₂; Hexane:EtOAc 4:1 R$_f$ = 0.14

3-(3-Bromo-phenyl)-5-methyl-isoxazole-4-carbaldehyde. (1.c.)

¹H NMR: (CDCl₃) δ 9.61 (s 1H), 7.65 (s 1H), 7.43 (s 1H), 7.35 (s 1H), 7.30 (s 1H), 2.76 (s 3H)

¹³C NMR: (CDCl₃) δ 186.56, 178.36, 168.03, 133.45, 129.78, 124.21, 121.89, 119.45, 13.05

TLC: SiO₂; Hexane:EtOAc 4:1 R$_f$ = 0.84

5-Methyl-3-phenyl-isoxazole-4-carbaldehyde. (1.a)

¹H NMR: (CDCl₃) δ9.90 (s 1H), 7.65 (d 2H J = 6.36Hz), 7.47 (d 2H J = 6.36Hz), 7.23 (s 1H), 2.72 (s 3H)

¹³C NMR: (CDCl₃) δ 194.36, 168.96, 166.03, 132.67, 130.05, 128.93, 128.05, 109.77, 12.31

TLC: SiO₂; Hexane:EtOAc 4:1 R$_f$ = 0.21**General synthesis of 2-Acetyl-3-[3-(4-bromo-phenyl)-5-methyl-isoxazol-4-yl]-acrylic acid ethyl ester**. (2.d.) An oven dried 50mL round bottom was charged with 0.95g of 5-methyl-3-phenyl-1,2-oxazole-4-carbaldehyde, 0.799g of Ethyl Acetoacetate, 4 mL of Benzene where added at room temperature. The solution was allowed to stir, and 0.1325g of glacial acidic acid and 0.054g of piperidine was added. The round bottom was then fitted with a Dean-Stark trap and a condenser. The solution was then allowed to reflux for three hours; with the reaction progress

monitored by TLC. The solution was then cooled to room temperature and the excess solvent was removed via rotovap. The solution was then purified via a silica column. The purification yielded yellow oil. (0.761g, 2.53 mmol, 52%)

^{1}H NMR: (CDCl$_3$) δ 7.54 (d 2H J = 9.78Hz), 7.40 (d 2H J = 8.56Hz), 7.33 (s 1H), 4.13 (q 2H J = 7.09Hz), 2.35 (s 3H), 2.19 (s 3H), 1.20 (t 3H J = 7.09Hz)

^{13}C NMR: (CDCl$_3$) δ 194.12, 169.17, 165.80, 160.44, 137.70, 132.11, 129.50, 131.45, 127.45, 124.46,109.55, 61.63, 13.75, 12.19

MS: *m/z* =377.03 (M+, 50% rel. intensity) 418.45 ([M+]+CH$_3$CN, 100)

TLC: SiO$_2$; Hexane:EtOAc 1:1 R$_f$ = 0.39

2-Acetyl-3-[3-(2-bromo-phenyl)-5-methyl-isoxazol-4-yl]-acrylic acid ethyl ester. (2.b.)

^{1}H NMR: (CDCl$_3$) δ 7.65 (s 1H), 7.54 (s 1H), 7.36 (s 1H) 7.24 (s 1H), 7.10 (s 1H), 4.17 (q 2H J = 6.57Hz), 2.37 (s 3H), 2.15 (s 3H), 1.17 (t 3h J = 6.98Hz)

^{13}C NMR: (CDCl$_3$) δ 194.36, 168.96, 166.03, 161.50, 138.26, 132.30, 130.71, 128.93, 128.05, 109.77, 61.60, 27.82, 13.79, 12.13

TLC: SiO$_2$; Hexane:EtOAc 1:1 R$_f$ = 0.41

2-Acetyl-3-[3-(3-bromo-phenyl)-5-methyl-isoxazol-4-yl]-acrylic acid ethyl ester. (2.c.)

^{1}H NMR: (CDCl$_3$) δ 7.65 (s 1H), 7.43 (s 1H), 7.35 (s 1H), 7.30 (s 1H), 7.68 (s 1H), 4.15 (q 2H J = 6.84Hz), 2.34 (s 3H), 2.17 (s 3H), 1.16 (t 3H J = 5.42Hz)

^{13}C NMR: (CDCl$_3$) δ 194.24, 169.12, 165.83, 162.78, 148.65, 137.68, 132.11, 130.41, 131.96, 124.93, 127.45, 110.15, 59.67, 24.65, 14.04, 12.18

TLC: SiO$_2$; Hexane:EtOAc 1:1 R$_f$ = 0.30

2-Acetyl-3-(5-methyl-3-phenyl-isoxazol-4-yl)-acrylic acid ethyl ester. (2.a.)

¹H NMR: (CDCl₃) δ 7.57 (d 2H J = 12.72Hz), 7.44 (d 2H J = 12.72Hz), 7.25 (s 1H), 3.99 (q 2H J = 7.52Hz), 2.40 (s 3H), 2.37 (s 3H), 1.14 (t 3H J = 6.05Hz)

¹³C NMR: (CDCl₃) δ 194.36, 168.96, 166.03, 161.50, 137.26, 132.67, 128.93, 128.05, 109.77, 61.60, 27.82, 13.79, 12.31

TLC: SiO₂; Hexane:EtOAc 1:1 R$_f$ = 0.39

Synthesis of 3-Oxo-butyric acid prop-2-ynyl ester. An oven dried round bottom(250mL) was charged with a magnetic stir bar, 4.64g of Ethyl Acetoacetate, 2.00g of propargyl alcohol, .22g of boric acid, and 40mL of Toluene added at room temperature. The round bottom was then fitted with a dean stark trap, a condenser and a drying tube. The solution was then heated to reflux and left for 144 hours. The reaction yielded a light red solution. The solution was then purified via a silica column. The purification compound yielded yellow oil. (2.868 g, 20.46 mmol, 57%)

¹H NMR: (CDCl₃) δ 4.68 (d 2H J = 2.45Hz), 3.46 (s 2H), 2.49 (t 1H J = 2.45Hz), 2.22 (s 3H),

¹³C NMR: (CDCl₃) δ 200.03, 166.27, 104.98, 89.06, 52.60, 49.56, 30.08

MS: m/z = 140.047 (M+, 100% rel. intensity) 142.07(M+2, 90), 183.78([M+2]+CH₃CN, 60)

TLC: SiO₂; Hexane:EtOAc 4:1 R$_f$ = 0.18

General Synthesis of 4-[3-(Bromo-phenyl)-5-methyl-isoxazol-4-yl]-2,6-dimethyl-1,4-dihydro-pyridine-3,5-dicarboxylic acid diethyl ester. (7.d.) An oven dried 100ml round bottom was charged with 0.107g (0.40mmol) of 3-(4-Bromo-phenyl)-5-methyl-isoxazole-4-carbaldehyde, 0.11g (0.014 mmol) of ethyl acetoacatate, 50ml of benzene

and a magnetic stir bar. The solution was allowed to stir at room temperature. 0.10ml of 30% aqueous ammonia was measured out along with 0.90ml of methanol, the mixture was then added to the 100ml round bound bottom containing (2Z)-2-[(5-methyl-3-pheyl-1,2-oxazol-4-yl)methylidene]-3-oxobutanoate. The round bottom was then fitted with an oven dried condenser and the solution was brought to reflux (70ºC). The reaction process was monitored via TLC. Once complete the solution was then cooled to room temperature and the excess solvent was removed via rotovap. The solution was then purified via recrystallized from ethyl acetate and hexanes to give yellow crystals (0.084g, 0.0411 mmol, 42.92%).

^{1}H NMR: (CDCl$_3$) δ 7.55 (d 2H J = 8.4Hz), 7.37 (d 2H J = 8.7Hz), 5.06 (s 1H), 5.02 (bs 1H), 3.52 (s 6H), 2.43 (s 3H)

^{13}C NMR: (CDCl$_3$) δ167.27, 166.26, 162.71, 145.31, 143.76, 143.52, 131.24, 130.72, 130.01, 122.88, 119.46, 101.14, 59.85, 51.31, 29.29, 29.16, 19.35, 14.46, 11.46

MS: *m/z* = 489.15 (M+, 100% rel. intensity), 530.36([M+]+CH$_3$CN, 70)

IR: cm^{-1} 2927.62, 2831.02, 1741.66, 1259.19, 1179.41, 1156.61, 727.32

TLC: SiO$_2$; Hexane:EtOAc 4:1 R$_f$ = 0.17

4-[3-(2-Bromo-phenyl)-5-methyl-isoxazol-4-yl]-2,6-dimethyl-1,4-dihydro-pyridine-3,5-dicarboxylic acid diethyl ester. (7.b.)

^{1}H NMR: (CDCl$_3$) δ 7.60 (d 1H J = 7.91Hz), 7.31 (d 1H J = 7.40Hz), 7.24 (d 1H J = 5.90Hz), 7.18 (d 1H J = 7.53Hz), 4.95 (s 1H), 4.15 (q 2H J = 4.64Hz), 4.13 (q 2H J = 4.64Hz), 2.58 (s 3H), 1.96 (s 6H), 1.25 (t 6H J = 7.15Hz)

^{13}C NMR: (CDCl$_3$) δ 167.33, 165.60, 162.95, 144.54, 132.46, 132.25, 130.00, 126.24, 125.01, 118.27, 100.47, 59.79, 29.24, 19.61, 14.61, 11.54

HRMS: calculated for $C_{23}H_{26}BrN_2O_5$ 489.1023 found 489.1025

MS: *m/z* = 489 (M+, 100)

IR: cm^{-1} 2917.91, 22831.02, 1734.06, 1361.76, 1213.60, 1164.17, 746.23

TLC: SiO$_2$; Hexane:EtOAc 4:1 R$_f$ = 0.07

4-[3-(3-Bromo-phenyl)-5-methyl-isoxazol-4-yl]-2,6-dimethyl-1,4-dihydro-pyridine-3,5-dicarboxylic acid diethyl ester. (7.c.)

^{1}H NMR: (CDCl$_3$) δ 7.59 (s 1H), 7.56 (s 1H), 7.55(s 1H), 7.33 (s 1H), 5.05 (s 1H), 4.16 (q 2H J = 3.76Hz), 4.09 (q 2H J = 3.76Hz), 2.54 (s 3H), 2.06 (s 6H), 1.25 (t 6H J = 7.03Hz)

^{13}C NMR: (CDCl$_3$) δ 167.27, 166.09, 162.48, 144.08, 133.18, 132.50, 129.21, 128.44, 121.64, 119.41, 101.00, 59.87, 29.41, 19.51, 14.51, 11.50

HRMS: calculated for $C_{23}H_{26}BrN_2O_5$ 489.1028 found 489.1025

MS: *m/z* = 489 (M+, 100) 530 ([M+2]+CH$_3$CN, 20)

IR: cm^{-1} 3001.51, 2975.15, 1737.86, 1351.12, 1224.92, 731.45

TLC: SiO$_2$; Hexane:EtOAc 4:1 R$_f$ = 0.26

2,6-Dimethyl-4-(5-methyl-3-phenyl-isoxazol-4-yl)-1,4-dihydro-pyridine-3,5-dicarboxylic acid diethyl ester. (7.a.)

^{1}H NMR: (CDCl$_3$) δ7.57 (d 2H J = 7.62Hz), 7.30 (d 2H J = 7.62Hz), 7.23 (s 1H), 4.98 (s 1H), 4.09 (q 2H J = 6.85Hz), 4. 01 (q 2H J = 4.89Hz), 2.49 (s 3H), 1.91 (s 6H), 1.18 (t 6H J = 7.09Hz)

^{13}C NMR: (CDCl$_3$) δ 171.23, 167.44, 166.32, 165. 81, 163.92, 147.32, 130.25, 128.63, 125.77, 121.32, 101.12, 59.81, 31.65, 20.87, 14.51, 12.34

TLC: SiO$_2$; Hexane:EtOAc 4:1 R$_f$ = 0.17

General Synthesis of 4-[3-(Bromo-phenyl)-5-methyl-isoxazol-4-yl]-2,6-dimethyl-1,4-dihydro-pyridine-3,5-dicarboxylic acid 3-ethyl ester 5-prop-2-ynyl ester (4.d.). An oven dried 100ml round bottom was charged with 0.82g (2.17 mmol) of ethyl (2Z)-2-[(5-methyl-3-pheyl-1,2-oxazol-4-yl)methylidene]-3-oxobutanoate, 0.305g (2.17 mmol) of prop-2-yn-1-yl 3-oxobutanoate, 50 ml of absolute ethanol and a magnetic stir bar the vessel was sealed and the solution was allowed to stirrer at room temperature. In a 10 ml graduated cylinder 0.47ml of 30% ammonia was measured out along with 0.53ml of absolute ethanol, the mixture was then added to the 100ml round bound bottom containing ethyl (2Z)-2-[(5-methyl-3-pheyl-1,2-oxazol-4-yl)methylidene]-3-oxobutanoate and prop-2-yn-1-yl 3-oxobutanoate. The 100ml round bottom was then placed on a heating mantel and fitted with a oven dried condenser. The solution was then refluxed (78ºC) for 12 hours during which time the solution turned yellow. The solution was then cooled to room temperature and the excess solvent was removed via rotovap. The solution was then purified via recrystallized from ethyl acetate and hexanes to give off yellow crystals. (0.355g, 0.713 mmol, 33%)

^{1}H NMR: (CDCl$_3$) δ 7.52 (d 2H J =7.83Hz), 7.29 (d 2H J = 8.31Hz), 5.01 (s 1H), 4.98 (s 2H) 4.56 (q, 2H J = 9.78Hz), 4.09 (qq, 2H J = 6.36Hz), 4.00 (qq, 2H J = 6.85Hz), 2.50 (s,3H), 2.47 (s, 3H), 2.05 (s 6H), 1.21 (t, 3H J = 7.03Hz)

^{13}C NMR: (CDCl$_3$) δ 167.28, 166.21, 162.70, 145.35, 143.78, 131.23, 130.72, 122.84, 119.47, 101.62, 101.12, 74.68, 59.85, 51.31, 29.69, 29.16, 19.35, 14.46, 11.46

MS: *m/z* = 499.35 (M+, 100% rel. intensity), 540.86 ([M+]+CH$_3$CN,60)

TLC: SiO$_2$; Hexane:EtOAc 4:1 R$_f$ = 0.12

4-[3-(2-Bromo-phenyl)-5-methyl-isoxazol-4-yl]-2,6-dimethyl-1,4-dihydro-pyridine-3,5-dicarboxylic acid 3-ethyl ester 5-prop-2-ynyl ester. (4.b.)

^{1}H NMR: (CDCl$_3$) δ 7.58 (d 1H J = 8.66Hz), 7.31 (d 1H J = 6.53Hz), 7.24 (d 1H J = 7.65Hz), 7.18 (d 1H J = 7.53Hz), 4.95 (s 1H), 4.67 (d 2H J = 3.04Hz), 4.15 (qq 2H J = 7.15Hz), 2.58 (s 3H), 2.05 (s 1H), 1.96 (s 6H), 1.25 (t 3H J = 7.15Hz)

^{13}C NMR: (CDCl$_3$) δ 167.33, 165.50, 162.95, 144.54, 132.46, 132.25, 132.11, 130.00, 126.24, 125.01, 118.27, 100.47, 100.47, 59.79, 29.24, 19.61, 14.61, 11.54

TLC: SiO$_2$; Hexane:EtOAc 4:1 R$_f$ = 0.12

4-[3-(3-Bromo-phenyl)-5-methyl-isoxazol-4-yl]-2,6-dimethyl-1,4-dihydro-pyridine-3,5-dicarboxylic acid 3-ethyl ester 5-prop-2-ynyl ester. (4.c.)

^{1}H NMR: (CDCl$_3$) δ 7.59 (s 1H), 7.56 (s 1H), 7.55 (s 1H), 7.33 (s 1H), 5.05 (s 1H), 4.65 (d 2H J = 2.51Hz), 4. 16 (qq 2H J = 7.15Hz), 2.54(s 3H), 2.08 (s 1H), 2.06 (s 6H), 1.25 (t 3H J = 7.03Hz)

^{13}C NMR: (CDCl$_3$) δ 167.27, 166.09, 162.48, 144.08, 133.18, 132.50,131.51, 129.21, 128.44, 121.64, 119.41, 101.00, 59.87, 29.41, 19.51, 14.51, 11.50

TLC: SiO$_2$; Hexane:EtOAc 4:1 R$_f$ = 0. 15

2,6-Dimethyl-4-(5-methyl-3-phenyl-isoxazol-4-yl)-1,4-dihydro-pyridine-3,5-dicarboxylic acid 3-ethyl ester 5-prop-2-ynyl ester. (4.a)

^{1}H NMR: (CDCl$_3$) δ 7.57 (d 2H J = 8.72Hz), 7.30 (d 2H J = 8.72Hz), 7.22 (s 1H), 5.37 (s 1H), 5.23 (s 1H), 4.98 (s 1H), 4.55 (q 2H J = 6.36Hz), 4.08 (q 2H J = 6.85Hz), 2.54 (s 3H), 2.08 (s 1H), 1.92 (s 6H), 1.18 (t 3H J = 7.09Hz)

^{13}C NMR: (CDCl$_3$) δ 171.18, 167.44, 166.41, 165.79, 163.81, 146.01, 144.39, 130.76, 129.52, 127.55, 119.43, 101.43, 74.59, 60.40, 29.20, 19.15, 14.47, 11.52

TLC: SiO_2 Hexane:EtOAc 4:1 R_f = 0. 18

Synthesis of (2-Azido-ethyl)-benzene. An oven dried 100mL round bottom was charged with 1.010g (8.268mmol) of 2-Phenyl-ethanol, a magnetic stir bar. Chloroform was then added and the round bottom was capped with a septum and the solution was then allowed to stir at room temperature. The round bottom was cooled in bath of a of $CaCl_2$ solution and water (25g/200mL). The round bottom was then placed in the $CaCl_2$/water solution and dry ice was added (to the cooling solution), the solution was then allowed to reach -35°C. Methanesulfonyl chloride (MsCl)1.031mL was then added via gas-tight syringe. The reaction was then kept at -35°C for two hours. The solution was then allowed to reach room temperate and was then left to stir at room temperature overnight. Excess solvent was removed via rotovap, to give a white solid. The same 100mL round bottom was then charged with 25mL of EtOH and 0.585g of NaN_3 at room temperature. The reaction was then allows to stir at room temperature over night. The reaction yielded an amber solution. The solution was then extracted with EtOAc and Brine three times, and dried over $NaSO_4$. The solution was then contracted via rotovap yielding a yellow-gold oil. (0.924g, 6.28 mmol, 77%)

^{1}H NMR: ($CDCl_3$) δ 7.24 (d, 2H J = 9.30Hz), 7.12 (d, 2H J = 8.85Hz), 7.11(s, 1H), 2.84(d, 2H J = 7.24Hz), 1.41(d,2H J = 7.30Hz)

TLC: SiO2; EtOAc R_f =.76

General Synthesis of 4-[3-(4-Bromo-phenyl)-5-methyl-isoxazol-4-yl]-2,6-dimethyl-1,4-dihydro-pyridine 3,5-dicarboxylic acid 3-ethyl ester 5-(1-phenethyl-1H-[1,2,3]triazol-4-ylmethyl) ester. (6.) An oven dried 100mL round bottom was charged with 0.038g (0.259mmol) of (2-Azido-ethyl)-benzene and a magnetic stir bar. The sample

was then taken up in freshly distilled THF and the solution was allowed to stir at room temperature. Once the (2-Azido-ethyl)-benzene was completely dissolved 0.129g (0.259mmol) of 4-[3-(Bromo-phenyl)-5-methyl-isoxazol-4-yl]-2,6-dimethyl-1,4-dihydro-pyridine-3,5-dicarboxylic acid 3-ethyl ester 5-prop-2-ynyl ester was added in potions. The round bottom was then capped with a rubber septum and the solution was allowed to stir. The solution was allowed to stir until all reagents where dissolved, 0.011g of Copper(I)-bromide was then added and the solution was allowed to stir at room temperature for 48 Hr. Reaction progress was monitored via TLC, once the compete excess solvent was removed via rotovap. The solution was then purified via silica column yielding yellow oil (0.0527g, 0.0816mmol, 32%)

^{1}H NMR: (CDCl$_3$) δ 7.51(d, 2H J = 8.53Hz), 7.30 (d, 2H J = 7.53Hz), 7.26(s, 1H), 7.24(d, 2H J = 9.29Hz), 7.12(d, 2H J = 8.28Hz), 5.15(q, 2H J = 12.30Hz), 5.03(s, 1H), 4.99(s, 1H), 4.56 (t, 2H J = 7.53Hz), 4.14 (q, 2H J = 7.03Hz), 4.07 (t 2H J = 7.03Hz), 3.20(t, 2H J = 7.28Hz), 2.35(s, 3H), 2.02(d, 6H J = 5.27Hz), 1.27(t, 3H J = 7.28Hz)

^{13}C NMR: (CDCl$_3$) δ 167.14, 167.04, 166.55, 144.59, 143.54, 136.89, 131.20, 130.79, 129.93, 128.85, 128.69, 127.13, 122.89, 101.52, 100.64, 60.43, 59.89, 56.88, 51.68, 45.91, 36.63, 26.39, 21.08, 19.46, 19.26, 14.45, 19.26, 14.45, 14.22, 11.33, 8.67

HRMS: calculated for C$_{23}$H$_{32}$BrN$_5$O$_5$ 646.1685 found 646.1665

MS: *m/z* = 645 (M (^{79}Br), 20% rel. intensity), 646 (M+, 80), 647([M+1]+, 35), 648 ([M+1]+(^{81}Br),78)

IR: cm^{-1} 2992.36, 1734.06, 1365.56, 1255.39, 1278.18, 1221.20, 761.51, 746.32

TLC: SiO$_2$; EtOAc:MeOH:CH$_2$Cl$_2$ (4:1:2) R$_f$ = 0.55

Synthesis of 2,6-Dimethyl-4-(5-methyl-3-phenyl-isoxazol-4-yl)-pyridine-3,5-dicarboxylic acid diethyl ester. (8.) The 2,6-Dimethyl-4-(5-methyl-3-phenyl-isoxazol-4-yl)-1,4-dihydro-pyridine-3,5-dicarboxylic acid diethyl ester was placed in a 50mL oven dried round bottom along with a magnetic stir bar and 0.085g of DI water. The solution was then allowed to stir at room temperature while, 0.227g of HNO3 and 0.0246g of H2SO4 was added. The solution was then heated to 110ºC and white foam was observed, after 10 min. at 110ºC the solution turned a light yellow. The solution was then allowed to cool to room temperature. The solution was then taken up in ice water and LiOH was added slowly until the solution was neutral. The solution was then added to a speratory funnel and extracted with CHCl$_3$ and Brine with 50mL three times. The solution was then dried over NaSO$_4$ and filtered; the excess solvent was then removed via rotovap yielding a pale yellow oil that was then crystallized with CH$_2$Cl$_2$ and Hexanes. (0.100g, 0.245 mmol, 98%)

^{1}H NMR: (CDCl$_3$) 7.46 (d, 2H, J = 7.28Hz), 7.34 (d, 2H, J = 7.11Hz), 7.29 (s, 1H), 4.03 (q, 2H, J = 9.56Hz), 2.59 (s, 3H), 2.25 (s, 3H), 0.97 (t, 3H, J = 7.01Hz)

^{13}C NMR: (CDCl$_3$) δ 167.18, 165.91, 159.70, 155.29, 134.52, 128.66, 127.56, 126.56, 109.18, 60.63, 22.09, 12.57, 10.38

HRMS: calculated for C$_{23}$H$_{24}$N$_2$O$_5$ 408.1685 found 408.1692

MS: *m/z* = 409 (M^{+1}, 100), 410 (M^{+2}, 40)

IR: cm^{-1} 3007.46, 1737.86, 1441.54, 1365.56, 1259.19, 1217.60, 746.32

TLC: SiO$_{2;}$ Hexanes:EtOAc (4:1) R$_f$ = 0.31

General Synthesis of 3-[1-(17-{4-[({4-[3-(4-bromophenyl)-5-methyl-1,2-oxazol-4-yl]-5-(ethoxycarbonyl)-2,6-dimethyl-1,4-dihydropyridin-3-yl}carbonyloxy)methyl]-1H-1,2,3-triazol-1-yl}-3,6,9,12,15-pentaoxaheptadecan-1-yl)-1H-1,2,3-triazol-4-yl]methyl 5-ethyl 4-[3-(4-bromophenyl)-5-methyl-1,2-oxazol-4-yl]-2,6-dimethyl-1,4-dihydropyridine-3,5-dicarboxylate. (5.d.) An oven dried 100ml round bottom was charged with 0.164g (.328mmol) of 4-[3-(4-Bromo-phenyl)-5-methyl-isoxazol-4-yl]-2,6-dimethyl-1,4-dihydro-pyridine-3,5-dicarboxylic acid 3-ethyl ester 5-prop-2-ynyl ester, 0.034g of 1-Azido-2-[2-(2-{2-[2-(2-azido-ethoxy)-ethoxy]-ethoxy}-ethoxy)-ethoxy]-ethane, 0.010g of Copper(I) bromide, 0.010g of Copper sulfate anhydride and a magnetic stir bar. 50ml of freshly distilled THF was then added and the solution was allowed to stir at room temperature. Sodium ascorbate (0.003g) was then added and the solution was allowed to react. The reaction progress was monitored by TLC, once the reaction was completed excess solvent was removed via rotovap. The solution was then purified via a silica column. The purification yielded yellow oil. (0.0067g, 0.005 mmol, 15.34%)

^{1}H NMR: (CDCl$_3$) δ 7.65 (s 2H), 7.49 (d 4H J = 8.28Hz), 7.22 (d 4H J = 8.28Hz), 4.99 (s 2H), 4.52 (q 4H J = 4.52Hz), 4.13 (q 2H J = 7.28Hz), 4.07 (q 2H J = 6.78Hz), 3.89 (t 3H J = 5.52Hz), 3.75 (t 4H J = 6.02Hz), 3.65 (m 16H), 2.33 (s 6H), 2.05 (s 9H), 1.19 (t 6H J =7.03Hz)

^{13}C NMR: (CDCl$_3$) δ 168.74, 166.68, 159.89, 156.71, 135.10, 131.91, 131.22, 130.77, 129.04, 128.17, 127.45, 124.90, 124.24, 109.43, 71.36, 70.59, 69.35, 69.303, 61.72, 58.48, 42.76, 37.76, 31.94, 29.71, 23.16, 14.13, 13.63, 11.25

HRMS: calculated for C$_{60}$H$_{71}$Br$_2$N$_{10}$O$_{15}$ 1329.3467 found 1329.3462

MS: m/z = 1327 (M (^{79}Br) 100% rel. intensity), 1328 (M, 62), 1329 (M^{+1}, 97), 1330

([M^{+1}](^{81}Br),60) 1331 ([M^{+1}]+(^{81}Br),60), 1332 ([M^{+1}]+2(^{81}Br),40)

IR: cm^{-1} 3014.92, 2962.68, 1746.26, 1492.10, 1369.40, 1216.41, 753.73

TLC: SiO$_2$; EtOAc:MeOH:CH$_2$Cl$_2$ (4:1:2) R$_f$ = 0.56

Then run a column in 4:1:3:2 (EtOAc:MeOH:Hexanes:CH$_2$Cl$_2$) R$_f$ = 0.23

3-[1-(17-{4-[({4-[3-(2-bromophenyl)-5-methyl-1,2-oxazol-4-yl]-5-(ethoxycarbonyl)-2,6-dimethyl-1,4-dihydropyridin-3-yl}carbonyloxy)methyl]-1H-1,2,3-triazol-1-yl}-3,6,9,12,15-pentaoxaheptadecan-1-yl)-1H-1,2,3-triazol-4-yl]methyl 5-ethyl 4-[3-(2-bromophenyl)-5-methyl-1,2-oxazol-4-yl]-2,6-dimethyl-1,4-dihydropyridine-3,5-dicarboxylate. (5.b.)

^{1}H NMR: (CDCl$_3$) δ 7.59 (d 2H J = 6.78Hz), 7.58 (d 2H J = 6.78Hz), 7.31 (d 2H J = 7.03Hz), 7.23 (s 2H J = 7.53Hz), 7.15 (d 2H J = 7.03Hz), 4.92 (s 2H), 4.54 (q 4H J = 5.52Hz), 4.10 (q 2H J = 8.78Hz), 3.97 (t 3H J = 5.77Hz), 3.81 (t 4H J = 6.27Hz), 3.66 (m 16H), 2.36 (s 6H), 1.96 (s 9H), 1.23 (t 6H J = 7.03Hz)

^{13}C NMR: (CDCl$_3$) δ 167.24, 132.21, 131.98, 130.28, 126.40, 100.36, 71.28, 70.56, 69.96, 69.47, 68.96, 65.56, 61.91, 59.69, 50.64, 47.62, 42.81, 37.70, 32.16, 30.48, 29.63, 23.41, 19.16, 15.14, 14.56, 11.28

HRMS: calculated for C$_{60}$H$_{71}$Br$_2$N$_{10}$O$_{15}$ 1329.3467 found 1329.3467

MS: m/z = 1327 (M (^{79}Br) 35% rel. intensity), 1328 (M, 30), 1329 (M^{+1}, 97), 1330

([M^{+1}](^{81}Br),50) 1331 ([M^{+1}]+(^{81}Br),100), 1332 ([M^{+1}]+2(^{81}Br),40)

IR: cm^{-1} 2917.91, 2850.74, 1731.34, 1496.26, 1261.19, 1164.17, 733.12

TLC: SiO$_2$; EtOAc:MeOH:CH$_2$Col$_2$ (4:1:2) R$_f$ = 0.48

3-[1-(17-{4-[({4-[3-(3-bromophenyl)-5-methyl-1,2-oxazol-4-yl]-5-(ethoxycarbonyl)-2,6-dimethyl-1,4-dihydropyridin-3-yl}carbonyloxy)methyl]-1H-1,2,3-triazol-1-yl}-3,6,9,12,15-pentaoxaheptadecan-1-yl)-1H-1,2,3-triazol-4-yl]methyl 5-ethyl 4-[3-(3-bromophenyl)-5-methyl-1,2-oxazol-4-yl]-2,6-dimethyl-1,4-dihydropyridine-3,5-dicarboxylate. (5.c.)

^{1}H NMR: (CDCl$_3$) δ 7.73 (s 2H), 7.64 (d 2H J = 5.52Hz), 7.51 (s 2H), 7.25 (s 2H), 7.18 (d 2H J = 10.54Hz), 4.98 (s 2H), 4.53 (q 4H J = 4.02Hz), 4.38 (q 2H J = 4.27Hz), 4.09 (q 2H J = 10.79Hz), 3.86 (t 3H J = 5.02Hz), 3.76 (t 4H J = 5.02Hz), 3.62 (m 16H), 2.35 (s 6H), 2.01 (s 9H), 1.19 (t 6H J = 7.28Hz)

^{13}C NMR: (CDCl$_3$) δ 167.18, 166.31, 162.49, 145.12, 144.12, 133.04, 132.73, 132.40, 131.54, 130.44, 13.026, 129.28, 128.39, 126.18, 124.96, 121.62, 199.30, 101.11, 100.33, 71.35, 70.62, 69.39, 69.01, 66.64, 59.85, 58.44, 56.92, 50.69, 43.38, 42.79, 41.44, 37.75, 29.41, 23.17, 23.09, 19.46, 19.29, 14.48, 13.62, 11.30

HRMS: calculated for C$_{60}$H$_{71}$Br$_2$N$_{10}$O$_{15}$ 1329.3467 found 1329.3450

MS: m/z = 1327 (M (^{79}Br) 35% rel. intensity), 1328 (M, 20), 1329 (M^{+1}, 100), 1330 ([M^{+1}](^{81}Br),60) 1331 ([M^{+1}]+(^{81}Br),100), 1332 ([M^{+1}]+2(^{81}Br),50)

IR: cm^{-1} 3007.46, 2970.14, 1738.80, 1432.83, 1227.61, 1216.41, 761.51

TLC: SiO$_2$; EtOAc:MeOH:CH$_2$Cl$_2$ (4:1:2) R$_f$ = 0.52

3-(1-{17-[4-(({[5-(ethoxycarbonyl)-2,6-dimethyl-4-(5-methyl-3-phenyl-1,2-oxazol-4-yl)-1,4-dihydropyridin-3-yl]carbonyloxy}methyl)-1H-1,2,3-triazol-1-yl]-3,6,9,12,15-pentaoxaheptadecan-1-yl}-1H-1,2,3-triazol-4-yl)methyl 5-ethyl 2,6-dimethyl-4-(5-methyl-3-phenyl-1,2-oxazol-4-yl)-1,4-dihydropyridine-3,5-dicarboxylate. (5.a.)

¹H NMR: (CDCl₃) δ 7.64 (s 2H), 7.52 (d 4H J = 8.28Hz), 7.25 (d 4H J = 8.28Hz), 4.98 (s 2H), 4.54 (q 4H J = 4.77Hz), 4.11 (q 2H J = 7.03Hz), 4.04 (q 2H J = 7.03Hz), 3.87 (t 3H J = 5.27Hz), 3.75 (t 4H J = 5.77Hz), 3.65 (m 16H), 2.36 (s 6H), 2.03 (d 9H J = 5.27Hz), 1.19 (t 6H J = 7.03Hz)

¹³C NMR: (CDCl₃) δ 171.15, 168.55, 167.21, 169.96, 151.03, 144.05, 130.90, 129.78, 129.44, 129.30, 128.68, 128.40, 127.51, 106.88, 101.17, 88.97, 71.28, 70.60, 70.51, 69.93, 69.37, 68.94, 66.48, 63.51, 61.56, 59.56, 55.57, 51.58, 50.65, 42.73, 37.64, 35.87, 29.57, 29.20, 23.50, 22.58, 21.50, 18.84, 15.10, 14.40, 14.02, 12.41, 11.06

HRMS: calculated for $C_{60}H_{71}N_{10}O_{15}$ 1171.5100 found 1171.5134

MS: *m/z* = 1169 ([M-2] 100 % rel. intensity), 1170 ([M-1] 70), 1171([M] 40), 1172 ([M+] 10)

IR: cm^{-1} 2972.26, 2831.20, 1734.06, 1571.92, 1357.96, 1225.00, 727.32

TLC: SiO_2; EtOAc:MeOH:CH_2Cl_2 (4:1:2) R_f = 0.52

3-[1-(2-{2-[2-(2-{4-[({4-[3-(4-bromophenyl)-5-methyl-1,2-oxazol-4-yl]-5-(ethoxycarbonyl)-2,6-dimethyl-1,4-dihydropyridin-3-yl}carbonyloxy)methyl]-1H-1,2,3-triazol-1-yl}ethoxy)ethoxy]ethoxy}ethyl)-1H-1,2,3-triazol-4-yl]methyl 5-ethyl 4-[3-(4-bromophenyl)-5-methyl-1,2-oxazol-4-yl]-2,6-dimethyl-1,4-dihydropyridine-3,5-dicarboxylate. (5.e)

¹H NMR: (CDCl₃) δ 7.60 (d 2H J = 5.52), 7.50 (t 4H J = 8.28Hz), 7.26 (t 4H J = 8.28Hz), 5.17 (m 4H), 4.99 (s 2H), 4.51 (q 4H J = 5.52Hz), 4.07 (q 2H J = 6.78Hz), 3.94 (q 2H J = 6.78Hz), 3.85 (t 4H J = 5.27Hz), 3.62 (m 8H), 2.34 (s 6H), 2.01 (d 9H J = 5.02Hz), 1.15 (t 6H J = 7.28Hz)

13C NMR: (CDCl$_3$) δ 167.21, 162.62, 145.12, 143.89, 131.90, 131.12, 130.78, 129.92, 129.02, 122.88, 119.54, 101.29, 100.39, 72.46, 70.67, 70.06, 69.34, 61.72, 59.81, 50.67, 42.84, 29.69, 19.03, 14.45, 11.30

HRMS: calculated for C$_{56}$H$_{63}$ N$_{10}$O$_{13}$Br$_2$ 1241.2943 found 1241.2950

MS: m/z = 1239 ([M(^{79}Br)] 60% rel. intensity), 1240 ([M] 40), 1241 ([M^{+1}] 100), 1242 ([M^{+1}](^{81}Br) 60), 1243([M+2] 70), 1244 ([M+3] 50)

IR: cm^{-1} 2917.91, 2850.74, 1731.31, 1496.26, 1261.19, 1164.17, 697.76

TLC: SiO$_2$; EtOAc:MeOH:CH$_2$Cl$_2$ (4:1:2) R$_f$ = 0.52

3-(1-{2-[2-(2-{4-[({4-[3-(4-bromophenyl)-5-methyl-1,2-oxazol-4-yl]-5-(ethoxycarbonyl)-2,6-dimethyl-1,4-dihydropyridin-3-yl}carbonyloxy)methyl]-1H-1,2,3-triazol-1-yl}ethoxy)ethoxy]ethyl}-1H-1,2,3-triazol-4-yl)methyl 5-ethyl 4-[3-(4-bromophenyl)-5-methyl-1,2-oxazol-4-yl]-2,6-dimethyl-1,4-dihydropyridine-3,5-dicarboxylate. (5.f.)

1H NMR: (CDCl$_3$) δ 7.61 (d 2H J = 7.53Hz), 7.49 (d 4H J = 8.28Hz), 7.25 (d 4H J = 8.53Hz), 5.17 (m 4H), 4.98 (s 2H), 4.51 (q 4H J = 5.27Hz), 4.06 (q 2H J = 6.83Hz), 3.88 (q 2H J = 5.02Hz), 3.72 (t 4H J = 6.02Hz), 3.64 (d 4H J = 6.27Hz), 2.33 (s 6H), 2.01 (s 9H), 1.15 (t 6H J = 7.28Hz)

13C NMR: (CDCl$_3$) δ 167.25, 143.96, 131.97, 131.18, 130.81, 129.89, 129.03, 122.98, 101.28, 71.30, 70.74, 70.47, 70.32, 69.15, 61.75, 59.83, 53.51, 50.67, 42.92, 29.70, 29.36, 19.04, 15.16, 14.46, 13.64, 11.36

HRMS: calculated for C$_{54}$H$_{59}$ N$_{10}$O$_{12}$Br$_2$ 1197.2633 found 1197.2681

MS: m/z = 1195 ([M(^{79}Br)] 80% rel. intensity), 1196 ([M] 60), 1197 ([M^{+1}] 100), 1198 ([M^{+1}](^{81}Br) 80), 1199 ([M+2] 100), 1200 ([M+3] 60)

IR: cm^{-1} 3014.92, 2962.68, 1746.26, 1429.10, 1369.40, 1216.41, 753.73

TLC: SiO$_2$; EtOAc:MeOH:CH$_2$Cl$_2$ (4:1:2) R$_f$ = 0.5

MDR-1 Assay.

Screening of IDHPs was performed by the Psychoactive Drug Screening Program (PDSP) of NIMH. The PDSP protocol utilizes live Caco-2 cells, which are derived from human colonic epithelium cells which express MDR-1.[9] The assay is based on the passive diffusion of calcein acetoxymethyl ester (Calcein-AM), which is hydrolyzed inside the cell to calcein, which is both fluorescent and negatively charged, and therefore trapped inside the cell. MDR-1 can transport non-fluorescent Calcein-AM from cells, but not hydrolyzed calcein. The assay measures the increase in calcein fluorescence as a function of time using a FlexStation II fluorimeter (Molecular Devices) in 96 well plates in which cells were preincubated with IDHPs (50 □M) for 30 minutes, upon which time calcein-AM was added to a final concentration of 150 nM. Fluorescence is monitored over 4 minutes, and each assay was performed in quadruplicate, with a 25 □M cyclosporin control. The value from untreated cells is 0% and the slope of the fluorescence is normalized taking the value for cyclosporin as 100%.[10]

The results are shown in **Table 4-1.**

mGluR$_5$ Assay

Screening of the IDHP was performed by the PDSP of the NIMH. IDHPs are tested using cell lines stably expressing Gq protein mGluR5 receptors in a functional assay. Cells are seeded and cultured in 96 well plates until a level of confluency is established around 3 to 4 days after seeding. After which the cells are incubated overnight and in a glutamine deprived medium along with myo-[3H]-inositol (NEN) to act as a label on the membrane

phosphoinosites of the cell. After incubation is complete the cells are washed with a Locke's buffer and a second round of incubation with the IDHP is carried out for 45 min at 37ºC in Lock's buffer containing 20 mM LiCl to hinder the degradation of the inositol phosphate. The incubation is then terminated via aspiration and [3H]inosital phosphates are extracted in 60 ul or 10 mM formic acid for 30 min. Samples of the aspirated media (40ul) is then transferred to opaque welled plates and incubated with polylysine-coated yttrium scintillation proximity assay (SPA) beads at room temperature for 1 hour with vigorous shaking. The sample is then allowed to incubate for an additional 8 hours with the SPA beads after which the inositol phosphates are quantified via a scintillation counter.

VGCC Assay

Binding to the Ca^{2+} channel was conducted by PDSP. The binding assay was carried out in 125 μl per well with 50mM Tris HCL, 50mM NaCl, 1mM $CaCl_2$, pH 7.4, at room temperature. The radioactive ligand, [^{3}H] Nitrendipine, was tested at a concentration close to its Kd of 4.77 ±1.75nM. Total binding and nonspecific binding is determined in the presence and absence of Nifedipine at 10 μM. Plates are incubated at room temperature in the dark for 90 min. Reactions are halted by vacuum filtration into a 0.3% polyethyleneimine (PEI) soaked 96-well filter mats utilizing a 96 well filtermate harvester. This is followed by washing with a cold wash buffer of 50 nM Tris HCl, pH 7.4. The scintillation cocktail was then melted into a microwave dried filter on a hot place. The radioactivity is then counted in a microbeta counter and the inhibition is calculated using excel.

Geometric parameters of 7c.

Fractional atomic coordinates and isotropic or equivalent isotropic displacement parameters ($Å^2$)

	x	y	z	U_{iso}*/U_{eq}
Br1	0.13632 (2)	0.25468 (2)	0.37558 (2)	0.02823 (9)
O1	0.43075 (9)	0.29377 (11)	0.11607 (10)	0.0283 (3)
O2	0.33685 (9)	0.38628 (9)	0.03190 (9)	0.0209 (3)
O3	−0.00779 (9)	0.29679 (11)	0.03098 (9)	0.0257 (3)
O4	0.05653 (8)	0.38995 (9)	−0.02185 (8)	0.0187 (3)
O5	0.23363 (9)	0.57903 (9)	0.13294 (9)	0.0217 (3)
N1	0.23174 (10)	0.19821 (10)	0.17407 (10)	0.0174 (3)
H1	0.2398	0.1592	0.2124	0.021*
N2	0.25085 (11)	0.54099 (11)	0.20923 (10)	0.0201 (3)
C1	0.29821 (12)	0.22402 (12)	0.15734 (11)	0.0169 (4)
C2	0.29080 (11)	0.29224 (12)	0.10686 (11)	0.0141 (3)
C3	0.21215 (11)	0.34605 (11)	0.07315 (10)	0.0130 (3)
H3	0.1986	0.3552	0.0142	0.016*
C4	0.14028 (11)	0.29744 (12)	0.08116 (11)	0.0139 (3)
C5	0.15317 (12)	0.23029 (12)	0.13390 (11)	0.0159 (4)
C6	0.08914 (14)	0.18422 (14)	0.15562 (13)	0.0245 (4)
H6A	0.1132	0.1316	0.1871	0.037*
H6B	0.0426	0.1677	0.1060	0.037*
H6C	0.0699	0.2233	0.1879	0.037*
C7	0.37467 (13)	0.17054 (14)	0.19898 (13)	0.0257 (4)
H7A	0.4155	0.2056	0.2415	0.039*
H7B	0.3974	0.1525	0.1595	0.039*
H7C	0.3609	0.1186	0.2232	0.039*
C8	0.36060 (12)	0.32102 (13)	0.08757 (12)	0.0186 (4)
C9	0.40158 (15)	0.42942 (16)	0.01577 (16)	0.0320 (5)

H9A	0.3787	0.4559	−0.0389	0.038*
H9B	0.4439	0.3862	0.0172	0.038*
C10	0.44005 (19)	0.4990 (2)	0.0777 (2)	0.0518 (8)
H10A	0.4833	0.5286	0.0658	0.078*
H10B	0.4641	0.4723	0.1316	0.078*
H10C	0.3979	0.5415	0.0764	0.078*
C11	0.05621 (11)	0.32540 (12)	0.03009 (11)	0.0169 (4)
C12	−0.02498 (12)	0.41577 (15)	−0.07884 (12)	0.0251 (4)
H12A	−0.0581	0.4380	−0.0492	0.030*
H12B	−0.0539	0.3649	−0.1117	0.030*
C13	−0.01450 (14)	0.48594 (15)	−0.13250 (13)	0.0265 (4)
H13A	−0.0687	0.5042	−0.1715	0.040*
H13B	0.0183	0.4633	−0.1615	0.040*
H13C	0.0137	0.5362	−0.0995	0.040*
C14	0.20205 (14)	0.54318 (14)	−0.00658 (13)	0.0255 (4)
H14A	0.1532	0.5807	−0.0259	0.038*
H14B	0.1924	0.4920	−0.0419	0.038*
H14C	0.2495	0.5759	−0.0074	0.038*
C15	0.21875 (12)	0.51432 (12)	0.07741 (12)	0.0178 (4)
C16	0.22413 (11)	0.43523 (12)	0.11286 (11)	0.0137 (3)
C17	0.24542 (11)	0.45621 (12)	0.19624 (11)	0.0146 (3)
C18	0.26466 (12)	0.39629 (12)	0.26628 (10)	0.0155 (4)
C19	0.20191 (12)	0.36074 (12)	0.28569 (11)	0.0169 (4)
H19	0.1460	0.3755	0.2551	0.020*
C20	0.22263 (13)	0.30334 (12)	0.35054 (11)	0.0196 (4)
C21	0.30353 (14)	0.28160 (13)	0.39662 (12)	0.0235 (4)
H21	0.3165	0.2426	0.4410	0.028*
C22	0.36550 (14)	0.31774 (14)	0.37688 (12)	0.0259 (4)

H22	0.4214	0.3034	0.4081	0.031*
C23	0.34645 (12)	0.37472 (13)	0.31184 (12)	0.0215 (4)
H23	0.3892	0.3989	0.2985	0.026*

Atomic displacement parameters ($\mathring{A}^2$)

	U^{11}	U^{22}	U^{33}	U^{12}	U^{13}	U^{23}
Br1	0.04300 (16)	0.02509 (13)	0.02490 (14)	−0.00891 (9)	0.02224 (11)	−0.00250 (8)
O1	0.0180 (7)	0.0354 (9)	0.0343 (8)	0.0043 (6)	0.0131 (6)	0.0014 (7)
O2	0.0214 (7)	0.0203 (7)	0.0271 (7)	−0.0033 (5)	0.0163 (6)	0.0006 (6)
O3	0.0157 (7)	0.0395 (9)	0.0204 (7)	−0.0050 (6)	0.0055 (5)	0.0005 (6)
O4	0.0146 (6)	0.0196 (7)	0.0179 (6)	0.0030 (5)	0.0022 (5)	0.0022 (5)
O5	0.0296 (8)	0.0110 (6)	0.0242 (7)	−0.0007 (5)	0.0100 (6)	0.0018 (5)
N1	0.0229 (8)	0.0126 (7)	0.0178 (7)	0.0012 (6)	0.0090 (6)	0.0034 (6)
N2	0.0249 (9)	0.0138 (8)	0.0204 (8)	−0.0003 (6)	0.0075 (7)	0.0005 (6)
C1	0.0198 (9)	0.0146 (8)	0.0167 (8)	0.0022 (7)	0.0074 (7)	−0.0019 (7)
C2	0.0141 (8)	0.0138 (8)	0.0154 (8)	0.0004 (6)	0.0068 (7)	−0.0020 (7)
C3	0.0152 (8)	0.0116 (8)	0.0133 (8)	−0.0002 (6)	0.0065 (6)	−0.0002 (6)
C4	0.0142 (8)	0.0141 (8)	0.0134 (8)	−0.0014 (6)	0.0055 (7)	−0.0024 (6)
C5	0.0195 (9)	0.0134 (8)	0.0162 (8)	−0.0038 (7)	0.0086 (7)	−0.0042 (7)
C6	0.0284 (11)	0.0225 (10)	0.0269 (10)	−0.0084 (8)	0.0154 (9)	0.0003 (8)
C7	0.0255 (10)	0.0235 (10)	0.0282 (10)	0.0110 (8)	0.0104 (9)	0.0070 (8)
C8	0.0193 (9)	0.0195 (9)	0.0202 (9)	−0.0014 (7)	0.0110 (7)	−0.0047 (7)
C9	0.0343 (12)	0.0296 (11)	0.0450 (13)	−0.0098 (9)	0.0297 (11)	−0.0020 (10)
C10	0.0417 (16)	0.0412 (15)	0.081 (2)	−0.0187 (12)	0.0336 (16)	−0.0231 (15)
C11	0.0166 (9)	0.0200 (9)	0.0134 (8)	−0.0012 (7)	0.0051 (7)	−0.0044 (7)
C12	0.0157 (9)	0.0327 (11)	0.0189 (9)	0.0044 (8)	−0.0020 (7)	−0.0001 (8)

C13	0.0242 (10)	0.0268 (11)	0.0218 (10)	0.0080 (8)	0.0017 (8)	−0.0017 (8)
C14	0.0321 (11)	0.0200 (10)	0.0250 (10)	0.0003 (8)	0.0117 (9)	0.0082 (8)
C15	0.0180 (9)	0.0141 (8)	0.0218 (9)	−0.0007 (7)	0.0083 (7)	0.0004 (7)
C16	0.0132 (8)	0.0129 (8)	0.0153 (8)	0.0001 (6)	0.0059 (6)	0.0010 (6)
C17	0.0133 (8)	0.0128 (8)	0.0178 (8)	−0.0005 (6)	0.0062 (7)	−0.0009 (7)
C18	0.0207 (9)	0.0118 (8)	0.0134 (8)	−0.0005 (7)	0.0058 (7)	−0.0024 (6)
C19	0.0218 (9)	0.0145 (8)	0.0155 (8)	0.0010 (7)	0.0084 (7)	−0.0024 (7)
C20	0.0318 (11)	0.0141 (8)	0.0167 (9)	−0.0038 (7)	0.0136 (8)	−0.0041 (7)
C21	0.0379 (12)	0.0154 (9)	0.0133 (9)	0.0008 (8)	0.0056 (8)	−0.0002 (7)
C22	0.0249 (10)	0.0236 (10)	0.0204 (10)	0.0014 (8)	−0.0007 (8)	0.0005 (8)
C23	0.0194 (9)	0.0207 (9)	0.0212 (9)	−0.0012 (7)	0.0043 (8)	−0.0011 (7)

Geometric parameters (Å, °)

Br1—C20	1.898 (2)	C9—H9A	0.9900
O1—C8	1.213 (2)	C9—H9B	0.9900
O2—C8	1.358 (2)	C9—C10	1.497 (4)
O2—C9	1.441 (2)	C10—H10A	0.9800
O3—C11	1.216 (2)	C10—H10B	0.9800
O4—C11	1.359 (2)	C10—H10C	0.9800
O4—C12	1.457 (2)	C12—H12A	0.9900
O5—N2	1.407 (2)	C12—H12B	0.9900
O5—C15	1.356 (2)	C12—C13	1.501 (3)
N1—H1	0.8800	C13—H13A	0.9800
N1—C1	1.375 (3)	C13—H13B	0.9800
N1—C5	1.379 (3)	C13—H13C	0.9800
N2—C17	1.315 (2)	C14—H14A	0.9800
C1—C2	1.355 (3)	C14—H14B	0.9800
C1—C7	1.504 (3)	C14—H14C	0.9800

C2—C3	1.521 (2)	C14—C15	1.485 (3)
C2—C8	1.469 (3)	C15—C16	1.354 (3)
C3—H3	1.0000	C16—C17	1.430 (2)
C3—C4	1.523 (2)	C17—C18	1.484 (2)
C3—C16	1.516 (2)	C18—C19	1.392 (3)
C4—C5	1.355 (3)	C18—C23	1.392 (3)
C4—C11	1.470 (3)	C19—H19	0.9500
C5—C6	1.505 (3)	C19—C20	1.388 (3)
C6—H6A	0.9800	C20—C21	1.382 (3)
C6—H6B	0.9800	C21—H21	0.9500
C6—H6C	0.9800	C21—C22	1.387 (3)
C7—H7A	0.9800	C22—H22	0.9500
C7—H7B	0.9800	C22—C23	1.389 (3)
C7—H7C	0.9800	C23—H23	0.9500
C8—O2—C9	116.28 (17)	H10A—C10—H10C	109.5
C11—O4—C12	114.35 (15)	H10B—C10—H10C	109.5
C15—O5—N2	108.62 (14)	O3—C11—O4	121.46 (17)
C1—N1—H1	118.3	O3—C11—C4	127.02 (18)
C1—N1—C5	123.44 (16)	O4—C11—C4	111.52 (15)
C5—N1—H1	118.3	O4—C12—H12A	110.1
C17—N2—O5	105.22 (15)	O4—C12—H12B	110.1
N1—C1—C7	114.20 (17)	O4—C12—C13	108.09 (17)
C2—C1—N1	119.89 (17)	H12A—C12—H12B	108.4
C2—C1—C7	125.92 (18)	C13—C12—H12A	110.1
C1—C2—C3	121.28 (16)	C13—C12—H12B	110.1
C1—C2—C8	121.10 (17)	C12—C13—H13A	109.5
C8—C2—C3	117.46 (16)	C12—C13—H13B	109.5
C2—C3—H3	107.6	C12—C13—H13C	109.5

C2—C3—C4	111.14 (14)	H13A—C13—H13B	109.5
C4—C3—H3	107.6	H13A—C13—H13C	109.5
C16—C3—C2	111.21 (14)	H13B—C13—H13C	109.5
C16—C3—H3	107.6	H14A—C14—H14B	109.5
C16—C3—C4	111.38 (14)	H14A—C14—H14C	109.5
C5—C4—C3	121.10 (16)	H14B—C14—H14C	109.5
C5—C4—C11	120.70 (17)	C15—C14—H14A	109.5
C11—C4—C3	118.19 (16)	C15—C14—H14B	109.5
N1—C5—C6	113.55 (17)	C15—C14—H14C	109.5
C4—C5—N1	119.78 (17)	O5—C15—C14	115.69 (16)
C4—C5—C6	126.67 (18)	C16—C15—O5	110.47 (16)
C5—C6—H6A	109.5	C16—C15—C14	133.83 (18)
C5—C6—H6B	109.5	C15—C16—C3	127.80 (16)
C5—C6—H6C	109.5	C15—C16—C17	103.46 (16)
H6A—C6—H6B	109.5	C17—C16—C3	128.74 (16)
H6A—C6—H6C	109.5	N2—C17—C16	112.22 (16)
H6B—C6—H6C	109.5	N2—C17—C18	118.86 (16)
C1—C7—H7A	109.5	C16—C17—C18	128.85 (16)
C1—C7—H7B	109.5	C19—C18—C17	120.71 (17)
C1—C7—H7C	109.5	C23—C18—C17	119.15 (17)
H7A—C7—H7B	109.5	C23—C18—C19	120.13 (17)
H7A—C7—H7C	109.5	C18—C19—H19	120.6
H7B—C7—H7C	109.5	C20—C19—C18	118.75 (18)
O1—C8—O2	122.32 (18)	C20—C19—H19	120.6
O1—C8—C2	127.38 (19)	C19—C20—Br1	118.22 (15)
O2—C8—C2	110.29 (16)	C21—C20—Br1	119.95 (15)
O2—C9—H9A	109.7	C21—C20—C19	121.84 (19)
O2—C9—H9B	109.7	C20—C21—H21	120.6

O2—C9—C10	110.00 (19)	C20—C21—C22	118.86 (18)
H9A—C9—H9B	108.2	C22—C21—H21	120.6
C10—C9—H9A	109.7	C21—C22—H22	119.8
C10—C9—H9B	109.7	C21—C22—C23	120.5 (2)
C9—C10—H10A	109.5	C23—C22—H22	119.8
C9—C10—H10B	109.5	C18—C23—H23	120.0
C9—C10—H10C	109.5	C22—C23—C18	119.93 (19)
H10A—C10—H10B	109.5	C22—C23—H23	120.0
Br1—C20—C21—C22	179.72 (15)	C5—C4—C11—O3	3.3 (3)
O5—N2—C17—C16	−0.6 (2)	C5—C4—C11—O4	−176.30 (16)
O5—N2—C17—C18	176.85 (15)	C7—C1—C2—C3	−175.27 (18)
O5—C15—C16—C3	−179.90 (17)	C7—C1—C2—C8	0.1 (3)
O5—C15—C16—C17	−1.1 (2)	C8—O2—C9—C10	−83.5 (3)
N1—C1—C2—C3	5.0 (3)	C8—C2—C3—C4	166.75 (15)
N1—C1—C2—C8	−179.71 (16)	C8—C2—C3—C16	−68.6 (2)
N2—O5—C15—C14	−178.08 (16)	C9—O2—C8—O1	−7.6 (3)
N2—O5—C15—C16	0.8 (2)	C9—O2—C8—C2	171.45 (16)
N2—C17—C18—C19	98.0 (2)	C11—O4—C12—C13	−179.11 (16)
N2—C17—C18—C23	−83.0 (2)	C11—C4—C5—N1	172.20 (16)
C1—N1—C5—C4	−7.5 (3)	C11—C4—C5—C6	−8.2 (3)
C1—N1—C5—C6	172.82 (17)	C12—O4—C11—O3	−4.5 (3)
C1—C2—C3—C4	−17.7 (2)	C12—O4—C11—C4	175.21 (15)
C1—C2—C3—C16	106.95 (19)	C14—C15—C16—C3	−1.3 (4)
C1—C2—C8—O1	−5.0 (3)	C14—C15—C16—C17	177.5 (2)
C1—C2—C8—O2	175.95 (17)	C15—O5—N2—C17	−0.2 (2)
C2—C3—C4—C5	19.2 (2)	C15—C16—C17—N2	1.0 (2)
C2—C3—C4—C11	−160.86 (15)	C15—C16—C17—C18	−176.04 (18)
C2—C3—C16—C15	117.1 (2)	C16—C3—C4—C5	−105.38 (19)

C2—C3—C16—C17	−61.4 (2)	C16—C3—C4—C11	74.53 (19)
C3—C2—C8—O1	170.49 (19)	C16—C17—C18—C19	−85.1 (2)
C3—C2—C8—O2	−8.5 (2)	C16—C17—C18—C23	93.9 (2)
C3—C4—C5—N1	−7.9 (3)	C17—C18—C19—C20	178.46 (16)
C3—C4—C5—C6	171.74 (17)	C17—C18—C23—C22	−179.06 (18)
C3—C4—C11—O3	−176.57 (18)	C18—C19—C20—Br1	−179.44 (13)
C3—C4—C11—O4	3.8 (2)	C18—C19—C20—C21	0.8 (3)
C3—C16—C17—N2	179.82 (17)	C19—C18—C23—C22	−0.1 (3)
C3—C16—C17—C18	2.7 (3)	C19—C20—C21—C22	−0.5 (3)
C4—C3—C16—C15	−118.3 (2)	C20—C21—C22—C23	−0.1 (3)
C4—C3—C16—C17	63.2 (2)	C21—C22—C23—C18	0.4 (3)
C5—N1—C1—C2	9.0 (3)	C23—C18—C19—C20	−0.5 (3)
C5—N1—C1—C7	−170.77 (17)		

Hydrogen-bond geometry (Å, °)

D—H$\cdots A$	D—H	H$\cdots A$	$D\cdots A$	D—H$\cdots A$
N1—H1$\cdots$N2[i]	0.88	2.26	3.125 (2)	169
C22—H22$\cdots$O3[ii]	0.95	2.58	3.302 (3)	134

Symmetry codes: (i) $-x+1/2$, $y-1/2$, $-z+1/2$; (ii) $x+1/2$, $-y+1/2$, $z+1/2$.

All esds (except the esd in the dihedral angle between two l.s. planes) are estimated using the full covariance matrix. The cell esds are taken into account individually in the estimation of esds in distances, angles and torsion angles; correlations between esds in cell parameters are only used when they are defined by crystal symmetry. An approximate (isotropic) treatment of cell esds is used for estimating esds involving l.s. planes.

Acknowledgement

4.7 References

1. Polgar, O.; Bates, E. ABC transporters in the balance: is there a role in multidrug resistance?, *Biochem. Soc. Trans.* **2005,** 33, 241-245

2. Tamaki, A., Ierano, C., Szakacs, G., Robey, R. W., and Bates, S. E. The controversial role of ABC transporters in clinical oncology, *Biochemistry* **2011,** 50, 209-232

3. Szakacs, G., Paterson, J. K., Ludwig, J. A., Booth-Genthe, C., and Gottesman, M. M. Targeting multidrug resistance in cancer, *Nat. Rev. Drug Discov*. **2006**, 5, 219-234

4. Nobili, S.; Landini, I.; Giglioni, B.; Mini, E. Pharmacological Strategies for Overcoming Multidrug Resistance. *Current Drug Targets,* **2006***, 7,* 861-879

5. Zhou, F.; Shao, O.; Coburn, R.A.; Morris, M.Quantitative structure-activity relationship and quantitative structure-pharmacokinetics relationship of 1,4-dihydropyridiens and pyridines as multidrug resistance modulators. *Pharm. Res*., **2005**, *22*, 1989-1996

6. Zhou, F.; Zhang, L.; Tseng, E.; Scott-Ramsay, E.; Schentag, J.; Coburn, A.; Morris, M. Effectis of dihydropyridines and pyridines on multidrug resistance mediated by breast cancer resistance protein. In vitro and vivo studies. *Drug Metab. Dispos*., **2005**, *33*, 321-328.

7. Linton, K.J. Structure and Function of ABC Transporters. *Physiology*, **2007**, *22*: 122-130

8. Shah, A.; Bariwal, J.; Molnár, J.; Kawase, M.; Motohashi, N. *Top. Heterocycl. Chem*. **2008**, *15*, 201

9. Mehdipour, A.R.; Javindnia, K.; Hemmateenejad, B.; Amirghorfran, Z.; Miri, R. *Chem. Biol. Drug. Design*. **2007**, *70*, 337-346

10. Voigt, B.; Coburger, C.; Monar, J.; Hilgeroth, A. *Bioorg. Med. Chem*., **2007**, *15*, 5110-5113

11. Matrosovich, M. N. Towards the development of antimicrobial drugs acting by inhibition of pathogen attachment to host cells: a need for polyvalency, *FEBS Lett. 252*, **1989,** 1-4

12. Ekins, S.; Ecker, G.F.; Chiba, P.; Swaan, W. Future directions for drug transporter modeling. *Xenobiotica,* **2007**, *37*, 1152-1170..

13. Crivori, P.; Reinach, B.; Pezzetta, D.; Poggesi, I. Computational models for identifying potential P-glycoprotein substrates and inhibitors. *Mol. Pharm.*, **2006**, *3*, 33-44.

14. Ecker, G.; Huber, M.; Schmid, D.; Chiba , P. The importance of a nitrogen atom in modulators of multidrug resistance. *Mol Pharmacol*., **1999**, 56:791–796

15. Rees, C.; Johnson, E.; Lewinson, O.; ABC transporters: the power of change. *Nat. Rev. Mol. Cell Biol.* **2009**, 10, 218-227

16. Ishigamin, M.; Tominaga, Y.; Nagao, K.; Kimura, Y.; Matsuo, M.; Kioka, N.; Ueda, K. ATPase activity of nucleotide binding domains of human MDR3 in the context of MDR1. *BIochim. Biophys Acta*. **2013**, 4, 683-690

17. Wang, J.; Casciano, N.; Clement, P.; Johnson, W. Active transport of fluorescent P-glycoprotein substrates: evaluation as markers and interaction with inhibitors. *Biochem Biophys Res Commun* **2001** *580-585*

18. Pires, M. M., Emmert, D., Hrycyna, C. A., and Chmielewski, J. Inhibition of P-glycoprotein-mediated paclitaxel resistance by reversibly linked quinine homodimers, *Mol. Pharmacol. 75*, **2009,** 92-100

19. Sauna, E.; Andrus, B.; Turner, M.; Ambudkar, V. Biochemical basis of polyvalency as a strategy for enhancing the efficacy of P-glycoprotein (ABCB1) modulators: Stipiamide homodimers separated with defined-length spacers reverse drug efflux with greater efficacy, *Biochemistry* **2004**, 2262-2271

20. Pires, M. M., Emmert, D., Hrycyna, C. A., and Chmielewski, J. Inhibition of P-glycoprotein-mediated paclitaxel resistance by reversibly linked quinine homodimers, *Mol. Pharmacol. 75*, **2009,** 92-100

21. Pires, M. M., Hrycyna, C. A., and Chmielewski, J. Bivalent probes of the human multidrug transporter P-glycoprotein, *Biochemistry 45*, **2006,** 11695-11702

22. Lugo, M. R. and Sharom, F. J. Interaction of LDS-751 and rhodamine 123 with P glycoprotein: evidence for simultaneous binding of both drugs. *Biochemistry 44*, **2005,** 14020-14029

23. Loo, T. W., Bartlett, M. C., and Clarke, D. M. Simultaneous binding of two different drugs in the binding pocket of the human multidrug resistance P-glycoprotein, *J. Biol. Chem. 278*, **2003,** 39706-39710

24. Szabon-Watola, Monika; Ulatowski, Sarah V.; George, Kathleen M.; Hayes, Christina D.; Steiger, Scott, Fluorescent probes of the Isoxazole-Dihydropyridine

Scaffold: MDR-1 binding and homology model. *Bioorganic & Medicinal Chemistry* **2014**, 24, 117-121

25. Kaymaz, A.; Tan, H.; Altug, T.; Buyukdevrim, A. The effect of calcium channel blockers, verapamil, nifeditpine and diltiazem, on metabolic control in dibabetic rats. *Diabetes Res Clin Pract.* **1995**, 201-205

26. Miri, R.; Javidnia, K.; Kebriae-Zadeh, A.; Niknahd, H.; Shaygani, N.; Semnanian,S.; Shafiee, A. Synthesis and evaluation of pharmacological activities of 3, 5-dialkyl 1, 4-dihydro-2,6-dimethyl-4-nitroimidazole-3, 5-pyridine dicarboxylates. *Pharm. Med. Chem.* **2003**, 422-428

27. Tsuruo, T.; Lida, H.; Nojiri, M.; Tsukagoshi, S.; Sakurai, Y. Circuvention of vincristine and adriamycin resistance in vitro and in vivo by calcium influx blockers. *Cancer Res*. **1983**, 2905-2910

28. Tsuruo, T.; Lida, H.; Yamashiro, M.; Tsukagoshi, S.; Sakurai, Y. Enhancement of vincristine- and adriamycin-induced cytotoxicity by verapamil in P388 leukemia and its sublines resistant to vincristine and adriamycin. *Cancer Res*. **1983**, 2905-2910

29. Miller, T.; Gorgan, T.; Dalton, W. P-glycoprotein expression in malignant lymphoma ans reversal of clinical drug resistance with chemotherapy plus high-dose verapamil. *J. Clin. Oncol*. **1991**, 17-24

30. McKay, S.; Finn, G. Click chemistry in complex mixtures: Bioorthogonal bioconjugation. *Chem Biol.* **2014**, 21, 11075-1101

31. Garrigos, M.;Mir, L.;Orlowski, S. Competitive and non-competitive inhibition of the multidrug-resistance-associated P-glycoprotein ATPase-further experimental evidence for a multisite model. *Eur J Biochem* **1997**, 664-673

32. Auffinger, P.; Hays, F. A.; Westhof, E.; Ho, P. S. Halogen bonds in biological molecules. *Proc. Natl Acad. Sci.* **2004,** 101, 16789–16794

33. Wilcken, R.; Zimmermann, M. O.; Lange, A.; Joerger, A. C.; Boeckler, F. M. Principle and applications of halogen bonding in medicinal chemistry and chemical biology. *J. Med. Chem.* **2013**, 56, 1363–1388

34. Hulubei, Victoria; Meikrantz, Scott B.; Quincy, David A.; Houle, Tina; McKenna, John I.; Rogers, Mark E.; Steiger, Scott; Natale, N. R., 4-Isoxazolyl-1,4-dihydropyridines exhibit binding at the multidrug-resistance transporter. *Bioorganic & Medicinal Chemistry* **2012**, 20, 6613-6620

35. Rautio, J.; Humphreys, JE.; Webster, L.; Balakrishnan, A.; Keogh, J.; Kunta, J.; Serabjit-Singh, C.; Polli, J. In vitro p-glycoprotein inhibition assays for assessment of clinical drug interaction potential of new drug candidates: a recommendation for probe substrates. *Drug Metab Dispos*. **2006,** 34, 786-92

Chapter 5

Synthesis of sterically hindered Isoxazolyl Dihydropyridines (IDHPs), and asymmetric
organocatalytic synthesis of IDHP and Isoxazolyl-Quinolones

5.1 Background

The impact of chirality on drug development has been well established, so much
so, that it is a factor that the Food and Drug Administration (FDA) [1] regulates with new
chemical entities. The reason for the FDAs involvement is based in the established
observation that there are observed differences in the pharmaceutical properties of
enantiomers. [2-4] The FDA has also compiled a list of recommendations regarding
switching enantiomers in treatment settings, which include among other things, switching
to a single enantiomer for an approved racemate where appropriate and that both
enantiomers of a new chemical entities should be tested independently. [5,6] As a general
statement, the toxicology, pharmacokinetics and pharmacodynamics of both enantiomers
of a drug can have widely different effects, and as such both enantiomers of a new
chemical entity should be studied and evaluated independently. Since the number of
chiral medicines increases annually, synthetic strategies that exhibit fine stereo control,
and can be efficiently performed on multi-gram scales are needed. [7, 8]

When considering the 1, 4-dyhidropyridine (DHP) ring; if the substituent's on the
C3 and C5 positions of the ring are non-identical, the molecule is chiral at the substituted
C4 center. The C3 and C5 positions are most commonly occupied by ester groups, there
arrangement with respect to the DHP ring and the interactions that they form, have been
proposed to be an influencing factor on the pharmacological activities of DHPs at the
voltage gated calcium channel (VGCC).[9] This along with the well established eudysmic

ratio that exists at the VGCC, makes it so the enantiomers of unsymmetrical DHPs usually differ in their biological activities [10,11] and could have all together opposite bioactivity profiles.[12]

The most common method for synthesizing DHPs is the Hantzsch pyridine synthesis. The synthesis has been known since 1882, and in that time there have been numerous efforts to improve or otherwise modify the reaction.[13-16] The Hantzsch pyridine synthesis consists of the condensation of an aldehyde with two equivalents of an active methylene carbonyl compounds (for example, ethyl acetoacetate) and a subsequent reaction with ammonia to yield a DHP.[17,18] The Hantzsch pyridine synthesis is what is known as a multi-component reaction, meaning that it is a chemical transformation in which three or more reagents form a product derived from all of the reactants.[19] As a comparison, two component reactions generally require a specific order of addition to generate a desired product. On the other hand, multi-component reactions such as the Hantzsch pyridine synthesis don't have the same requirements and the reagents can be added in any order as long as all the reagents are present the final product will still be produced. [20] With this flexibility in the order of addition, multi-component reactions do have a major drawback. Their ability to resist catalysis, this is in large part a result of the aforementioned multiple methods that the reaction can take place. This is further exemplified in the Hantzsch pyridine synthesis by the fact that more than a century has passed between the discovery of the reaction and the discovery of the first catalysts for the synthesis. [21]

In the synthesis of symmetrical DHPs, the reaction is a multi-component reaction or to be more specific, it can be termed a four component reaction. The dicarbonyl

compounds are independent variables and are incorporated twice to produce symmetrical products. The limitation of only producing symmetrical DHPs can be avoided by making modifications to the starting materials. The synthesis can be carried out with one equivalent of either an enamine or a Knoevenagel condensation product with another equivalent of a dicarbonyl compound. The two fragments will react in what is known as a Michael addition to form what will be the C4 center of the DHP. Additionally, if the two fragments are non-identical they will produce a C4 center that is now chiral. This is followed by a proton transfer, and finally an intermolecular enamine formation followed by the loss of water to give the desired DHP final product.

The classical Hantzsch reaction is carried out by reacting the given reagents via refluxing them in either acetic acid or alcohol. [22] Without a catalysis the reaction, involves long reaction times, relatively harsh conditions, and often utilizes large quantities of volatile solvents. There have been attempts over the years, to improve on the harsh reaction conditions that are required for the un-catalyzed synthesis to be successful. [23-27] With more recent research into catalyzing the synthesis, asymmetric or otherwise, the possibility of synthesizing previously unattainable compounds becomes possible. This attention has resulted in a substantial amount of effort being put into discovering a useful catalysis for the reaction. As such, we focused on this recent work to modify our synthetic efforts to generate our next generation of compounds. Rare earth metal Lewis acids, such a $Yb(OTf)_3$ and $Sc(OTf)_3$ have gained the highest rate of adoption as a useful catalysis. $Yb(OTf)_3$, which was discovered in 2005, nearly 120 years after the discovery of the reaction itself, has been shown to give synthetically useful yields for the reaction as well as address a number of the issues that arise from the un-catalyzed

reaction method. [28] Other Lewis acid catalysis such as Proline and PhB(OH)$_2$ have also been shown to catalyze the reaction, but do to by-product formation or additional purification being needed, they have not seen the same adoption rate. [29-32]

But, even utilizing a catalysis the reaction still has one major drawback, it produces racemic mixtures. As mentioned above, we want to explore chiralitys effect on MDR1 inhibition and as such we need a means to synthesis IDHPs stereoselectively.[33-35] The formation of enantiomers and their separation by means of crystallization or preparative chromatography has been historically the predominate means of resolving racemic DHP. But, our goal in this research is to develop a method to asymmetrically produce enatio-pure compounds. With this being said, there have been attempts that have recently discovered effective enantioselective asymmetric synthetic methods for DHPs in the literature. With this research forming the bases of our effort in asymmetric synthesis, we now have the mean to modify established synthetic methods to produce our desired final products.

5.2 Chiral resolution of DHPs

The use of classical resolving methods have been the predominate mean of separating enantiomers of DHPs in the literature. But, it isn't the only potential means of obtaining enantiomers. Resolutions of racemic DHPs have been shown to be possible if a carboxylic acid is present on the DHP ring. DHPs with C3-carboxylic acids can be resolved via diastereomeric salts. [36] This method utilizes diastereomeric salts that are formed in the presents of a chiral amine base that functions as a resolving agent. [36] The most preferred and most successful resolving agents are cinchonidine, [37-39] cinchonine[40,41] and quinidine.[42] Common factors in these separations, is that a racemic

DHP is treated with a chiral base, which forms a crystalline diastereomeric salt. The diastereomeric purity of the salt is improved by repeat crystallization; but to obtain enantiomerically pure DHPs, the salt needs to be removed, this is usually done via acidification. The recovery of the monoacid from the mother liquor can then be treated with another chiral base that will complex the crystalline optical antipode; and after repeated crystallization the opposite enantiomers can be obtained. A benefit of this method is that both enantiomers can be obtained. But the need for repeated crystallization lowers the yield and with this step being essential to obtain a high ee's it makes the purification method impractical on small scales. Additionally, chiral acids such as camphorsulphonic acid and substituted tartaric acids have also been used to separate enantiomers of basic DHP compounds. [43] The resolution of racemic amlodipine has been carried out using (-) camphanic acid chloride, and the diastereomeric amides is then separated via chromatographic methods to give a pure product.[44] This method of separation is the most suitable for DHPs with basic substituent's at the 2 position of the DHP ring.[44]

Chiral resolution of enantiomers by HPLC is another resolution method that is historically very predominate for obtaining DHP enantiomers. Both enantiomers can be obtained using conventional stationary phase chromatography. Alternatively, enantiomers can be directly analyzed on chiral stationary phases.[45] The direct chromatographic enatio separation of unsymmetrical DHPs on chiral stationary phases has been widely used for the determination of enantiomeric purity,[46] and for preparing small quantities of enantiomers,[47][48] for biological investigation.[49,50]

5.3 Asymmetric synthesis of the Hantzsch pyridine synthesis
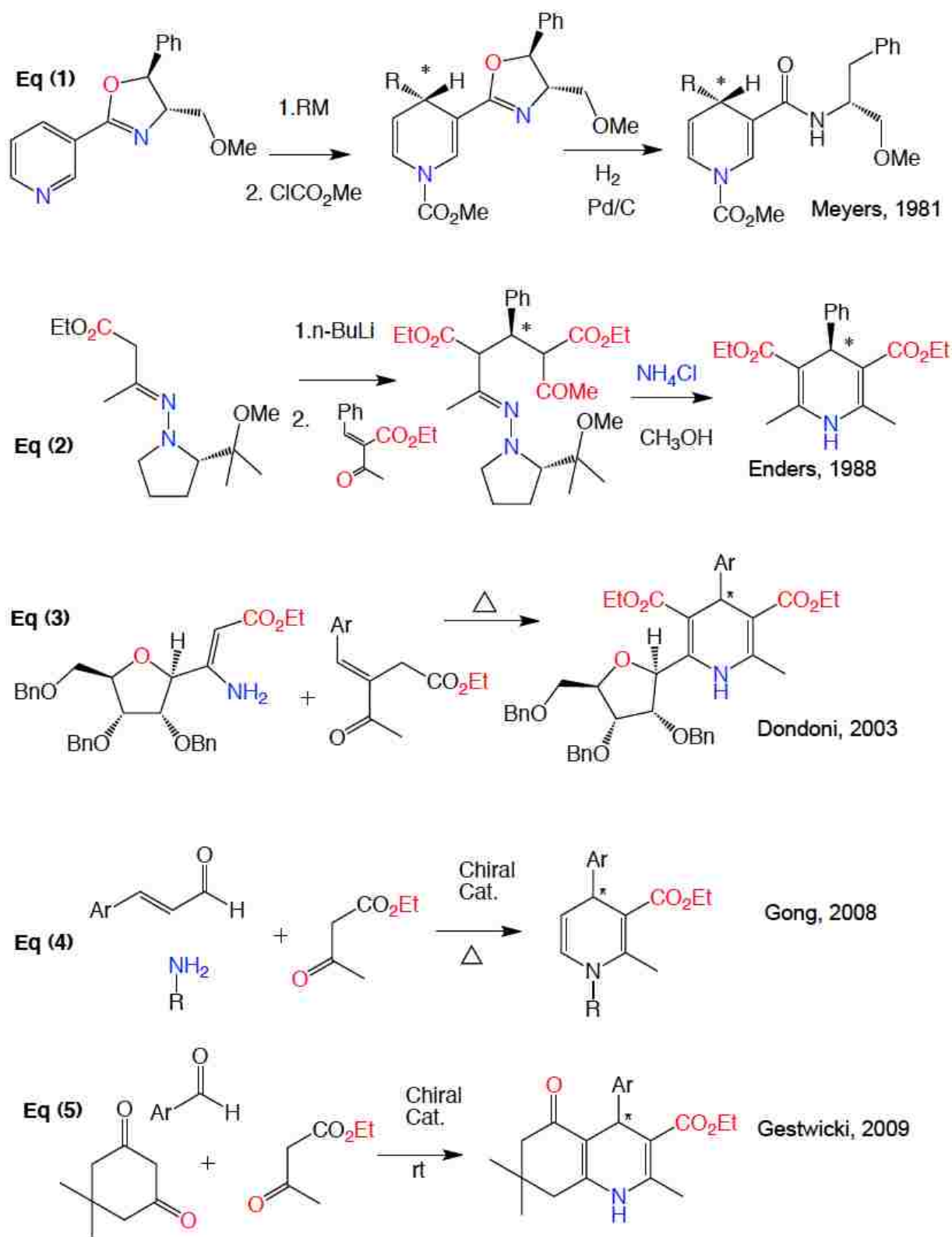
Figure 5.1: Historical evolution of the chiral asymmetric synthesis of DHPs

The use of asymmetric synthetic methods for DHPs has been explored sense the discovery of the Hantzsch pyridine synthesis with varying degrees of success. Historically, the first synthetic strategys involves the synthesis of diastereomeric DHPs with an easily removable chiral auxiliary. This was then followed by the separation of the diastereomers by means of chromatography or fractional crystallization; although this can also be followed by regioselective removal of the group containing the chiral auxiliary. [51][78] This method was further explored by leaving the chiral auxiliary on the DHP and using the auxiliary to assign the C4 chiral center. [52]

Other synthetic methods include the use of amino heterocycles that have been incorporated into the enamine component before the critical Michael addition. The use of different enamines permits the isolation of unsymmetrical DHPs, with the reaction requiring that the enamine be used in combination with an active methylene carbonyl compound to achieve the desired result. [53-55] The mechanism for the reaction involves an aldehyde that is condensed with an active methylene compound to give α,β-unsaturated ketone in a reaction known as a Knoevenagel condensation. The product can then be reacted with a secondary amine to form an enamine that can be reacted with another equivalent of an active methylene compound to give an unsymmetrical and definably chiral DHP.[56] Enantioselective synthetic methods utilizing chiral auxiliaries attached to the nitrogen atom as described above have proven to be practically useful.[57] However, low yields of N-substituted DHP and formation of cyclohexenes as by-products have been observed.[58] As a general statement, this alternative synthetic method of first

141

synthesizing a Knoevenagel or enamine product and then reacting it usually gives good results when the traditional Hantzsch synthesis fails.

5.4 Chiral BIONL phosphoric acids

The development of chiral ester of phosphoric acid as catalysts was initially slower than that of the corresponding phosphor amides, with far fewer examples of the phosphoric acid class of ligand being reported. More recently however interest in phosphoric acids as catalysts has grown; initial work done by two research groups' first explored phosphoric acids as catalysts. Terada and Akiyama independently reported on the catalytic activity of phosphoric acids esters. [59,60] Terada reported the use of a binaphthyl mono-phosphoric acid being utilized in highly enantioselective 1,2-aza Freidal-Crafts reactions, generating the product in a good enantiomeric excess.[61] Akiyama reported the use of a chiral phosphoric acid ester in the enantioselective Mannich-type reaction of ketene silyl acetals with aldimines. Akiyama studies also explored the effect that the R groups present in the 3, 3-positions of the BINOL scaffold, have on the enantiomeric excess of the product. [62]

Many chiral phosphoric acid esters are based on the 1, 1-binaphthol (BINOL) scaffold. Synthetically obtaining the phosphoric acid ester is done via reacting the BINOL diol with phosphoryl chloride in the presence of a base. This is followed by an aqueous work up to give a phosphoric acid ester. The phosphoric acid ester allows the molecule to act as a bi-functional catalyst that contains both a Bronsted acid and Lewis base.[60] Additionally, the phosphoric acid ester is conformationally rigid with one proton being highly acidic, and as such it has been predicted to form hydrogen bonding interactions in transition states.[79] Moving out from the phosphoric acid ester to other

areas of the catalysis, the 3,3-substituents on the BINOL can be varied to change the properties of the catalyst. Studies done where the substituent's at the 3 positions where modified showed the general trend that sterically bulky groups enhance enantioselectivity, whereas less sterically demanding groups gave diminished enantiomeric excesses. [64]

As a class of catalysts, phosphoric acids have been shown to have a wide array of potential uses synthetically. Most commonly phosphoric acid catalysis have been used as hydrogen bonding catalysts for a wide variety of reactions.[65] Additionally, chiral BINOL phosphoric acids have been reported to be used as a chiral resolving agent, but the predominate application of the compound has been it uses as a catalysis.[66]

There have been examples of asymmetric catalysis of the Hantzsch reaction, recently reported by Gong and Gestwicki. [67-69] Phosphoric acid esters exhibit comparable chemical reactivity to Yb (OTf)$_3$ and have been shown to induced high enantioselectivity. Building on this work we have decided to utilize Yb (OTf)$_3$ to produce racemic isoxazole-dihydropyridines (IDHP) s and isoxazol-hydroquinolines (IHQ) s. This will then be follow up with the use of a chiral phosphoric acid ester to produce enatio enriched IDHPs and IHQs for the next generations of drug development.

5.5 Next Generation of Compounds

Examining the variations that we have introduced into each generation of IDHP analog development up to this point allows us to pinpoint areas in the SAR that we still want to address. The R2 position (Figure 5.11) and the chirality of IDHP are the remaining aspects that we decided to explore. With these two goals in place, we focused our efforts on pursuing a series of IHQ analogs. Literature pertaining to the 4-aryl-

hydroquinolines has been observed to produce compounds that possess reduced calcium channel activity; this added benefit of being less selective at VGCC is another aspect that makes this sub-structure an ideal lead scaffold to examine. Additionally, to date the compounds haven't been tested at MDR1. The hydroquinolines also contain a chiral center, and this also allows us to examine the effect that chirality has on MDR1 inhibitory activity. With this being said, the need to establish an alternative method of synthesis is key to the next generations of drug development. There have been similar synthetic methods that will allow us to produce our desired product but, the differences that our starting materials have verses the known methods will need to be considered and taken into account; the exploration of these methods will be discussed later in the chapter.

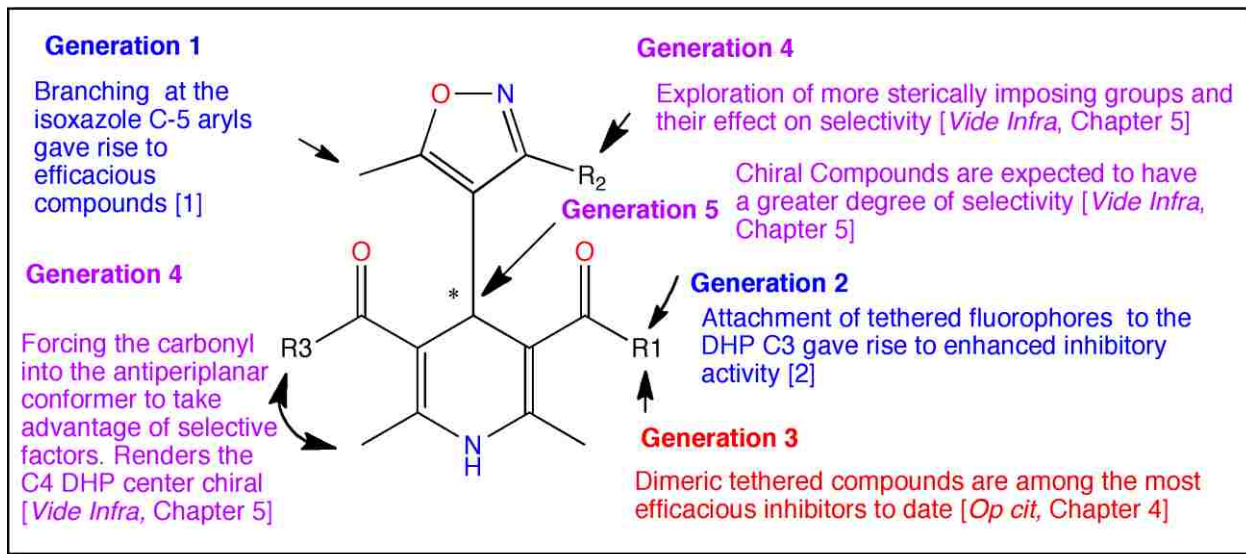Figure 5.2: The breakdown of the generations of drug development as it relate to this project.

Generation 4 compounds will function as a bridging generation of compounds, which will work to both explore a remaining aspect of the SAR and function as stepping stones to set up the 5th generation of chiral compounds by producing racemic IDHPs and IHQs. Going back to generation 1 compounds and comparing it with generation 3

144

monomers we observe a defined increase in activity as we go from Cl to Br IDHP

analogs. The observation that as groups in this position become more sterically imposing

there is an increase in MDR1 inhibition is an SAR factor that we want to examine further.

Thus, we decided to pursue synthetic targets that would examine the degree of steric bulk

that would allow for optimal MDR1 inhibitory activity. Additionally, we have the

opportunity to examine the potential effect halogen bonding interactions could have with

binding to MDR1. In chapter 2 and 3 we observed halogen bonding interactions in the

crystal structure, and as such we want to see if the increase in activity is potentially due to

steric bulk or halogen bonding interactions. Also previous work that relates to the

selectivity of similar compounds was done by Triggle and Natale. Both groups noted that

more steric aryl-DHPs and IDHPs have reduced calcium channel activity. [70-72] As such,

we are looking to take advantage of this SAR factor to allow for more MDR1 selective

compounds. But, we are encouraged to not utilize the conventional un-catalysized

Hantzsch pyridine synthesis. The un-catalyzed Hantzsch pyridine synthesis isn't an

optimal synthetic strategy for synthesizing more steric compounds due to that previous

studies attempting to produce more sterically demanding compounds often results in

almost none of the desired product being formed due; to what has been termed the tennis

racket effect. Thus, a new synthetic method is needed to synthesize the desired target

compounds. As mentioned above, the use of Ytterbium (III) trifluoromethanesulfonate

(Yb) was recently reported as a catalysis for synthesizing aryl-hydroquinolines. [73] As

such, we manipulated the method to work as a catalysis to produce our desired generation

4 IDHPs and IHQs compounds. Using Yb III as a catalysis also requires less harsh

reaction conditions and as a general statement provides higher yields.

Entry	R	% yield	HRMS calc'd	Found
1a	1'-Naphthyl	64.04	501.2026	501.2019
2a	1'-(2'-methoxy-Naphthyl)	50.21	491.2182	491.2205
3a	9'-Anthryl	41.98	511.2233	511.2228
4a	3,4-Bis –benzyloxy-benzene	67.95	469.1975	469.1990
5a	3-Phenoxy-benzene	60.98	501.2026	501.2019
6a	4-Methoxy-benzene	60.96	441.2026	441.2057
7a	2,4-Dimethoxy-benzene	63.98	623.2757	623.2709
8a	3,4-Dimethoxy-benzene	53.19	623.2757	623.2807
9a	4-Biphenyl	46.23	487.2233	487.2256

Table 5.1. Lanthanide catalyzed synthesis of sterically hindered isoxazolyl-dihydropyrdines

The fifth generation of compounds will focus on establishing a eudysmic ratio for the IHQs and IDHPs at MDR1. Given Triggles work on aryl-DHPs, a syn-periplanar conformation for the carbonyl groups at C3 and C5 on the DHP ring is suggested as a common feature of DHPs that lead to their calcium channel antagonist activity. [74-76] To capitalize on this factor and increase the selectivity of our compounds while still focusing on producing chiral center at the C4 center of the DHP ring. We propose that one of the carbonyl groups can be forced into an anti-periplanar conformation. This can be accomplished by using dimedone as one equivalent of our dicarbonyl fragment, while using ethyl acetate as the second equivalent in a standard Hantzsch pyridine synthesis. Additionally, as a proof of concept that the modification leads to reduced VGCC activity 4-aryl-hydroquinolones have been observed to have weak calcium channel activity [77] when compared to their DHP counterparts. This could be contributed to the aforementioned locking of the carbonyl group, thus giving us the bases to pursue IHQs that should show less activity at the VGCC and be more selective for MDR1. Additionally, the modification introduces chirality at the C4 center and will allow us to take advantage of the eudysmic ratio that is known at the VGCC. It consequently, allows

us to examine if there is also a lack of a eudysmic ratio at MDR1. The synthesis and exploration of the proposed concepts will be discussed later in the chapter.

5.6 Generation 4 Synthesis
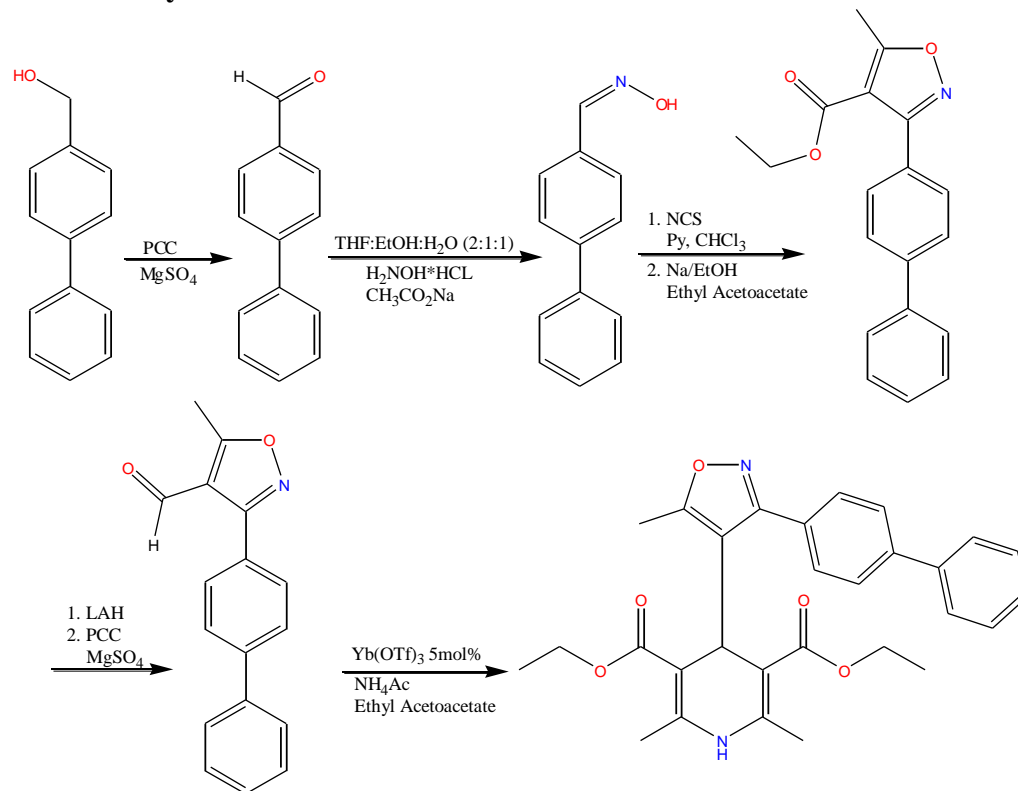
Figure 5.3: Representative Synthetic Route for sterically hindered IDHP compounds.

The synthetic route proposed to obtain generation 4 compounds is similar to methods used in previous generations of drug development. The utilization of an alcohol as a starting material requires that the alcohol needs to be oxidized to an aldehyde *via* Pyridinium chlorochromate (PCC) to allow for the formation of an oxime. But, once an oxime is in hand the synthetic methods for the formation of the isoxazolyl-aldehyde is identical to that described in earlier chapters. The notable exception to generation 3 synthetic methods is that the Hantzsch pyridine synthesis is carried out with the Yb (III) catalysis. This method allows for better yields and more sterically hindered systems to be synthesized effectively. The catalyzed method also requires less solvent and it can be ran

at room temperature, with the one down side that it requires longer reaction times for larger reaction scales. We also wanted to examine unsymmetrical IHQ derivatives in the next generation of compounds so we synthesized, racemic IHQs using the Yb (III) catalytic method.
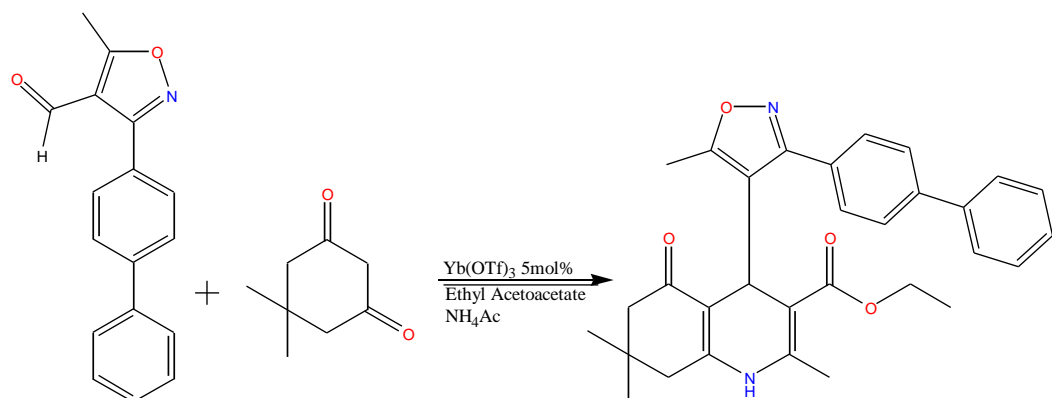
Figure 5.4: Synthetic Route for IHQs utilizing Yb (III) catalytic method

The exact mechanism for the YB (III) catalyzed reaction isn't known with certainty, but it is speculated on in the literature. Generally the mechanism involves the Yb (III) catalysis complexing with an activated methylene compound in its enol form. The activated enol can then react with an aldehyde to give rise to a Knoevenagel product. The Knoevenagel product then reacts in a Michael addition with an equivalent of dimedone or ethyl acetoacetate to from an intermediate where the catalysis is released. From this point in the mechanism the remaining steps in the standard Hantzsch pyridine synthesis are allow to occur to produce a IDHP or IHQ.
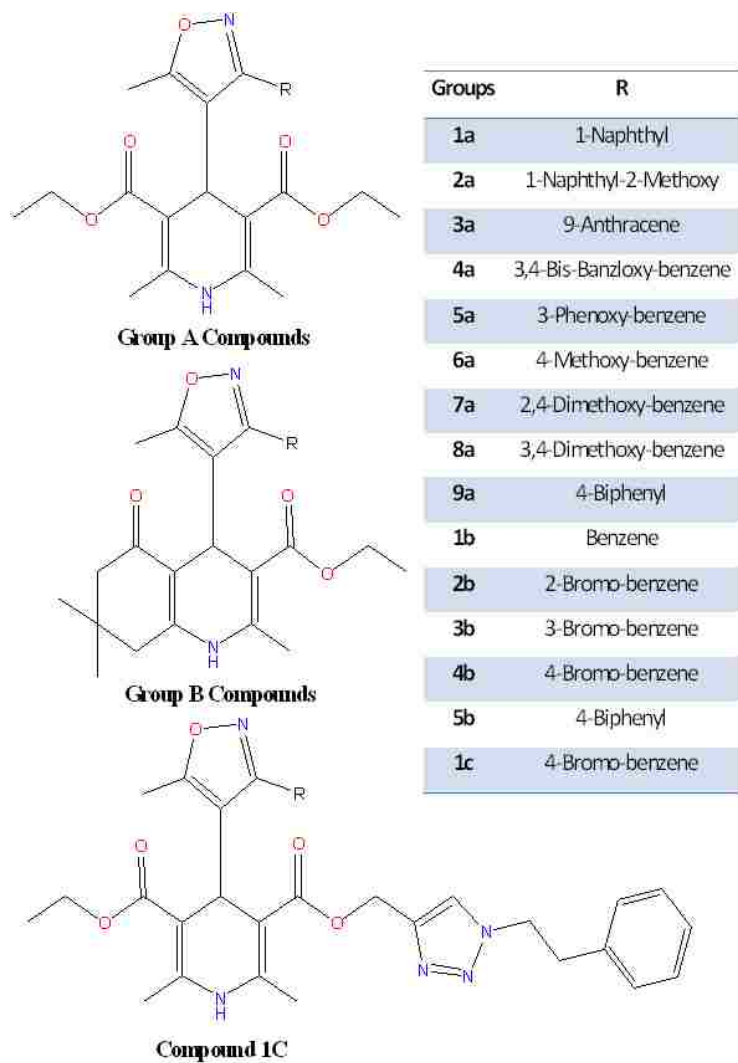
Figure 5.5: Generation 4 library of compounds, using Yb (III) catalyst method

5.7 **Generation 4 Compound (1a, 2a, 1b) Crystal Structures**

A
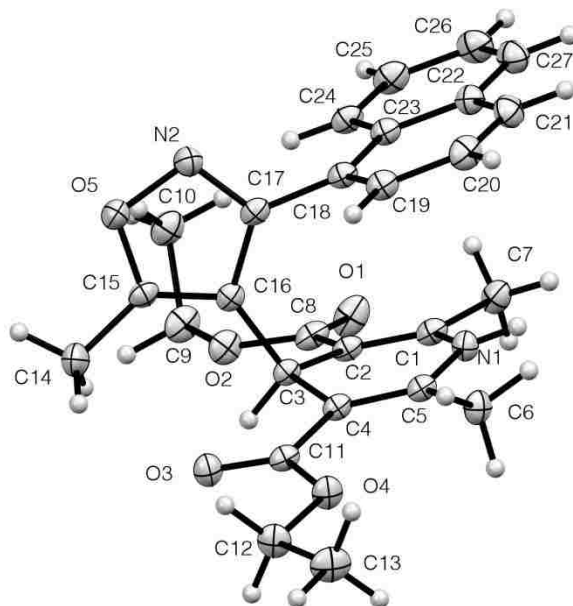
Crystal data

C$_{27}$H$_{28}$N$_2$O$_5$	?
M_r = 460.51	D_x = 1.305 Mg m^{-3}
Monoclinic, $P2_1/c$	Melting point: ? K
Hall symbol: ?	Mo $K\alpha$ radiation, λ = 0.71073 Å
a = 8.2709 (7) Å	Cell parameters from 9866 reflections
b = 20.1782 (16) Å	θ = ?°
c = 14.0531 (12) Å	μ = 0.09 mm^{-1}
β = 92.412 (4)°	T = 100 K
V = 2343.3 (3) Å^3	Prism, translucent white
Z = 4	0.44 × 0.30 × 0.17 mm
$F(000)$ = 976	

Data collection

Bruker SMART BREEZE CCD diffractometer	5938 independent reflections
Radiation source: 2 kW sealed X-ray tube	4468 reflections with $I > 2\sigma(I)$
Graphite monochromator	R_{int} = 0.048

150

Detector resolution: ? pixels mm^{-1}	$\theta_{max} = \underline{28.9}°$, $\theta_{min} = \underline{1.8}°$
$\underline{\varphi \text{ and } \omega \text{ scans}}$	$h = \underline{-11}\quad\underline{11}$
Absorption correction: $\underline{\text{multi-scan}}$ $\underline{SADABS \text{ v2012/1 (Bruker AXS Inc.)}}$	$k = \underline{-27}\quad\underline{25}$
$T_{min} = \underline{0.703}$, $T_{max} = \underline{1.000}$	$l = \underline{-18}\quad\underline{13}$
$\underline{20554}$ measured reflections	

Refinement

Refinement on $\underline{F^2}$	Secondary atom site location: $\underline{?}$
Least-squares matrix: $\underline{\text{full}}$	Hydrogen site location: $\underline{\text{inferred from}}$ $\underline{\text{neighbouring sites}}$
$R[F^2 > 2\sigma(F^2)] = \underline{0.051}$	$\underline{\text{H-atom parameters constrained}}$
$wR(F^2) = \underline{0.142}$	$\underline{w = 1/[\sigma^2(F_o^2) + (0.0695P)^2 + 0.5936P]}$ $\underline{\text{where } P = (F_o^2 + 2F_c^2)/3}$
$S = \underline{1.04}$	$(\Delta/\sigma)_{max} = \underline{0.001}$
$\underline{5938}$ reflections	$\Delta\rho_{max} = \underline{0.38}$ e Å^{-3}
$\underline{312}$ parameters	$\Delta\rho_{min} = \underline{-0.33}$ e Å^{-3}
$\underline{0}$ restraints	Extinction correction: $\underline{\text{none}}$
$\underline{?}$ constraints	Extinction coefficient: $\underline{?}$
Primary atom site location: $\underline{\text{structure-}}$ $\underline{\text{invariant direct methods}}$	

B

Crystal data

C$_{28}$H$_{30}$N$_2$O$_6$	calculated from global refinement
M_r = 490.54	D_x = 1.331 Mg m^{-3}
Monoclinic, C2/c	Melting point: ? K
Hall symbol: -C 2yc	Cu $K\alpha$ radiation, λ = 1.54178 Å
a = 19.5698 (9) Å	Cell parameters from 5879 reflections
b = 15.3341 (7) Å	θ = 2.7–68.4°
c = 17.2324 (7) Å	μ = 0.77 mm^{-1}
β = 108.724 (3)°	T = 100 K
V = 4897.5 (4) Å^3	Prism, translucent pale yellow
Z = 8	0.31 × 0.15 × 0.06 mm
$F(000)$ = 2080	

Data collection

Bruker D8 Venture PHOTON 100 CMOS diffractometer	4278 independent reflections
Radiation source: INCOATEC ImuS micro-focus source	2418 reflections with $I > 2\sigma(I)$
Mirrors monochromator	R_{int} = 0.076

Detector resolution: 10.4167 pixels mm^{-1}	$\theta_{max} = 66.6°$, $\theta_{min} = 3.7°$
ω and phi scans	$h = -23 \quad 22$
Absorption correction: numerical SADABS V2008/1 (Bruker AXS Inc.)	$k = -18 \quad 15$
$T_{min} = 0.70$, $T_{max} = 0.96$	$l = -19 \quad 20$
16347 measured reflections	

Refinement

Refinement on F^2	Secondary atom site location: difference Fourier map
Least-squares matrix: full	Hydrogen site location: inferred from neighbouring sites
$R[F^2 > 2\sigma(F^2)] = 0.091$	H atoms treated by a mixture of independent and constrained refinement
$wR(F^2) = 0.265$	$w = 1/[\sigma^2(F_o^2) + (0.1199P)^2 + 11.9275P]$ where $P = (F_o^2 + 2F_c^2)/3$
$S = 1.03$	$(\Delta/\sigma)_{max} = 0.005$
4278 reflections	$\Delta\rho_{max} = 0.88$ e Å^{-3}
335 parameters	$\Delta\rho_{min} = -0.26$ e Å^{-3}
0 restraints	Extinction correction: none
? constraints	Extinction coefficient: ?
Primary atom site location: structure-invariant direct methods	

C

Crystal data

<u>C$_{25}$H$_{28}$N$_2$O$_4$</u>	<u>?</u>
M_r = <u>420.49</u>	D_x = <u>1.286</u> Mg m^{-3}
Monoclinic, <u>$P2_1/c$</u>	Melting point: ? K
Hall symbol: <u>?</u>	<u>Mo $K\alpha$ radiation, λ = 0.71073</u> Å
a = <u>16.0832 (7)</u> Å	Cell parameters from <u>7766</u> reflections
b = <u>9.8265 (4)</u> Å	θ = <u>2.5–27.5</u>°
c = <u>13.7577 (6)</u> Å	μ = <u>0.09</u> mm^{-1}
β = <u>93.053 (3)</u>°	T = <u>100</u> K
V = <u>2171.20 (16)</u> Å^3	<u>Prism, yellow</u>
Z = <u>4</u>	<u>0.18 × 0.13 × 0.13</u> mm
$F(000)$ = <u>896</u>	

Data collection

<u>Bruker SMART BREEZE CCD</u> diffractometer	<u>4980</u> independent reflections
Radiation source: <u>2 kW sealed X-ray tube</u>	<u>3220</u> reflections with <u>$I > 2\sigma(I)$</u>
<u>Graphite</u> monochromator	R_{int} = <u>0.068</u>
Detector resolution: ? pixels mm^{-1}	θ_{max} = <u>27.5</u>°, θ_{min} = <u>1.3</u>°

φ and ω scans	$h = -17 \quad 20$
Absorption correction: multi-scan *SADABS* v2012/1 (Bruker AXS Inc.)	$k = -12 \quad 12$
$T_{min} = 0.938$, $T_{max} = 1.000$	$l = -17 \quad 17$
30941 measured reflections	

Refinement

Refinement on F^2	Secondary atom site location: ?
Least-squares matrix: full	Hydrogen site location: inferred from neighbouring sites
$R[F^2 > 2\sigma(F^2)] = 0.052$	H-atom parameters constrained
$wR(F^2) = 0.120$	$w = 1/[\sigma^2(F_o^2) + (0.0472P)^2 + 0.7827P]$ where $P = (F_o^2 + 2F_c^2)/3$
$S = 1.02$	$(\Delta/\sigma)_{max} \leq 0.001$
4980 reflections	$\Delta\rho_{max} = 0.34$ e Å^{-3}
285 parameters	$\Delta\rho_{min} = -0.34$ e Å^{-3}
0 restraints	Extinction correction: none
? constraints	Extinction coefficient: ?
Primary atom site location: structure-invariant direct methods	

Figure 5.6 ORTEPs of (A) **Naphthyl**-**2**. (B) Methoxy-Naphthyl-**2. (C)** IQ **3a,** 50% probability ellipsoids. Complete crystallographic information files (cif's) are available from the authors upon request.

Single crystal x-ray diffractometry (sc-xrd) was used to characterize the conformation of IDHPs **1a**, **2a** and IHQ **1b**. Interestingly, the both hindered naphthyl IDHPs 1a and **2a,** adopt a solid state conformation where the isoxazole is *endo* to the DHP, likely due to crystal packing forces. In contrast, the IHQ **1b** orients the C-3 isoxazole phenyl *exo* to the hydroquinolines ring, probably due to the influence of the axial of the geminal dimethyls on the hydroquinolines B ring.

5.8 HPLC Traces

The generation 4 IHQs and IDHP that where synthesized above were made to examine both SAR elements and to establish racemic compounds to allow for a comparison to generation 5 chiral compounds. To set the ground work for this comparison to take place, traces of the racemic IHQs and IDHPs were collected to compare to the chiral IHQ and IDHP in generation 5. The racemic IHQ and IDHP compounds were analyzed on a cellulose based chiral pack AD chiral stationary phase (CSP) column (Fig. 5.7).
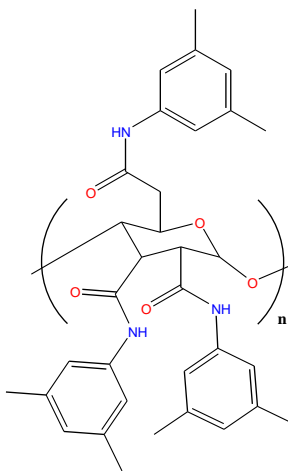
Figure 5.7: Structure of Cellulose Based Chiral Stationary Phase (CSP) Column

As one would expect with racemic compounds, both enantiomers can be observed in the HPLC traces (Figure 5.8). This establishes a control resolution of the IHQ and IDHP enantiomers and will be utilized in the analysis of putative asymmetric induction (*vide infra*). The mobile phase solution that was used in the process was a 90/10 HPLC grade hexane/isopropanol solution at a flow rate of 0.85 mL/min.
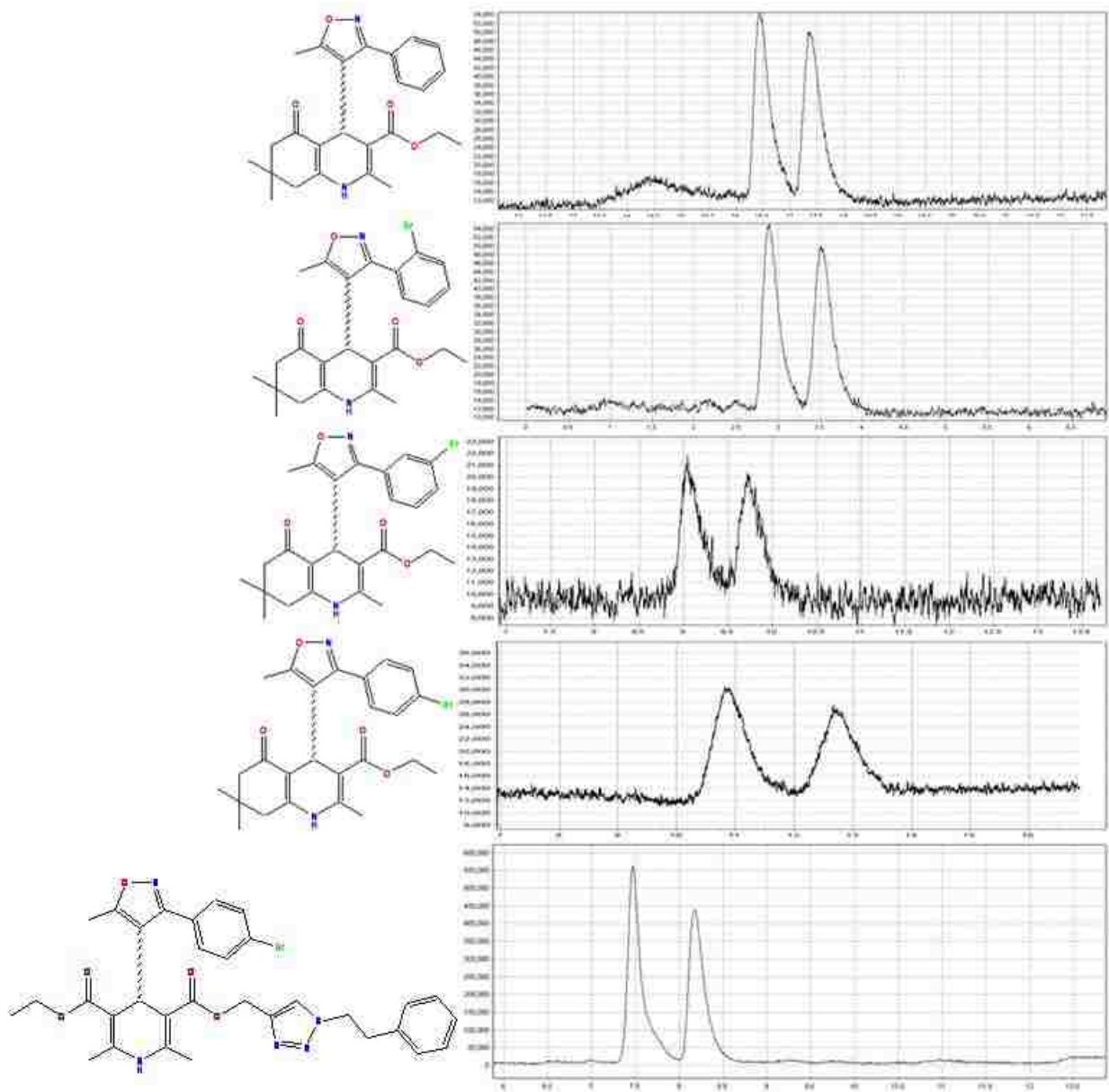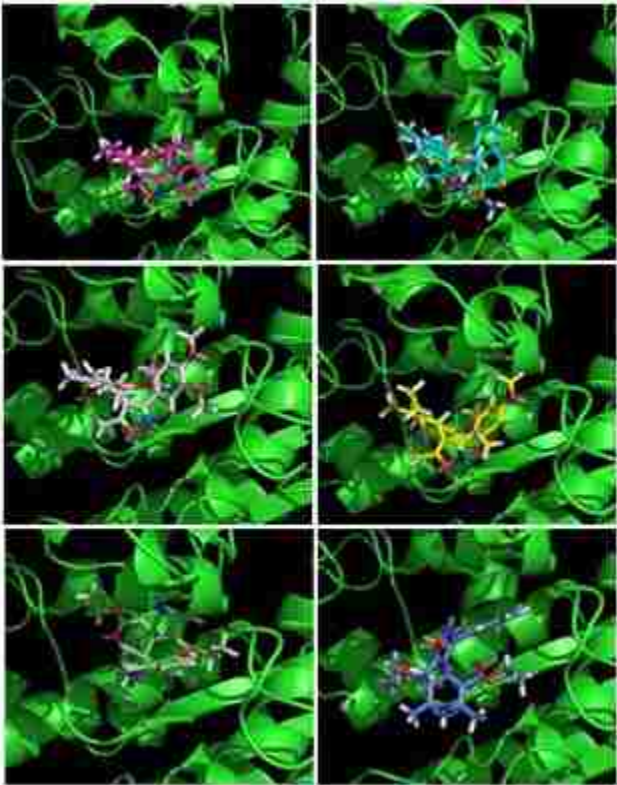
Figure 5.8: HPLC trace of the Racemic Generation 4 compounds

With racemic traces of our desired compounds in hand we moved on to examine the potential interaction that generation 4 compounds could have with MDR1 and see if we could establish a tentative SAR before moving on to synthesizing generation 5 compounds.

5.9 Computational modeling for generation 4 compounds

Due to a lack of biological data for this generation of compounds, computational modeling was employed and the compounds were bound into the previously established homology model. This process is identical to the process used in previous generations of drug development, with the exception that we utilized CHEM PLP scores to establish a gradation between the proposed compounds. As a result of this we used CHEM PLP scores to establishing the lead compound in this generation of drug development and to allow us to have a reason to examine one compounds SAR factors over another. The library of compounds was localized and binding calculations were done identically to the past generations of compounds, as such the process isn't described in detail here.

R	CHEMPLP
1-Naphthyl	51.88
1-Naphthyl-2-Methoxy	48.46
9-Anthracene	44.82
3-Phenoxy-benzene	52.77
4-Methoxy-benzene	47.25
2,4-Dimethoxy-benzene	49.07
3,4-Dimethoxy-benzene	50.65
4-Biphenyl	54.07

Figure 5.9: Generation 4 binding energies predicted using ChemPLP.

The most energetically favorable compound is predicted to be the 4-biphenyl IDHP. The establishment of an SAR was identical to previous generations, and as such

the compound was isolated and a 6 Å sphere was examined to establish the close binding

contacts.
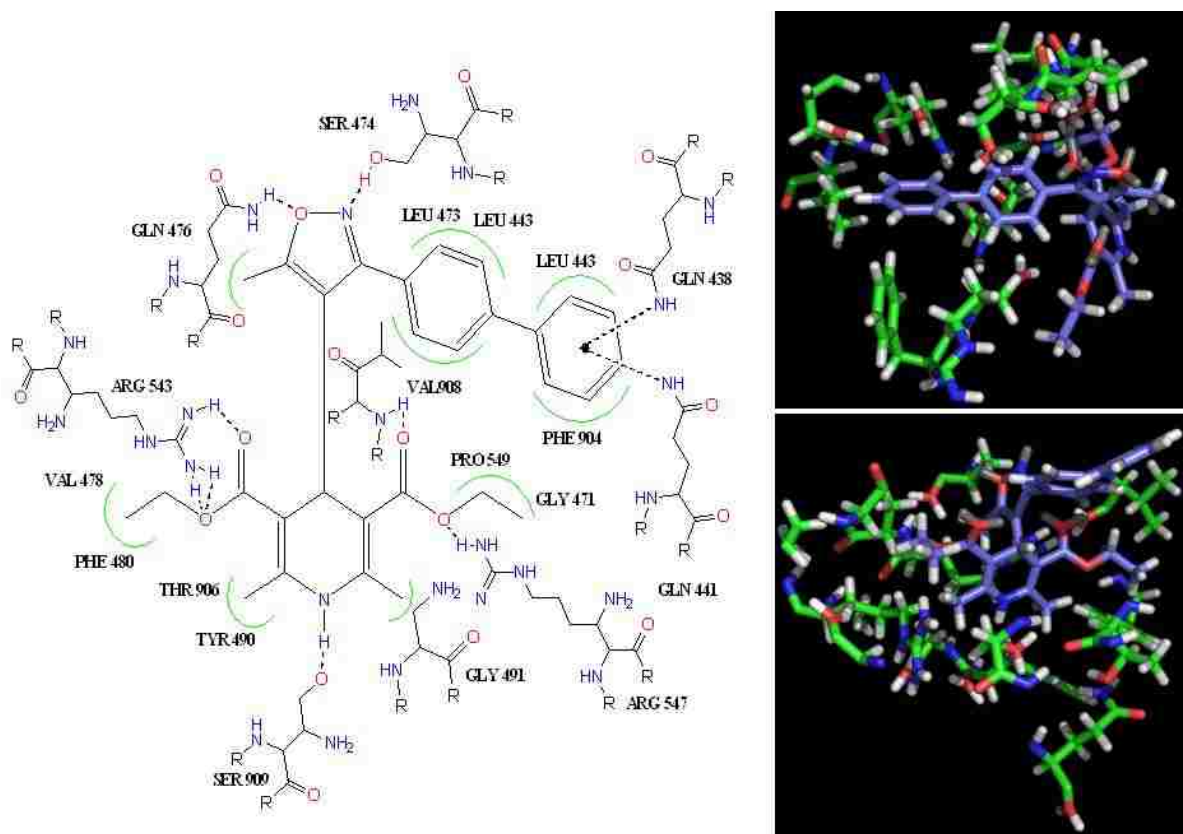
Figure 5.10 Computational prediction for binding box interactions and SAR of compound
9a.

The anchoring interactions that are observed in the calculated best binder are far

more spread throughout the structure when compared to the past generations of drug

development. The DHP substructure is a more substantial anchoring point in this

generation. We also observe that the isoxazole has two key anchoring residues: GLN476

and SER 474 which further validates the inclusion of both the DHP and isoxazole

substructures. Additionally, the inclusion of the more steric and liphophilic groups in the

3-isoxazole position of the IDHPs, increase the calculated binding energies. The overall

SAR that can be taken from the 4th generation of compounds is that both of the isoxazole

and DHP substructures should be maintained in future drug development cycles.

159

Additionally, the inclusion of more steric and liphophilic groups produces compounds that are calculated to be more active. This also tentatively excludes the prediction that halogen bonding is having an effect on increasing MDR1 inhibition. Computational modeling of compounds in generation 4 that could potentially halogen bond don't show this interaction, and the increase in activity seems to be attributed to the increase in steric bulk.

5.10 Chiral IHQ and IDHP synthesis

With generation 4 racemic compounds in hand, we then shifted our attention to synthesizing chiral IHQs and IDHPs. As mentioned above, chiral phosphoric acid BINOL catalyses have been used to synthesize chiral aryl-DHPs. The asymmetric induction is the result of the BINOL catalysis forcing the Hantzsch pyridine synthesis to react in a very defined and deliberate way. The reaction for the IHQs requires a specific order of addition to be successful in producing the desired chiral product. 1.5 equivalents of dimedone and 1 equivalent of ethyl acetoacetate are added in the presents of the chiral BINOL catalysis. This is then followed by the addition of the aldehyde and ammonium acetate. The mixture is then allowed to stir at room temperature and the product can be isolated.
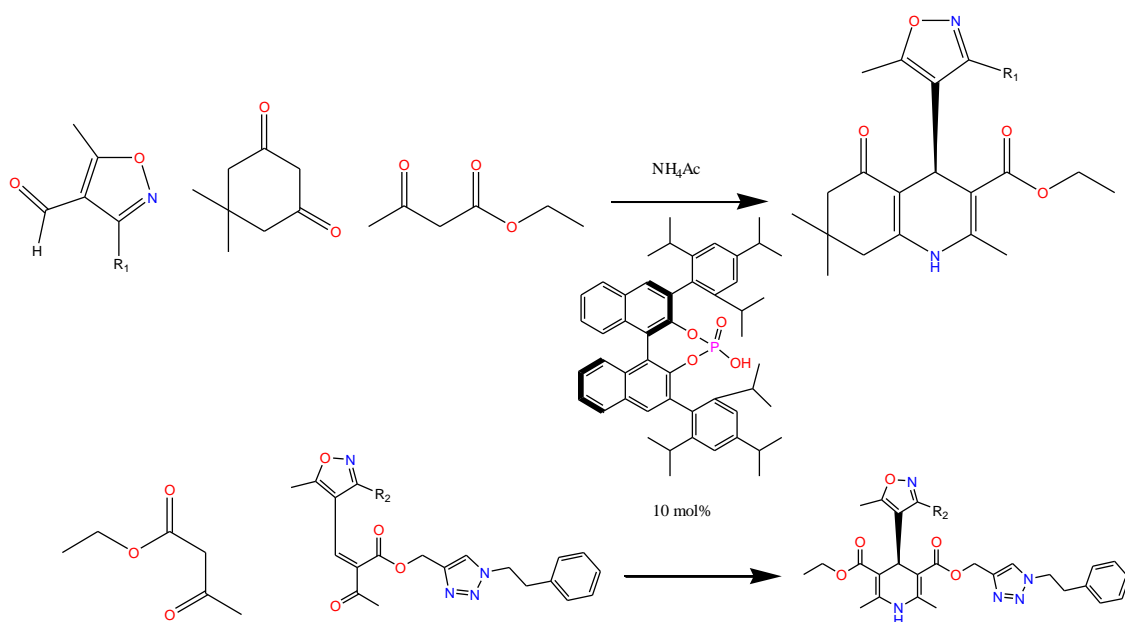
Figure 5.11: Asymmetric organocatalytic syntheses of 4-isoxazolyl-Quinolones.

R$_1$	Catalyst	Yield	$[\alpha]_D$
-Ph	Yb(OTf)$_3$	30.25	
	(R)-BINOL	25.92	-11.2
-o-Br-Ph	Yb(OTf)$_3$	71.60	
	(R)-BINOL	64.35	-13.5
-m-Br-Ph	Yb(OTf)$_3$	62.07	
	(R)-BINOL	60.40	-2.36
-p-Br-Ph	Yb(OTf)$_3$	67.19	
	(R)-BINOL	65.34	-0.032
R$_2$	Catalyst	Yield	$[\alpha]_D$
-p-Br-Ph	Yb(OTf)$_3$	31.56	
	(R)-BINOL	21.32	-2.68

Table 5.2 Asymmetric organocatalytic synthesis of 4-isoxazolyl-Quinolones.

The difference in the activity between the dimedone and ethyl acetoacetate is

what we are hypothesizing as the main factor that leads to the asymmetric induction. The

bases of our argument is an observation made by Gestwicki, during his studies with a

similar BIONL catalysis. He ran reactions with equal equivalents of ethyl acetoacetate

and dimedone, the end result of the study was that 20-30% of the recovered yield was

symmetrical ethyl acetoacetate DHP. This would suggest that ethyl acetoacetate is 20-

30% more reactive with the BIONL catalysis then dimedone. The catalysis allows the

ethyl acetoacetate to react faster than dimedone and to form the enolate. This then leads to the subsequent Knoevenagel reaction to be held in place by the BIONL catalysis. The mechanism for the catalysis isn't known with any certainty, but the suggested route is similar to a reaction mechanism proposed by Gong in his studies with a similar catalysis. This also suggest that the Michael addition that occurs to form the C4 center, occurs by the Knoevenagel product being held in place by the BINOL and the slower reacting dimedone reacts to form the C4 center, again showing similarities to the reaction mechanism proposed by Gong.(Figure 5.11) This would also explain why there is a need to add an additional half of an equivalent of dimedone to the reaction to compensate for the lower reactivity and to aide in the addition to allow for the desired IHQ product being formed.

Another factor leading to the stereo-selective synthesis is what has been termed the stereo-controlling groups at the 3' positions of the BINOL. These groups allow for the selectivity of both a specific geometric isomer and a stereo face for the reaction to occur. The most energetically favorable combination of these factors being the E geometric isomer and the Si face (Figure 5.11). The three other combinations ether place the fragments to far from one another to react or showed extremely unfavorable steric interaction with the stereo-controlling groups. The BINOL catalysis has the most favorable interactions with the E geometric isomer while only allowing the si face to be accessible for any addition. The end result of this is that a si face attack occurs during the Michael addition, leading to the synthesis of the S enantiomer. The control that the BINOL catalysis maintains on both the geometric isomer and facial selectivity allows for the reaction to produce enatio pure compounds.
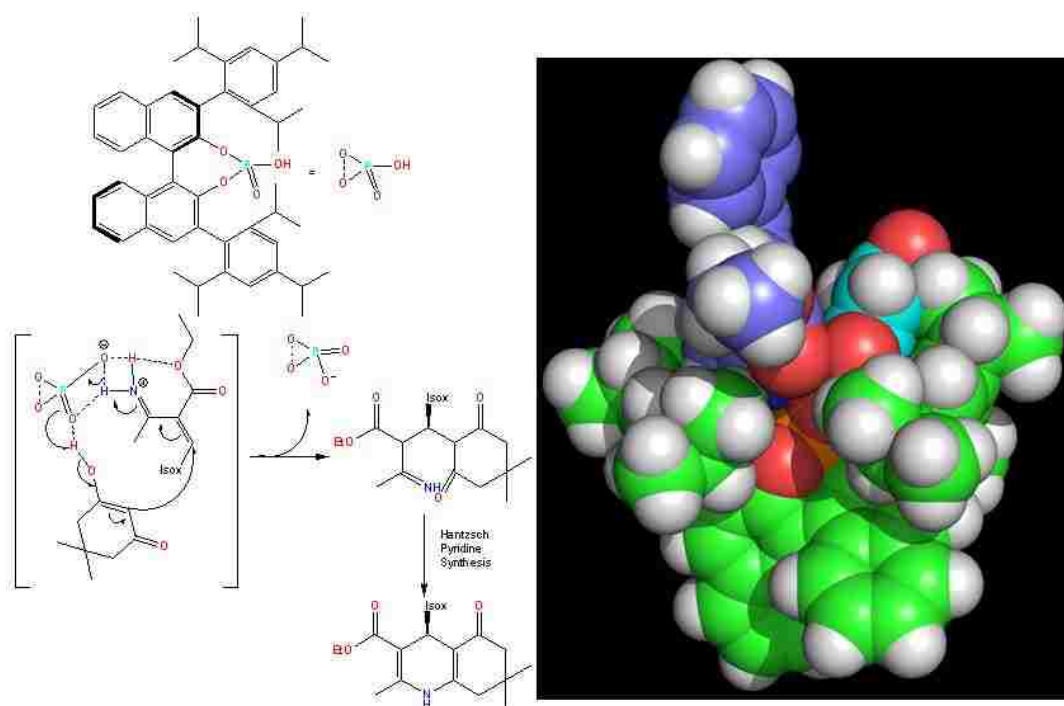
Figure 5.12: Predicted reaction mechanism for the BINOL catalysis. (Left) The predicted critical Michael addition for the reaction, the reaction show several similarities with a predicted reaction that Gong et al. made for a similar reaction with a similar catalysis. (Right) Computational representation of the key Michael addition in the Hantzsch pyridine synthesis, showing the most favorable E geometric isomer and the si face.

The order of addition for the click control, (1c) diverges from the IHQs chiral synthesis in that a Knoevenagel condensation is preformed with 3-Oxo-butyric acid prop-2-ynyl ester and an isoxazole aldehyde to produce an isoxazole α, β-unsaturated ketone before being introduced to the BINOL catalysis. The product is then reacted with the phenylethyl azide in a click reaction to give one fragment in the Hantzsch pyridine synthesis (Figure 5.12). This was done due to that there is essentially no difference in the activity between the first equivalent of a transesterified ethyl acetoacetate and the second equivalent of ethyl acetoacetate to form an enolate. As such the pre-assembly of the Knoevenagel condensation and reacting the product in a click reaction allows us to introduce a larger more sterically encumbered fragment that allows for a difference in

163

activity verses the second equivalent of ethyl acetoacetate. This allows for a difference in how the fragments interact with the catalysis. This difference allows for the catalysis to force the same specific order of addition between the two fragments in the Michael addition and as a result allows for enatio pure compounds to be produced.
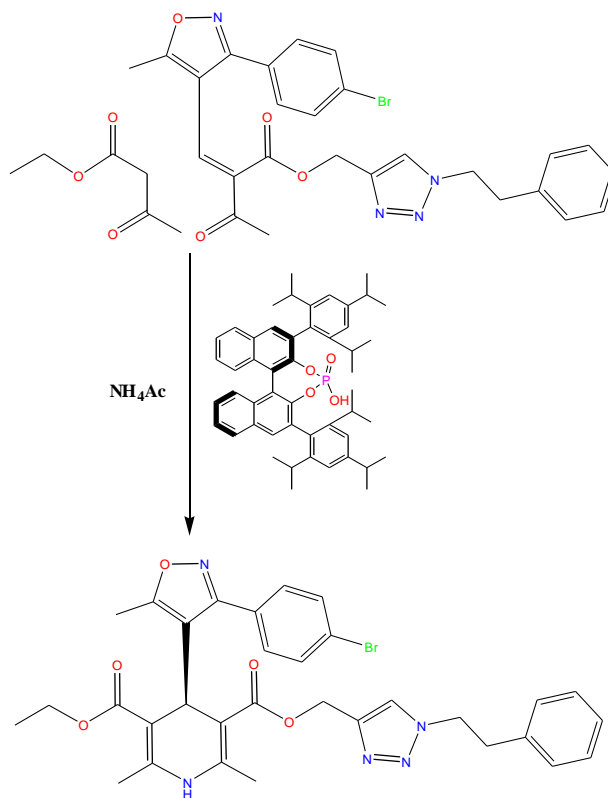
Figure 5.13: Reaction scheme for 1c.

Once the Michael addition is complete, the remaining steps of the Hantzsch pyridine synthesis occur to give either an IDHP or an IHQ product. The remaining reactions that occur to finish off the Hantzsch pyridine synthesis don't have additional effects on the C4 center thus the stereo center that is formed in the Michael reaction remains unchanged, and the center is retained until the final product is formed.

5.11 Chiral HPLC Traces

164

The same chiral cellulose based column that was utilized in the racemic IHQs was utilized again here. As you would expect only one enantiomer is observed with the main source of error being the baseline. As such, while the reaction seems to produce 100%ee product we can only prove that the reaction produces compounds that are around 95% ee due to the aforementioned baseline errors.
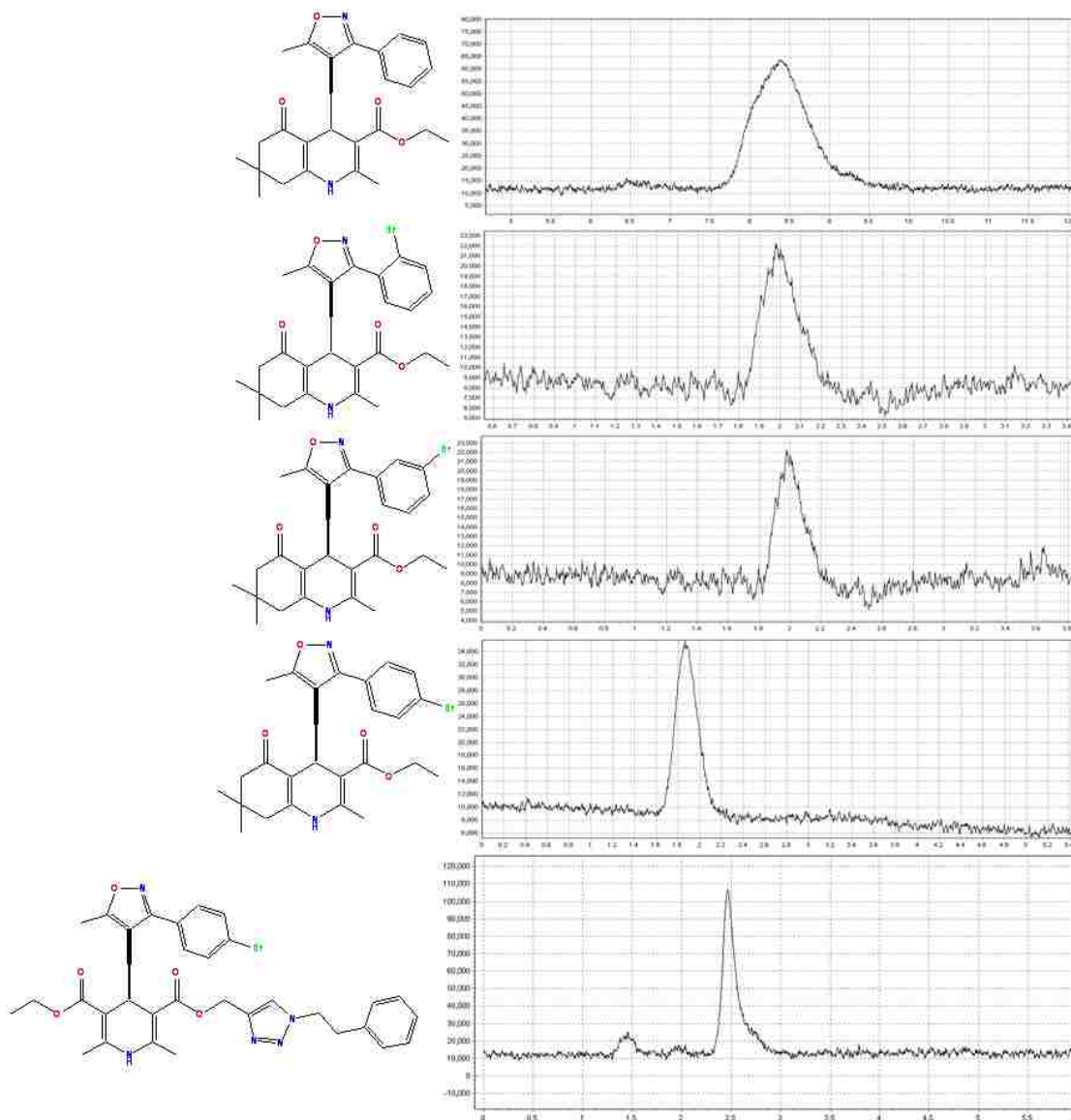
Figure 5.14: HPLC trace of chiral generation 5 compounds

Now with both racemic HPLC traces and chiral HPLC traces in hand we can compare and contrast the two traces.

165
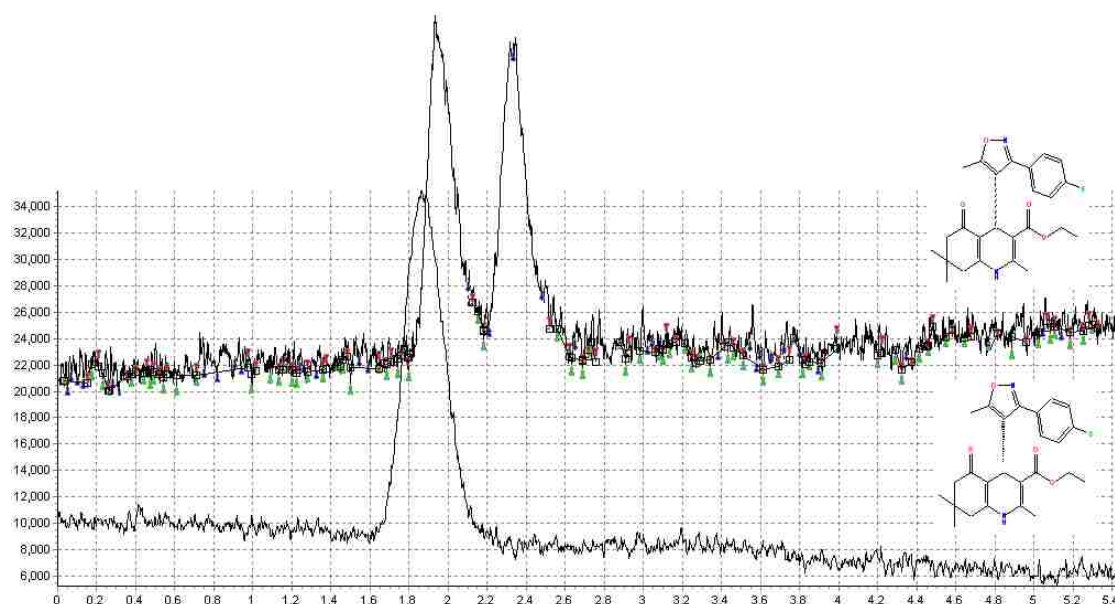
Figure 5.15: Combined HPLC trace of the chiral and racemic IHQs

As a final step we combined the traces of the enatio-enriched IHQ and the racemic IHQ (Figure 5.11). This allows us to make a tentative assignment that the first peak in the HPLC trace is the (-) enantiomer with the second peak being the (+) enantiomer. The absolute configuration was assigned via unpublished work done by Dr. Schade. A personal communication with Dr. Schade informed us that in a similar 4-aryl-hydroquinolones series, compounds that showed a (-) rotation were assigned as the S enantiomer. Dr. Schade's assignment of the absolute conformation was established via x-ray crystallography. As such, we can conclude that our compounds that gave a (-) rotation are the S enantiomer by association.

With both racemic and chiral compounds in hand biological testing would allow for the examination and establishment of a eudysmic ratio at MDR1 for IDHPs and IHQs. Computational modeling for this generation wasn't conducted due to that the literature in the field has established that MDR1 has a minimal eudysmic ratio for aryl-DHPs. This

166

coupled with the several papers that detail the eudysmic ratio at the calcium channel; we can make an informed hypothesis. With experimental results already in place to predict the outcome of this study, computational modeling wasn't employed as a predictive tool. Additionally, from the previous generations of drug development we would predict that the most active and selective compound in the library would be the (S)-m-Br IHQ.

Our prediction for the results of the biological testing is that there shouldn't be a eudysmic ratio at MDR1. The basis for this argument is that a similar experiment has be conducted by Hollt et al. Hollt observed that 4-aryl-DHPs showed a defined eudysmic ratio at the calcium channel, but his work also showed that MDR1 didn't discriminate between different enantiomers. As such, we would propose that the lack of a eudysmic ratio at MDR1 can be used to our advantage. If the S enantiomer is utilized the compound will be less active at the VGCC, while still retaining an unchanged level of activity at MDR1. This synthetic modification allows us to engineer selectivity into compounds and reduce off target polypharmacology. This coupled with the lower doses that will be needed to treat MDR due to the increase penetration rate of drug to MDR cells will give options in treatment to both treat MDR cells and allow for lower doses to be utilized to achieve a desired pharmacological effect. Both of these factors will allow for safer and more effective cancer treatment and should be considered as a vast improvement on current methods of treatment in MDR cancer chemotherapy.

5.12 **Generation 4 experimental**

General synthesis for Biphenyl-4-Carbaldehyde: An oven dried 100mL round bottom was charged with 2.00g (10.855mmol) of Biphenyl-4-yl-methanol, 30ml of Chloroform, 10.5g of anhydrous magnesium sulfate and a magnetic stir bar. The solution was then allowed to stir until the solution was homologous, 4.5 g of Pyridinium chlorochromate was then added and the vessel was sealed and allowed to react for 3 hours. Reaction progress was checked by TLC; once the reaction was complete excess solvent was removed via rotovap. The solution was then purified via a silica column. The purification yielded yellow oil that was then re-crystallized into a white crystalline solid with hexane and dichloromethane. (1.90g, 10.43mmol, 96%)

^{1}H NMR: (CDCl$_3$) δ ppm 9.82 (s, 1H) 7.36 - 7.41 (m, 2 H) 7.45 - 7.50 (m, 4 H) 7.55 (s, 1 H) 7.59 - 7.64 (m, 4 H)

TLC: SiO$_2$; Hexane:EtOAc 4:1 R$_f$ = 0.54

General synthesis of Biphenyl-4-carbaldehyde oxime. An oven dried round 100mL bottom was charged with 1.90g (10.43mmol) of Biphenyl-4-carbaldehyde, 1.49g of NH$_2$OH*HCl, 2.54g of NaCH$_3$CO$_2$, and a magnetic stir bar. A solution of THF:EtOH:H$_2$O(2:1:1) was made (40mL) and added at room temperature to the round bottom. The round bottom was then capped and allowed to stir for 72 hours. The reaction progress was monitored via TLC, once the reaction went to completion the solution as place on a rotovap to remove EtOH from the solution. The remaining mixture was then extracted with CHCl$_3$ and Brine three times, and dried over NaSO$_4$. The solution was then concnentrated via rotovap yielding a white solid. (2.01g, 10.19 mmol, 98%)

¹H NMR: (CDCl₃) δ ppm 8.18 (s, 1H) 7.36 - 7.41 (m, 2 H) 7.45 - 7.50 (m, 4 H) 7.55 (s, 1 H) 7.59 - 7.64 (m, 4 H)

TLC: SiO₂; Hexane:EtOAc 4:1 R_f = 0.65

General synthesis of 3-Biphenyl-4-yl-5-methyl-isoxazole-4-carboxylic acid ethyl ester. An oven dried round bottom 100mL was charged with 2.01g of Biphenyl-4-carbaldehyde oxime, a magnetic stir bar. The solution was then allowed to stir at room temperature until the mixture was homologous. 0.117 mL of pyridine was then added along with 2.12g of N-chlorosuccinimide, the round bottom was then capped and allowed to stir at room temperature for 3 hours. The reaction mixture was extracted with brine and CHCl₃, the mixture was then dried over NaSO₄, then filtered and concentrated via rotovap. The resulting Biphenyl-4-benzohydroximinoyl chloride was then left under the high vacuum. Another oven dried round bottom 250mL was charged with 100mL of EtOH, and a magnetic stir bar, the round bottom was then capped with a rubber septum and placed under an argon environment. 0.523g of Na was then weight out and placed in the EtOH, the solution was then stirred and the Na was allowed to dissolve. Once dissolved 2.97g of ethyl acetoacetate was then added and the solution was allowed to stir at room temperature. The 100mL round bottom containing Biphenyl-4-benzohydroximinoyl chloride was then removed from the high vacuum and capped with a rubber septum and placed under an argon environment. The Biphenyl-4-benzohydroximinoyl chloride was then taken up in a minimal amount of EtOH and added to the Na/EtOH mixture at room temperature. The round bottom was then capped with a rubber septum and placed under an argon environment. The solution was then allowed to stirred over night. The solution was then extracted with CHCl₃ and Brine three times, and

dried over NaSO$_4$. The solution was then concentrated via rotovap yielding a yellow oil. The solution was then purified via a silica column. (1.96g, 6.38 mmol, 61.9%)

¹H NMR: (CDCl$_3$) δ ppm 7.36 - 7.41 (m, 2 H) 7.45 - 7.50 (m, 4 H) 7.55 (s, 1 H) 7.59 - 7.64 (m, 4 H) 4.11 (q 2H J = 8.02Hz), 1.99(s 3H), 1.18 (t 3H J = 6.84Hz)

TLC: SiO$_2$; Hexane:EtOAc 4:1 R$_f$ = 0.73

General synthesis of (3-Biphenyl-4-yl-5-methyl-isoxazol-4-yl)-methanol. An oven dried 100ml 2-neck round bottom was charged with 2.04g of 3-Biphenyl-4-yl-5-methyl-isoxazole-4-carboxylic acid ethyl ester, a magnetic stir bar and the vessel was sealed and placed under a vacuum. An oven dried condenser was then attached to the 2 neck round bottom and the system was seal and placed under a vacuum and flushed with argon, this process was done three times. The 2-neck round bottom was then placed in an ice bath and was allowed to reach 0ºC. 100mL of freshly distilled THF was then added to the 2-neck round bottom and the solution was again allowed to reach 0ºC. 0.198g of LiAlH$_4$ was then added in potions to the solution, there was slight foaming that was observed. The reaction was then left to react and was allowed to come to room temperature. Reaction process was monitored by TLC after the reaction was completed the mixture was quenched with sodium sulfate decahydrate, foaming was observed. The solution was then purified via filtering it threw a silica plug with Et$_2$O, the resulting solution was then concentrated via rotovap yielding a yellow oil. (1.33g, 5.01mmol, 75.6%)

¹H NMR: (CDCl$_3$) δ ppm 7.36 - 7.41 (m, 2 H) 7.45 - 7.50 (m, 4 H) 7.55 (s, 1 H) 7.59 - 7.64 (m, 4 H) 5.24 (s 3H), 2.54 (s 3H)

TLC: SiO$_2$; Hexane:EtOAc 4:1 R$_f$ = 0.51

General synthesis of 3-Biphenyl-4-yl-5-methyl-isoxazole-4-carbaldehyde. An oven

dried 100mL round bottom was charged with 0.481g of 3-Biphenyl-4-yl-5-methyl-

isoxazol-4-yl)-methanol, 50ml of dichloromethane, 1.76g of anhydrous magnesium

sulfate and a magnetic stir bar. 0.75g of pyridinium chlorochromate was then added and

the vessel was capped with a rubber septa and was allowed to react for 3 hours. Reaction

progress was monitored via TLC, once the reaction was complete excess solvent was

removed via rotovap. The solution was then purified via a silica column and recrystalized

via slow evaporation using hexanes and EtOH. The re-crystallization yielded clear

crystals. (0.356g 1.35 mmol, 74.8%)

^{1}H NMR: (CDCl$_3$) δ ppm 9.88 (s 1H) 7.36 - 7.41 (m, 2 H) 7.45 - 7.50 (m, 4 H) 7.55 (s, 1

H) 7.59 - 7.64 (m, 4 H), 2.62 (s 3H)

TLC: SiO$_2$; Hexane:EtOAc 4:1 R$_f$ = 0.52

General Synthesis of 4-(3-Biphenyl-4-yl-5-methyl-isoxazol-4-yl)-2,6-dimethyl-1,4-

dihydro-pyridine-3,5-dicarboxylic acid diethyl ester. An oven dried 100mL round

bottom was charged with 0.356g of 3-Biphenyl-4-yl-5-methyl-isoxazole-4-carbaldehyde,

0.37g of ethyl acetoacatate, 50ml of EtOH and a magnetic stir bar. The solution was

allowed to stir at room temperature until homologues. 0.337ml of 30% ammonia

hydroxide was then added and the round bottom was fitted with a dean stark trap. The

round bottom was then fitted with an oven dried condenser and the solution was brought

to reflux. The reaction process was monitored via TLC. Once complete the solution was

then cooled to room temperature and the excess solvent was removed via rotovap. The

solution was then purified via a silica column yielding yellow oil (0.309g, 1.35 mmol,

46.2%)

¹H NMR: (CDCl₃) δ 7.58 - 7.68 (m, 4 H) 7.55 (s, 1 H) 7.48 (s, 4 H) 7.33 - 7.42 (m, 1 H) 5.22 (br. s., 1 H) 5.05 (s, 1 H) 4.04 - 4.17 (m, 3 H) 3.93 - 4.04 (m, 2 H) 2.44 - 2.52 (m, 3 H) 1.99 (s, 5 H) 1.18 (t, J=7.15 Hz, 5 H)

¹³C NMR: (CDCl₃) δ 167.41, 165.86, 163.52, 143.87, 141.15, 140.47, 13.09, 129.01, 127.01, 126.15, 119.58, 101.17, 59.82, 29.35, 19.44, 14.51, 11.50

HRMS: calculated for $C_{29}H_{31}N_2O_5$ 487.2233 found 487.2256

MS: m/z = 486 ([M] 40), 487 ([M^{+1}] 100), 488 ([M^{+1}] 30)

TLC: SiO₂; Hexane:EtOAc 4:1 R_f = 0.23

4-(3-Anthracen-9-yl-5-methyl-isoxazol-4-yl)-2,6-dimethyl-1,4-dihydro-pyridine-3,5-dicarboxylic acid diethyl ester

¹H NMR: (CDCl₃) δ 8.49 (s, 1 H) 8.11 (s, 1 H) 7.97 (d, J=9.03 Hz, 1 H) 7.41 - 7.54 (m, 3 H) 7.30 - 7.40 (m, 1 H) 4.96 (s, 1 H) 4.09 - 4.28 (m, 4 H) 2.75 (s, 3 H) 1.20 - 1.38 (m, 6 H) 0.88 (s, 6 H)

¹³C NMR: (CDCl₃) δ 167.13, 166.10, 161.10, 145.05, 131.24, 131.06, 129.77, 127.78, 126.46, 125.87, 125.50, 119.89, 99.22, 59.71, 29.44, 18.17, 14.69, 11.72

HRMS: calculated for $C_{31}H_{31}N_2O_5$ 511.2233 found 511.2228

MS: m/z = 509 ([M-1] 80), 510 ([M] 30), 511([M^{+1}] 100), 512 ([M^{+1}] 30)

TLC: SiO₂; Hexane:EtOAc 4:1 R_f = 0.14

4-[3-(2-Methoxy-naphthalen-1-yl)-5-methyl-isoxazol-4-yl]-2,6-dimethyl-1,4-dihydro-pyridine-3,5-dicarboxylic acid diethyl ester

¹H NMR: (CDCl₃) δ 7.89 (d, J=8.91 Hz, 1 H) 7.69 - 7.77 (m, 1 H) 7.23 - 7.38 (m, 5 H) 7.18 (s, 1 H) 4.96 (s, 1 H) 4.09 - 4.25 (m, 4 H) 3.79 (s, 3 H) 2.64 (s, 3 H) 1.87 (s, 3 H) 1.28 (dt, J=8.85, 7.18 Hz, 6 H) 1.01 (s, 3 H)

^{13}C NMR: (CDCl$_3$) δ 167.36, 165.52, 159.42, 155.23, 144.61, 143.98, 134.18, 130.49, 128.29, 127.29, 126.70, 125.09, 123.56, 119.49, 113.22, 112.25, 99.94, 99.80, 59.65, 59.57, 56.17, 29.46, 19.14, 18.33, 14.67, 14.58, 11.67

HRMS: calculated for C$_{28}$H$_{31}$ N$_2$O$_6$ 491.2182 found 491.2205

MS: *m/z* =489 ([M-1] 100), 490 ([M] 30), 491([M^{+1}] 70), 512 ([M^{+1}] 30)

TLC: SiO$_2$; Hexane:EtOAc 4:1 R$_f$ = 0.18

2,6-Dimethyl-4-(5-methyl-3-naphthalen-1-yl-isoxazol-4-yl)-1,4-dihydro-pyridine-3,5-dicarboxylic acid diethyl ester

^{1}H NMR: (CDCl$_3$) δ 7.89 (d, J= 8.28Hz, 2H), 7.83(d, J=8.03Hz, 1H), 7.46(m, 2H), 7.36(m, 2H), 4.96 (s, 1 H), 4.16 (q, J=7.15Hz, 4 H) 2.65 (s, 3 H) 1.41 (bs, 6 H) 1.29 (t, *J*=7.09 Hz, 6 H)

^{13}C NMR: (CDCl$_3$) δ 167.27, 165.35, 162.54, 144.67, 133.00, 132.84, 128.79, 128.45, 127.99, 127.57, 126.40, 126.40, 126.08, 124.68, 199.38, 99.98, 59.76, 29.38, 18.81, 14.62, 11.57

HRMS: calculated for C$_{27}$H$_{29}$ N$_2$O$_5$ 460.2076 found 461.2087

MS: *m/z* =461 ([M+1] 100), 462 ([M+2] 50)

TLC: SiO$_2$; Hexane:EtOAc 4:1 R$_f$ = 0.28

4-[3-(4-Methoxy-phenyl)-5-methyl-isoxazol-4-yl]-2,6-dimethyl-1,4-dihydro-pyridine-3,5-dicarboxylic acid diethyl ester

^{1}H NMR: (CDCl$_3$) δ 7.21 - 7.26 (m, 2 H) 6.79 - 6.86 (m, 2 H) 4.93 (s, 1 H) 4.79 (s, 1 H) 3.99 - 4.09 (m, 2 H) 3.89 - 3.99 (m, 2 H) 3.77 (s, 3 H) 2.39 - 2.43 (m, 3 H) 1.94 (s, 6 H) 1.13 (t, *J*=7.03 Hz, 6 H)

^{13}C NMR: (CDCl$_3$) δ 167.68, 157.90, 143.49, 140.33, 128.99, 113.20, 104.48, 59.71, 55.16, 38.76, 19.65, 14.29

HRMS: calculated for C$_{24}$H$_{29}$ N$_2$O$_6$ 441.2026 found 441.2057

MS: *m/z* =439 ([M-1] 80), 440 ([M] 20), 441([M^{+1}] 100), 442 ([M^{+2}] 30)

TLC: SiO$_2$; Hexane:EtOAc 4:1 R$_f$ = 0.18

4-[3-(3,4-Dimethoxy-phenyl)-5-methyl-isoxazol-4-yl]-2,6-dimethyl-1,4-dihydro-pyridine-3,5-dicarboxylic acid diethyl ester

^{1}H NMR: (CDCl$_3$) δ 6.95 - 7.01 (m, 2 H) 6.80 - 6.86 (m, 1 H) 6.60 (s, 1 H) 5.62 (s, 1 H) 5.00 (s, 1 H) 3.98 - 4.12 (m, 2 H) 3.86 - 3.97 (m, 2 H) 3.83 (s, 3 H) 3.79 (s, 3 H) 2.39 (s, 3H) 1.95 (s, 6 H) 1.08 - 1.15 (q, 6H)

^{13}C NMR: (CDCl$_3$) δ 167.53, 166.14, 163.26, 149.27, 148.33, 144.21, 123.33, 122.14, 119.59, 112.87, 110.48, 100.68, 59.68, 55.99, 29.30, 18.93, 14.42, 11.43

HRMS: calculated for C$_{25}$H$_{29}$ N$_2$O$_7$ 469.1975 found 469.1990

MS: *m/z* =469 ([M-1] 100), 470 ([M] 40), 471([M^{+1}] 80), 472 ([M^{+1}] 20)

TLC: SiO$_2$; Hexane:EtOAc 4:1 R$_f$ = 0.07

2,6-Dimethyl-4-[5-methyl-3-(3-phenoxy-phenyl)-isoxazol-4-yl]-1,4-dihydro-pyridine-3,5-dicarboxylic acid diethyl ester

^{1}H NMR: (CDCl$_3$) δ 7.28 - 7.35 (m, 1 H) 7.13 - 7.21 (m, 1 H) 7.01 - 7.11 (m, 1 H) 6.94 - 7.01 (m, 2 H) 6.76 (ddd, *J*=8.03, 2.51, 1.00 Hz, 1 H) 5.48 (bs, 1 H) 4.87 (s, 1 H) 3.98 - 4.21 (m, 4 H) 2.33 (s, 3 H) 2.18 (s, 6 H) 1.20 (q, 6 H)

^{13}C NMR: (CDCl$_3$) δ 167.50, 157.53, 156.72, 149.81, 143.96, 129.58, 129.01, 123.06, 118.81, 116.57, 103.97, 59.76, 39.53, 30.96, 19.60, 14.26

HRMS: calculated for C$_{29}$H$_{29}$ N$_2$O$_6$ 501.2026 found 501.2019

MS: *m/z* =500 ([M-1] 20), 501 ([M] 100), 502([M^{+1}] 60)

TLC: SiO$_2$; Hexane:EtOAc 4:1 R$_f$ = 0.28

4-[3-(2,4-Dimethoxy-phenyl)-5-methyl-isoxazol-4-yl]-2,6-dimethyl-1,4-dihydro-pyridine-3,5-dicarboxylic acid diethyl ester

^{1}H NMR: (CDCl$_3$) δ 7.27 (s, 2 H) 7.11 (s, 1 H) 6.48 (s, 1 H) 4.93 (s, 1 H) 4.80 (s, 1 H) 4.05 - 4.19 (m, 4 H) 3.95 (s, 3 H) 3.69 (s, 3 H) 2.54 (s, 3 H) 2.00 (s, 6 H) 1.25(q, 6 H)

^{13}C NMR: (CDCl$_3$) δ 167.36, 165.13, 159.79, 157.70, 156.11, 143.87, 132.19, 119.27, 112.68, 100.66, 95.72, 59.74, 56.42, 55.95, 29.44, 19.31, 14.53, 11.52

HRMS: calculated for C$_{25}$H$_{31}$ N$_2$O$_7$ 623.2757 found 623.2709

MS: *m/z* = 469 ([M-1] 30), 470 ([M] 20), 471([M^{+1}] 100), 472 ([M^{+2}] 30)

TLC: SiO$_2$; Hexane:EtOAc 4:1 R$_f$ = 0.05

4-[3-(3,4-Bis-benzyloxy-phenyl)-5-methyl-isoxazol-4-yl]-2,6-dimethyl-1,4-dihydro-pyridine-3,5-dicarboxylic acid diethyl ester

^{1}H NMR: (CDCl$_3$) δ 7.19 - 7.41 (m, 13 H), 6.92 (s, 2H), 6.76 (s, 2H), 5.21 (s, 1 H) 5.03 (t, *J*=3.76 Hz, 3 H) 4.85 (m, 1 H) 3.88 - 4.12 (m, 4 H) 2.39 (s, 3 H) 2.19 (s, 3 H) 1.73 (s, 3 H) 1.12 (t, *J*=12.30 Hz 6H)

^{13}C NMR: (CDCl$_3$) δ 167.60, 167.4, 165.53, 163.52, 148.68. 148.16, 144.00, 143.56,141.33,137.88, 137.68, 137.63, 136.88, 128.69, 128.56, 128.42, 128.40, 128.11, 128.02, 127.66, 127.61, 127.56, 127.46, 127.32, 127.26, 124.20, 122.92, 120.92, 119.15, 116.29, 115.51, 114.77, 114.41, 104.17, 100.72, 77.36, 77.25, 77.04, 76.72, 71.44, 71.38, 71.34, 70.69, 59.76, 59.70, 38.86, 29.25, 19.63, 19.08, 14.51, 14.35, 11.46,

HRMS: calculated for C$_{37}$H$_{39}$ N$_2$O$_7$ 623.2757 found 623.2807

MS: *m/z* = 621 ([M-1] 20), 622 ([M] 10), 623([M^{+1}] 100), 624 ([M^{+2}] 50)

TLC: SiO_2; Hexane:EtOAc 4:1 $R_f = 0.16$

5.9 Generation 5 experimental

General synthesis for 2,7,7-Trimethyl-4-(5-methyl-3-phenyl-isoxazol-4-yl)-5-oxo-1,4,5,6,7,8-hexahydro-quinoline-3-carboxylic acid ethyl ester: An oven dried 50mL round bottom was charged with 0.27g (1.44mmol) of starting material, 0.202g of dimedone, 0.187g of ethyl acetoacetate, 0.046g of Ytterbium (III) trifluoromethanesulfonate and a magnetic stir bar. The mixture is then taken up in 3.61mL of absolute Ethanol and is allowed to stir at room temperature. Once homologues 0.11g of ammonium acetate is added to the stirring solution and the round bottom is capped. The solution is then allowed to stir at room temperature for 48hr. After which reaction progress was monitored via TLC. Once the reaction was complete excess solvent was removed via rotovap. The solution was then purified via a silica column.

^{1}H NMR: ($CDCl_3$) δ 7.50 (d, J=9.03Hz 2H), 7.38 (s 1H), 7.36 (d, J=11.04Hz 2H), 5.73 (s, 1H), 5.01 (s, 1H), 4.05 (m, 2H), 3.89 (m, 2H), 2.54 (s, 3H), 2.15 (d, J=4.02Hz 2H), 2.00 (s, 2H), 1.08 (t, J=7.28Hz, 3H), 0.99 (s, 6H)

^{13}C NMR: ($CDCl_3$) δ 195.48, 167.15, 166.70, 163.40, 148.45, 143.86, 130.90, 129.60, 128.58, 127.70, 118.74, 109.21, 103.32, 59.78, 50.75, 40.66, 32.33, 28.52, 28.42, 26.50, 19.05, 14.31, 11.47

HRMS: calculated for $C_{25}H_{29} N_2O_4$ 421.2127 found 421.2132

MS: m/z = 419 ([M^{-1}] 10), 421 ([M^{+1}] 100), 422 ([M^{+2}] 30)

TLC: SiO_2; Hexane:EtOAc 3:2 $R_f = 0.23$

4-[3-(2-Bromo-phenyl)-5-methyl-isoxazol-4-yl]-2,7,7-trimethyl-5-oxo-1,4,5,6,7,8-hexahydro-quinoline-3-carboxylic acid ethyl ester

^{1}H NMR: (CDCl$_3$) δ 7.59 (d, J=7.78Hz 1H), 7.32 (t, J=7.53Hz 1H), 7.23 (m, 1H), 7.16 (m, 1H), 4.97 (s, 1H), 4.94 (s, 1H),4.12 (q, J=7.28Hz, 2H), 4.11(q, J=7.03Hz, 2H), 2.68 (s, 3H), 2.05 (s, 2H), 1.96(s, 2H), 1.24 (t, J=7.28Hz 3H), 1.08 (s, 3H), 0.98 (s, 6H)

^{13}C NMR: (CDCl$_3$) δ 195.47, 167.07, 166.58, 162.43, 148.09, 144.42, 132.42, 132.42, 132.30, 130.04, 126.24, 124.82, 117.30, 109.20, 102.30, 60.41, 58.89, 50.56, 40.94, 32.99, 26.27, 19.52, 14.50, 11.45

HRMS: calculated for C$_{25}$H$_{28}$N$_2$O$_4$Br 499.1232 found 499.1248

MS: *m/z* = 499 ([M] 90), 500 ([M^{+1}] 40), 501 ([M^{+1}] 100) 502 ([M^{+2}] 30)

TLC: SiO$_2$; Hexane:EtOAc 3:2 R$_f$ = 0.21

4-[3-(3-Bromo-phenyl)-5-methyl-isoxazol-4-yl]-2,7,7-trimethyl-5-oxo-1,4,5,6,7,8-hexahydro-quinoline-3-carboxylic acid ethyl ester

^{1}H NMR: (CDCl$_3$) δ 7.67 (s, 1H), 7.48 (d, J=8.78Hz 1H), 7.27 (s, 1H), 7.24 (d, J=8.03Hz 1H), 6.50 (s, 1H), 4.98 (s, 1H), 4.04 (q, J=10.79Hz 2H), 3.89 (q, J=10.79Hz 2H), 2.51 (s,3H), 2.14 (d, J=6.53Hz 2H), 1.99 (s, 2H), 1.07(t, J=7.03Hz 3H), 0.97 (s, 6H)

^{13}C NMR: (CDCl$_3$) δ 195.68, 167.25, 167.09, 162.00, 149.19, 144.24, 132.91, 132.91, 132.31, 131.71, 129.46, 128.25, 121.78, 119.11, 108.86, 103.05, 59.79, 50.75, 40.39, 32.23, 28.52, 28.30, 26.67, 18.87, 14.31, 11.52

HRMS: calculated for C$_{25}$H$_{27}$N$_2$O$_4$Br 499.1232 found 499.1324

MS: *m/z* = 499 ([M] 100), 500 ([M^{+1}] 50), 501 ([M^{+2}] 90), 502 ([M^{+3}] 30)

TLC: SiO$_2$; Hexane:EtOAc 4:1 R$_f$ = 0.23

4-[3-(4-Bromo-phenyl)-5-methyl-isoxazol-4-yl]-2,7,7-trimethyl-5-oxo-1,4,5,6,7,8-hexahydro-quinoline-3-carboxylic acid ethyl ester

^{1}H NMR: (CDCl$_3$) δ 7.54 (d, J=8.53Hz 2H), 7.51 (d, J=8.53Hz 2H), 5.24 (bs, 1H), 5.02 (s, 1H), 4.06 (m, J=7.03Hz 2H), 3.88 (m, J=7.28Hz 2H), 2.52(s, 3H), 2.18 (d, J=5.27Hz 2H), 2.10 (s, 2H), 1.08 (t, J=6.78Hz 3H), 1.03 (s 6H)

^{13}C NMR: (CDCl$_3$) δ 195.36, 167.21, 166.95, 162.28, 147.76, 143.06, 131.27, 130.91, 130.09, 122.99, 118.78, 109.59, 103.88, 59.92, 50.68, 41.03, 32.45, 28.58, 28.36, 26.52,19.27, 14.24, 11.47

HRMS: calculated for C$_{25}$H$_{28}$ N$_2$O$_4$Br 499.1232 found 499.1251

MS: m/z = 499 ([M] 100), 500 ([M^{+1}] 30), 501 ([M^{+1}] 90), 502 ([M^{+2}] 30)

TLC: SiO$_2$; Hexane:EtOAc 3:2 R$_f$ = 0.18

4-(3-Biphenyl-4-yl-5-methyl-isoxazol-4-yl)-2,7,7-trimethyl-5-oxo-1,4,5,6,7,8-hexahydro-quinoline-3-carboxylic acid ethyl ester

^{1}H NMR: (CDCl$_3$) δ 7.69 (d, J=7.78Hz 2H), 7.61 (t, J=8.53Hz 2H), 7.53 (s 1H), 7.45 (t, J=7.28Hz 2H), 7.36 (t, J=7.28Hz 2H), 6.57 (bs, 1H), 5.05 (s, 1H), 4.02 (m, J=10.54Hz 2H), 3.79 (m, J=10.54Hz 2H), 2.44 (s, 3H), 2.12 (d, J=2.76Hz, 2H), 2.04 (s, 2H), 1.95 (s, 2H), 0.99 (t, J=7.03Hz 3H), 0.94 (s, 6H)

^{13}C NMR: (CDCl$_3$) δ 195.77, 167.21, 167.11, 162.95, 149.11, 143.97, 141.49, 140.53, 129.90, 129.81, 128.96, 127.70, 127.05, 126.49, 119.49, 109.04, 103.37, 59.71, 50.75, 40.42, 32.24, 28.52, 28.25, 26.55, 18.79, 14.22, 11.47

HRMS: calculated for C$_{31}$H$_{31}$ N$_2$O$_4$ 495.2284 found 495.2309

MS: m/z = 495 ([M] 100), 496 ([M^{+1}] 50), 497 ([M^{+1}] 60)

TLC: SiO$_2$; Hexane:EtOAc 4:1 R$_f$ = 0.23

The general synthesis of (-)- 2,7,7-Trimethyl-4-(5-methyl-3-phenyl-isoxazol-4-yl)-5-oxo-1,4,5,6,7,8-hexahydro-quinoline-3-carboxylic acid ethyl ester. An oven dried 50mL round bottom was charged with 0.027g (1.5eq) of dimedone, 0.025g of ethyl acetoacetate, and 0.014g (10mol%) of (R)- 4-Oxo-2,6-bis-(2,4,6-triisopropyl-phenyl)-3,5-dioxa-4l5-phospha-cyclohepta[2,1-a;3,4-a']dinaphthalen-4-ol and a magnetic stir bar. The mixture was then taken up in 1.5mL of acetonitrile, capped and put under an inert atmosphere of argon, after which the solution was allowed to stir at room temperature for 20 minutes. Once homologues 0.036g (0.193mmol) of aldehyde and 0.015g of ammonium acetate is added to the stirring solution, the solution is then allowed to stir at room temperature for 48hr. After which reaction progress was monitored via TLC. Once the reaction was complete excess solvent was removed via rotovap. The solution was then purified via a silica column.

^{1}H NMR: (CDCl$_3$) δ 7.46 (d, J=9.03Hz 2H), 7.39 (s 1H), 7.38 (d, J=11.54Hz 2H), 5.02 (s, 1H), 4.14-4.06 (m, 1H), 3.96-3.92 (m, 1H), 2.57 (s, 3H), 2.18 (d, J=2.76Hz 2H), 2.03 (s, 3H), 1.13 (t, J=7.28Hz, 3H), 1.04 (s, 3H), 1.03 (s, 3H)

^{13}C NMR: (CDCl$_3$) δ 194.29, 165.90, 166.72, 147.85, 143.51, 137.74, 129.72, 129.23, 127.63, 115.26, 109.56, 103.56, 59.87, 57.53, 50.71, 40.98, 32.57, 32.48, 28.66, 28.42, 26.49, 24.58,19.34,14.32. [α]$_D$ - 11.2 (c = 0.09 CH$_3$OH)

(-)-4-[3-(2-Bromo-phenyl)-5-methyl-isoxazol-4-yl]-2,7,7-trimethyl-5-oxo-1,4,5,6,7,8-hexahydro-quinoline-3-carboxylic acid ethyl ester

^{1}H NMR: (CDCl$_3$) δ 7.61 (d, J=7.78Hz 1H), 7.33 (t, J=7.28Hz 1H), 7.24 (m, 1H), 7.19 (d, J=7.53Hz 2H), 4.97 (s, 1H), 4.77 (s, 1H),4.12 (q, J=7.28Hz, 2H), 2.68 (s, 3H), 2.30 (d,

J=16.31Hz 2H), 2.17 (d, J=16.31Hz 2H), 1.97 (s,3H), 1.25 (t, J=7.03Hz 3H), 1.98 (s, 3H), 0.99 (s, 3H)

¹³C NMR: (CDCl₃) δ 195.45, 167.06, 166.60, 147.95, 144.30, 132.49, 132.31, 130.01, 126.24, 124.86, 117.24, 109.28, 102.39, 60.41, 59.92, 50.55, 41.03, 33.02, 26.26, 19.59, 14.49, 11.44... [α]$_D$ -13.5 (c = 0.15, CH₃OH)

(-)-4-[3-(3-Bromo-phenyl)-5-methyl-isoxazol-4-yl]-2,7,7-trimethyl-5-oxo-1,4,5,6,7,8-hexahydro-quinoline-3-carboxylic acid ethyl ester

¹H NMR: (CDCl₃) δ 7.62 (s, 1H), 7.54 (d, J=8.03Hz 1H), 7.42 (d, J=7.53Hz 1H), 7.30 (d, J=7.53Hz 1H), 5.18 (s, 1H), 5.01 (s, 1H), 4.12-4.06 (m,1H), 4.00-3.95 (m,1H), 2.60 (s,3H), 2.20 (d, J=14.81Hz 2H), 2.07(d, J=16.31Hz 2H), 2.04(s,3H), 1.14 (t, J=7.03Hz 3H), 1.06 (s, 6H)

¹³C NMR: (CDCl₃) δ 195.54, 167.60, 166.89, 163.57, 149.96, 144.52, 132.50, 132.30, 132.31, 131.84, 129.68, 127.56, 125.61, 118.11, 108.65, 102.42, 58.67, 50.62, 40.69, 33.25, 27.62, 26.74, 18.65, 14.53, 11.52. [α]$_D$ - 2.36 (c = 0.28, CH₃OH).

(-)-4-[3-(4-Bromo-phenyl)-5-methyl-isoxazol-4-yl]-2,7,7-trimethyl-5-oxo-1,4,5,6,7,8-hexahydro-quinoline-3-carboxylic acid ethyl ester

¹H NMR: (CDCl₃) δ 7.56 (d, J=8.28Hz 2H), 7.51 (d, J=8.28Hz 2H), 5.21 (bs, 1H), 5.02 (s, 1H), 4.08-4.04 (m,1H), 3.90-3.86 (m,1H), 2.52(s, 3H), 2.18 (d, J=5.02Hz 2H), 2.11 (s, 3H), 2.09 (d, J=9.29Hz 2H), 1.08 (t, J=7.28Hz 3H), 1.04 (s 6H)

¹³C NMR: (CDCl₃) δ 195.37, 167.22, 166.95, 162.29, 147.77, 131.28, 130.92, 130.09, 123.00, 118.79, 109.59, 103.89, 59.93, 50.68, 41.04, 32.45, 28.58, 28.37, 26.53,19.28, 14.25, 11.48. [α]$_D$ - 0.032 (c = 0.08, CH₃OH)

(-)-4-[3-(4-Bromo-phenyl)-5-methyl-isoxazol-4-yl]-2,6-dimethyl-1,4-dihydro-pyridine-3,5-dicarboxylic acid 3-ethyl ester 5-(1-phenethyl-1H-[1,2,3]triazol-4-ylmethyl) ester

^{1}H NMR: (CDCl$_3$) δ 7.41(d, 2H J = 8.28Hz), 7.18 (d, 2H J = 8.28Hz), 7.07(s, 1H), 7.24(d, 2H J = 9.29Hz), 7.01(d, 2H J = 6.78Hz), 5.73(s, 1H), 5.09 (d, 2H J = 12.80Hz), 4.97 (d, 2H J = 12.80Hz), 4.90(s, 1H), 4.48 (t, 2H J = 7.28Hz), 4.05 (q, 2H J = 7.03Hz), 4.07 (q 2H J = 7.03Hz), 3.11(t, 2H J = 7.53Hz), 2.26(s, 3H), 1.92(d, 6H J = 8.03Hz), 1.06(t, 3H J = 7.03Hz)

^{13}C NMR: (CDCl$_3$) δ 167.35, 167.11, 166.63, 144.30, 142.98, 136.86, 131.09, 130.82, 128.82, 128.66, 127.11, 122.95, 119.76, 101.09, 59.80, 58.25, 56.72, 51.63, 42.90, 36.59, 29.36,19.03, 18.85, 18.40, 14.45, 14.43, 11.33. [α]$_D$ -2.68 (c = 0.48, CH$_3$OH).

5.14 References

1. FDA's Policy statement for the development of new stereoisomeric drugs. *Chirality.* **1992**, 4, 338-340

2. Daniels,D., Nestmann, R., Kerr, A. Development of Stereoisomeric drugs: A Brief Review of Scientific and Regulatory Considerations. *Drug inf. J,.* **1997**, 31, 639-646

3. Agrana, I., Caner. H., Caldwell. J. Putting chirality to work: the strategy of chiral switches. *Nature Rev. Drug Discovery*. **2002**, 1, 753-768

4. Hillier,C., Reider,J. Stereoselective synthesis from a process research perspective *Drug Discov. Today.* **200**2,7,303-314

5. Daniels, D., Nestmann, R., Kerr,A. Development of stereoisomeric (chirl) drugs: A brief review of scientific and regulatory considerations. *Drug inf. J.* **1997**, 31, 639-646

6. Strong,M. FDA policy and regulation of stereoisomers: paradigm shift and the future of safer more effective drugs. *Food Drug Law J.* **1999**, 54, 463-487

7. Agranat, I., Caner, H., Caldwell, J. Putting chirality to work: the strategy of chiral switches. *Nat. Review Drug Discovery.***2002**, 1, 753-768

8. Aboul-Enein, H., Wainer, I. The impact of stereochemistry on drug development and use. John& Wiley & Sons, **1997**, 728

9. Golman, S., Stoltefuss, 1,4-Dihydropyridines: Effects of chirality and conformation on the calcium antagonist and calcium agonist activities. *J. Angew. Chem.* **1991**, 30, 1559-1578

10. Ashimori, A., Uchida, T., Ohtaki, Y., Tanaka, M., Ohe, K., Fukaya, C., Watanabe, M., Kagitani, M., Yokoyama, K. Synthesis and pharmacological effects of optically active 2-[4-(4-benzhydryl-1-piperazinyl)phenyl]-ethyl methyl 1,4-dihydro-2,6-dimethyl-4-93-nitrophenyl)-3,5-pyridinedicarboxylate hydrochloride. *Chem Pharm. Bull*. **1991**, 39, 108-11

11. Alajarin, R., Vaquero, J., Alvarez-Builla, J., Pastor, M., Sunkel, C., Fau de Casas-Juana, M., priego, J., Statkow, P., Sanz-Aparicco, J., Fonsecca, I. Candida antarcita lipase-catalyzed hydrolysis of 4-substituted bis(ethoxycarbonylmethyl) 1,4-dihydropyridine-3,5-dicarboxylates as the key step in the synthesis of optically active dihydropyridines. *J. Med. Chem.* **1995**, 38, 2830-2841

12. Kamp, T., Sanguinetti, M., Miller, R. Voltage and use- dependent modulation of cardiac calcium channels by the dihydropyridine (+)-202-791. *Circulation research*. **1989**, 64, 338-351

13. Eisner, U., Kuthan, J. Chemistry of dihydropyridines. *Chem. Rev.* **1972**, 72-,1-42

14. Sausins, A., Duburs, G. Synthesis of 1,4-dihydropyridines by cyclocondensation reactions. *Heterocycles.* **1988**, 27, 269-289

15. Stout, D., Meyers, I. Recent advances in the chemistry of dihydropyridines. *Chem. Rev.* **1982**, 82, 223-243

16. Natale, N. Learing from the hantzsch synthesis. *Chemical Innovation*. **2000**, 30, 22-28

17. Sausin, A., Chekavichus, B., Lusis, V., Dubur, G. 1-aryl and 1-benzyl-3, 5-diethoxycarbonyl-1,4-dihydropyridines. *Chemistry of Heterocyclic Compounds*. **1980**, 377-385

18. Uldrikis, J., Durbur, G., Dipan, I., Chekavichus, B. *Chemistry of Heterocyclic Compounds.* **1975**, 1070-1076

19. Zhu J, Bienayme H. Multicomponent Reactions. **2005**

20. Weber L, Illgen K, Almstetter M. Discovery of new multi component reactions with combinatorial methods. *Synlett* **1999**, 366-374

21. Ramon, J., Yus, M. Asymmetric multicomponent reactions(AMCRs): the new frontier. *Angew Chem Int.* **2005**,44, 1602-1634

22. Loev, B.; Snader, K.; The Hantzsch reaction. I. Oxidative dalkylation of certain dihydropyridines. *J. Org. Chem.*, 1965, 30 (6), pp 1914–1916

23. S.-J. Tu, J.-F. Zhou, X. Deng, P.-J. Cai, H. Wang, J.-C. Feng. One step synthesis of 4-arylpolyhydroquinoline derivatives using microwave irradiation. Chin. J. Org. Chem., 21 (2001), pp. 313–316

24. G. Sabitha, G.S.K.K. Reddy, C.S. Reddy, J.S. Yadav. A novel TMSI-mediated synthesis of Hantzsch 1,4-dihydropyridines at ambient temperature. Tetrahedron Lett., 44 (2003), pp. 4129–4131

25. S.J. Ji, Z.Q. Jiang, J. Lu, T.P. Loh. Facile ionic liquids-promoted one-pot synthesis of polyhydroquinoline derivatives under solvent free conditions. Synlett (2004), pp. 831–835

26. J.G. Breitenbucher, G. Figliozzi. Solid-phase synthesis of 4-aryl-1,4-dihydropyridines via the hantzsch three component condensation. Tetrahedron Lett., 41 (2000), pp. 4311–4315

27. A. Dondoni, A. Massi, E. Minghini, V. Bertolasi. Multicomponent hantzsch cyclocondensation as a route to highly functionalized 2 and 4

dihydropyridylalanines, 2 and 4 pyridylalanines, and their N-oxides: preparation via a polymerassisted solution-phase approach. Tetrahedron, 60 (2004), pp. 2311–2326

28. Wang, M., Sheng, J., Zhang, L., Han, J-W., Fan, Z-Y., Tian, H., Qian, C-T. Facile Yb(OTf)3-promoted one-pot synthesis of polyhydroquinoline derivatives through Hantzsch reaction. *Tetrahedron*. **2005**, 6, 1539-1543

29. Wang, M., Sheng, J., Zhang, L., Han, J-W., Fan, Z-Y., Tian, H., Qian, C-T. Facile Yb(OTf)3-promoted one-pot synthesis of polyhydroquinoline derivatives through Hantzsch reaction. *Tetrahedron*. **2005**, 6, 1539-1543

30. Debache A., Boulcina, R., Belfaitah, A., Rhouati, S., Carboni, B. Onepot synthesis of 1,4-dihydropyridines via a phenylboronic acid catalyzed Hantzsch three-component reaction. *Synlett.* **2008**, 509-512

31. Kumar, A., Maurya, R., Synthesis of polyhydroquinoline derivatives through unsymmetric Hantzsch reaction using organocatalysts. *Tetrahedron* **2007**, 63, 1946-1952

32. Ko, S., Yao, C-F. Ceric ammonium nitrate (CAN) catalyzes the one-pot synthesis of polyhydroquinoline via the Hantzsch reaction. *Tetrahedron*. **2006**, 62,7293-7299

33. Golman, S., Stoltefuss, 1,4-Dihydropyridines: Effects of chirality and conformation on the calcium antagonist and calcium agonist activities. *J. Angew. Chem.* **1991**, 30, 1559-1578

34. Achiwa, K., Kato, T. Asymmetric synthesis of optically active 1,4-dihydropyridines as calcium antagonist. *Curr. Org. Chem.* **1999**, 3, 77-106

35. Marchalin, S., Chudik, M., Mastihuba, V., Decroix, B. Use of enzymes in preparation of enantiopure 1,4-dihydropyridines. *Heterocycles.* **1998**, 48, 1943-1957

36. Genain, G. Eropene Patent #0273349, 1988

37. Ashimori, A., Uchida, T., Ohtaki, Y., Tanaka, M., Ohe, K., Fukaya, C.,Watanabe, M., Kagitani, M., Yokoyama, K. Synthesis and pharmacological effects of optically active 2-[4-(4-benzhydryl-1-piperazinyl) phenyl]-ethyl methyl 1, 4-dihydro-2, 6-dimethyl-4-(3-nitrophenyl)-3, 5-pyridinedicarboxylate hydrochloride. *Chem. Pharm. Bull.* **1991**, 39, 108-111

38. Ogawa, T., Matsumoto, K., Yokoo, C., Hatayama, K., Kitamura, K., Synthesis and configurational assignment of methyl 3-nitrooxypropyl 1, 4-dihydro-2, 6-dimethyl-4-(3-nitrophenyl) pyridine-3, 5-dicarboxylate. *J. Chem. Soc. Perkin Trans.* **1993**,4, 525-528

39. Vincent, J. Bryan, Alex D. Sokolowski, Thanh V. Nguyen, and Gyula Vigh. A family of single-isomer chiral resolving agents for capillary electrophoresis. 1. Heptakis (2, 3-diacetyl-6-sulfato)-β-cyclodextrin. *Analytical Chemistry* **1997**, 69, 4226-4233

40. Ogawa, T.; Matsumoto, K.; Yokoo, C.; Hatayama, K.; Kitamura, K., J. Chem. Soc. Perkin Trans. 1993, 525-528

41. Shibanuma, T; Iwanai, M.; Okuda, K.; Takenaka, T.; Murakamin, M., Chem. Pharm. Bull. 1980,28, 2809-2812

42. Ashimori, A.; Uchida, T.; Ohtaki, Y.; Tanaka, M.; Ohe, K.; Fukaya, C.;Watanabe, M.; Kagitani, M.; Yokoyama, K. Chem. Pharm. Bull. 1991, 39, 108-111

43. Golman, S., Stoltefuss, 1,4-Dihydropyridines: Effects of chirality and conformation on the calcium antagonist and calcium agonist activities. *J. Angew. Chem.* **1991**, 30, 1559-1578

44. Goldman, S., Stoltefuss, J., Born, L. Determination of the absolute configuration of the active amlodipine enantiomer as (-)-S: a correction *J. Med. Chem.* **1992,** 35, 3341-3344

45. Tokuma, Y., Noguchi, H. Stereoselective pharmacokinetics of dihydropyridine calcium antagonists. *J. Chromatogr. A.* **1995**, 694, 181-193

46. Ebiike, H., Maruyama, K., Ozawa, Y., Yamazaki, Y., Achiwa, K. Asymmetric synthesis of (R)-nilvadipine and (S)-NB 818 via regioselective bromination of chiral 1, 4-dihydropyridines as a key step and enzymatic resolution of racemic 2-hydroxymethyl-1, 4-dihydropyridine derivatives. *Chem. Pharm Bull.* **1997**, 45, 869-876

47. Caccamese, S.; Chillemi, R.; Principato, G. Fluorenone 1, 4-dihydropyridine derivatives with cardiodepressant activity: Enantiomeric separation by chiral HPLC and conformational aspects. *Chirality* **1996**, 8, 281-290

48. Alajarin, R.; Vaquero, J.; Alvarez-Builla, J.; Pastor, M.; Sunkel, C.; Fau de Casa-Juana, M.; Priego, J.; Statkow, P.; Sanz-Aparicio, J.; Fonseca, I. Synthesis, structure, and pharmacological evaluation of the stereoisomers of furnidipine. *J. Med. Chem.* **1995**, 38, 2830-2841

49. Soons, P.; Rossemalen, m.; Breimer, D., Enantioselective determination of felodipine and other chiral dihydropyridine calcium entry blockers in human plasma. *J. Chromatogr.* **1990**, 528, 343-356

50. Uno, T.; Ohkubo, T.; Sugawara, K. Effects of grapefruit juice on the stereoselective disposition of nicardipine in humans: evidence for dominant presystemic elimination at the gut site. *J. Chromatrogr. B*. **1997**, 698, 181-186

51. Meyers, A., Natale, N., Wettlaufer, D. Chiral 1,4-dihydropyridines. Synthesis and absolute configuration. *Tettrahedron Lett*. **1981**, 22, 5123-5126

52. Ducatti, D., Massi, A., Noseda, M., Duarte, E., Dondoni, A. Dihydropyridine C-glycoconjugates by organocatalytic hantzsch cyclocondensation. Stereoselective synthesis of α- threofuranose C-nucleoside enatiomers. *Org. Biomol. Chem.* **2009**, 7, 1980-1986

53. Petrow, V. New synthesis of heterocyclic compounds. Part VII. 9-amino-6:8-dimethyl-7: 10-diazaphenanthrenes. *J. Chem. Soc.* **1946**, 884-888

54. Katritzky, A., Ostercamp, D., Yousaf, T. The mechanism of the hantzsch pyridine synthesis: a study by 15N and 13C NMR spectroscopy. *Tetrahedron.* **1986**, 42, 5729-5738

55. Li, Jie. Hantzsch pyridine synthesis. *Name Reactions*. **2002**, 152-153

56. Vigante, B., Ozols, Y., Dubur, G., Beilis, Y., Belash, M., Prezhdo, V. Esters of 1,4-dihydropyridine-3-and-3,5-carbothiolic acids. *Chemistry of Heterocyclic Compounds*, **1982**, 18, 170-178

57. Ender, D.; Muller, S.; Demir, A.; Enantioselective Hantzsch dihydropyridine synthesis via metalated chiral alkyl acetoacetale hydrazone. Tettrahedon Lett. 29,49, 6437-6440, 1988

58. Goldmann, S., Stolefuss, J. 1, 4-Dihydropyridines: Effects of Chirality and Conformation on the Calcium Antagonist and Calcium Agonist Activities. *Angew*. **1991**, 30, 1559-1578

59. Uraguchi, D., Sorimachi, K., Terada, M. Organocatalytic asymmetric aza-Friedel-Crafts alkylation of furan. *J. Am. Chem. Soc*. **2004**, 126, 11804-11805

60. Akiyama, T. Strong Bronsted Acids. *Chem. Review*, **2007**, 107, 5744-5758

61. Uraguchi, D.; Sorimachi, K.; Terada, M. Organocatalytic Asymmetric Aza-Freidel-crafts alkylation of furan. *J. Am. Chem. Soc.* **2004**, 126, 11804-11805

62. Akiyama, T. Strong Bronsted Acids. *Chem. Review*, **2007**, 107, 5744-5758

63. Feringa, L. Phosphoramidites: marvellous ligands in catalytic asymmetric conjugate addition. *Acc. Chem. Res.* **2000**, 33, 346

64. Akiyama, A., Mortia, H., Bachu, P., Mori, K., Yamanaka, M., Hiraka, T. Chiral Bronsted acid-catalyzed hydrophosphonylation of imines-DFT study on the effect of substituents of phosphoric acid. *Tetrahedron*, **2009**, 65, 4950-4956

65. Storer, R., Carrera, E., Ni, Y., MacMillan, W. Enantioselective organocatalytic reductive amination. *J. Am. Chem. Soc.* **2005**, 128,84-86

66. Akiyama, T. Strong Bronsted Acids. *Chem. Review*, **2007**, 107, 5744-5758

67. Evans, G., Gestwicki, E. Enantioselective organocatalytic Hantzsch synthesis of polyhydroquinolines. *Org Lett.* **2009**,11, 2957-2959

68. Li, N.; Chen, X.; Song, J.; Luo, S.; Fan, W.; Gong, L. Highly enantioselective organocatalytic biginelli and bigineeli-like condensations: reversal of the stereochemistry by turing the 3,3'-disubstituents of phosphoric acids. *J. Am. Chem. Soc.*, **2009**, 131, 1501-15310

69. Jiang, J.; Yu, J.; Sun, X.; Rao, Q.; Gong, L. Organocatalytic asymmetric three-component cyclization of cinnamaldehydes and primary amines with 1,3-dicarbonyl compounds: straightforward acces to enantiomerically enriched dihydropyridnes. *Angew. Chem. Int. Ed.* **2008**, 47, 2458-2462

70. Triggle, D. Calcium channel antagonists: past and future. *Pharmaceutical new*, **2002**, 9, 463-471

71. Triggle, D. The 1,4-dihydopyridines nucleus: a pharmacophoric templat part1. Actions at ion channels. *Mini Rev. Med. Chem.*, **2003**, 3, 215-223

72. Zamponi, G.; Stotz, S.; Staples, R.; Andro, T.; Nelson, J.; Hulubei, V.; Blumenfeld, A.; Natale, N. Unique structure activity relatiohsip for 4-isoxazolyl-1,4-dihydropyridines. *J. Med. Chem.* **2003**, 2, 87-96)

73. Schade, D., Lanier. M., Willems, E., Okolotowicz, K., Bushway, P., Wahiguist, C., Gilley, C., Mercola, M., Cashman, J. Synthesis and SAR of b-annulated 1,4-dihydropyridiens defines cardiomyogenic compounds as novel inhibitors of TGFβ signaling. *J. Med. Chem.* **2012**, 26, 9946-9957

74. Rose, U. Hexahydroquinolinones with calcium-modulatory Effects synthesis and pharmacologic action. *Arch. Pharm.* **1990**, 323, 281−286

75. Aydin, F., Safak, C., Simsek, R., Erol, K., Ulgen, M., Linden, A. Studies on condensed 1,4-dihydropyridine derivatives and their calcium modulatory activities. *Pharmazie* **2006**, 61, 655−659

76. Takahashi, D., Oyunzul, L., Onoue, S., Ito, Y., Uchida, S., Simsek, R., Gunduz, M. G., Safak, C., Yamada, S. Structure−activity relationships of receptor binding of 1,4-dihydropyridine derivatives. *Biol. Pharm. Bull.* **2008**, 31, 473−479

77. Willems, E., Teixeira, J., Schade, D., Cai, W., Reeves, P., Bushway, J., Lanier, M., Walsh, C., Kirchhausen, T., Izpizua Belmonte, C., Cashman, J., Mercola, M. Small molecule-mediated TGFβ Type II receptor degradation promotes cardiomyogenesis in embryonic stem cells. *Cell Stem Cell* **2012**, 11, 242– 252

78. Meyers, A. I.; Oppenlaender, T. An asymmetric synthesis of chiral nifedipine analogues. *Journal of the Chemical Society, Chemical Communications* **1986,**12, 920-921

79. Connon, S. Chiral Phosphoric Acids: Powerful Organocatalysts for asymmetric addition reactions to imines. *Angew. Chem. Int. Ed.* **2006**, 45, 3909-3912